

國立交通大學

機械工程學系

碩士論文

分數階變革式奈米 Duffing 共振器系統的渾沌及
其同步與反控制

**Chaos, Its Synchronization and Anticontrol of
Fractional Order Modified Nano Duffing
Resonator Systems**



研究生：歐展義

指導教授：戈正銘 教授

中華民國九十五年六月

分數階變革式奈米 Duffing 共振器系統的渾沌及
其同步與反控制

**Chaos, Its Synchronization and Anticontrol of
Fractional Order Modified Nano Duffing
Resonator Systems**

研究生：歐展義

Student : Chan-Yi Ou

指導教授：戈正銘

Advisor : Zheng-Ming Ge



A Thesis
Submitted to Department of Mechanical Engineering
College of Engineering
National Chiao Tung University
in Partial Fulfillment of the Requirement
for the Degree of Master of Science
in
Mechanical Engineering
June 2006
Hsinchu, Taiwan, Republic of China
中華民國九十五年六月

分數階變革式奈米 Duffing 共振器系統的渾沌及其 同步與反控制

學生：歐展義

指導教授：戈正銘

摘要

本篇論文以相圖、龐卡萊映射圖及分歧圖等數值方法研究分數階變革式奈米 Duffing 共振器系統的渾沌行為。基於頻域的觀點，零到一階之間的分數階積分器可以線性轉移函數的近似計算而得。可以發現系統總階數 1.8、1.9、2.0、2.1 時，系統具有渾沌現象。兩個沒有耦合的分數階變革式奈米 Duffing 共振器系統之渾沌同步可以藉以第三渾沌系統的渾沌狀態變數之相同函數取代它們相對應的參數而達成。此方法稱為參數激發渾沌同步。渾沌同步可成功地以很低的總分數階數 0.2 獲得，數值模擬見於相圖、龐卡萊映射圖和狀態誤差圖。最後研究分數階變革式奈米 Duffing 共振器系統的反控制。首先，以第二個全同的系統之狀態變數的函數作為添加項，渾沌反控制即可獲得。接著以白噪訊、Rayleigh 噪訊、Rician 噪訊、均勻噪訊等分別作為添加項，渾沌反控制亦可獲得。渾沌反控制可成功地以很低的總分數階數 0.2 達成。數值模擬以相圖、龐卡萊映射圖表示。

Chaos, Its Synchronization and Anticontrol of Fractional Order Modified Nano Duffing Resonator Systems

Student : Chan-Yi-Ou

Advisor : Zheng-Ming-Ge

ABSTRACT

In this thesis, the chaotic behaviors in a fractional order modified nano Duffing resonator system are studied numerically by phase portraits, Poincaré maps and bifurcation diagrams. Linear transfer function approximations of the fractional integrator block are calculated for a set of fractional orders in $(0,1]$, based on frequency domain arguments. The total system orders found for chaos to exist in such systems are 1.8, 1.9, 2.0 and 2.1. The chaos synchronizations of two uncoupled fractional order chaotic modified nano Duffing resonator systems are obtained. By replacing their corresponding parameters by the same function of chaotic state variables of a third chaotic system, the chaos synchronization can be obtained. The method is named parameter excited chaos synchronization which can be successfully obtained for very low total fractional order 0.2. Numerical simulations are illustrated by phase portrait, Poincaré map and state error plots. Anti-control of chaos of a fractional order modified nano Duffing resonator system is studied. First, by using the functions of state variable of a second identical system as the added term, the anti-control of chaos can be obtained. Second, by using the white noise, Rayleigh noise, Rician noise and uniform noise as the added term respectively, the anti-control of chaos can be obtained. Anti-control of chaos can be successfully obtained for very low total fractional order 0.2. Numerical simulations are illustrated by phase portraits and Poincaré maps.

誌謝

此篇論文及碩士學業之完成，首先感謝指導教授 戈正銘老師的耐心指導及諄諄教誨。老師在讀書、人生、真理方面的經驗是令學生敬佩的，無論是兩個金字塔、特定人誕生之機率、剃刀原則等等皆讓我受益無窮；而老師的博學也令學生見識到大師的風采，特別是詩詞方面令學生體會到傳統中國文化之美。

在兩年的碩士光陰，經歷了兩場親人的死別和自身的一場車禍，在這要感謝我的同學易昌賢、張安瑞和徐茂原在課業上的幫忙及生活上的協助；也感謝學弟李乾豪、李式中、吳宗訓及學妹翁郁婷陪伴我度過最後一年碩士生涯。感謝我的家人，在我求學期間能使我無後顧之憂完成我的學業，特別要感謝的是父親對我求學之路上的支持。在新竹的兩年，要感謝女友小君在生活上的相伴及學業上的支持與鼓勵；感謝陳爸爸、陳媽媽在生活上的照顧。



Contents

ABSTRACT	i
ACKNOWLEDGMENT	iii
CONTENTS	iv
LIST OF FIGURES	v
Chapter 1 Introduction	1
Chapter 2 Chaos in a Fractional Order Modified Nano Duffing Resonator System	4
2.1 Fractional Derivative and Its Approximation	4
2.2 A Fractional Order Modified Nano Duffing Resonator System	5
2.3 Simulation Results	7
Chapter 3 Chaos Synchronization of Fractional Order Modified Nano Duffing Resonator Systems with Parameters Excited by a Chaotic Signal	34
3.1 Preliminaries	34
3.2 Numerical Simulations for Chaos Synchronization with Parameter Driven by a Chaotic Signal	34
Chapter 4 Anti-control of Chaos of a Fractional Order Modified Nano Duffing Resonator System	47
4.1 Regular Dynamics of a Fractional Modified Nano Duffing Resonator System	47
4.2 Anti-control of Chaos	47
4.2.1 Adding the term kx_1	48
4.2.2 Adding the term $k \sin x_1$	49
Chapter 5 Anti-control of Chaos of a Fractional Order Modified Nano Duffing Resonator System by Adding Noise	59
5.1 Preliminaries	59
5.2 Anti-control of Chaos by Adding Noise	59
5.2.1 Adding the white noise	59
5.2.2 Adding the Rayleigh noise	60
5.2.3 Adding the Rician noise	61
5.2.4 Adding the Uniform noise	62
Chapter 6 Conclusions	71
References	72
Appendix	79
Paper List	80

LIST OF FIGURES

Figure 2.1	The phase portraits, Poincaré maps and the bifurcation diagram for the fractional order modified nano Duffing resonator system, x versus y and b versus x, $(q_1, q_2) = (1.5, 0.3)$.	8
Figure 2.2	The phase portraits, Poincaré maps and the bifurcation diagram for the fractional order modified nano Duffing resonator system, x versus y and b versus x, $(q_1, q_2) = (1.3, 0.5)$.	9
Figure 2.3	The phase portraits, Poincaré maps and the bifurcation diagram for the fractional order modified nano Duffing resonator system, x versus y and b versus x, $(q_1, q_2) = (0.3, 1.5)$.	10
Figure 2.4	The phase portraits, Poincaré maps and the bifurcation diagram for the fractional order modified nano Duffing resonator system, x versus y and b versus x, $(q_1, q_2) = (0.5, 1.3)$.	11
Figure 2.5	The phase portraits, Poincaré maps and the bifurcation diagram for the fractional order modified nano Duffing resonator system, x versus y and b versus x, $(q_1, q_2) = (1.8, 0.1)$.	12
Figure 2.6	The phase portraits, Poincaré maps and the bifurcation diagram for the fractional order modified nano Duffing resonator system, x versus y and b versus x, $(q_1, q_2) = (1.6, 0.3)$.	13
Figure 2.7	The phase portraits, Poincaré maps and the bifurcation diagram for the fractional order modified nano Duffing resonator system, x versus y and b versus x, $(q_1, q_2) = (1.5, 0.4)$.	14
Figure 2.8	The phase portraits, Poincaré maps and the bifurcation diagram for the fractional order modified nano Duffing resonator system, x versus y and b versus x, $(q_1, q_2) = (1.4, 0.5)$.	15
Figure 2.9	The phase portraits, Poincaré maps and the bifurcation diagram for the fractional order modified nano Duffing resonator system, x versus y and b versus x, $(q_1, q_2) = (1.3, 0.6)$.	16
Figure 2.10	The phase portraits, Poincaré maps and the bifurcation diagram for the fractional order modified nano Duffing resonator system, x versus y and b versus x, $(q_1, q_2) = (1.1, 0.8)$.	17

Figure 2.11	The phase portraits, Poincaré maps and the bifurcation diagram for the fractional order modified nano Duffing resonator system, x versus y and b versus x, $(q_1, q_2) = (0.1, 1.8)$.	18
Figure 2.12	The phase portraits, Poincaré maps and the bifurcation diagram for the fractional order modified nano Duffing resonator system, x versus y and b versus x, $(q_1, q_2) = (0.3, 1.6)$.	19
Figure 2.13	The phase portraits, Poincaré maps and the bifurcation diagram for the fractional order modified nano Duffing resonator system, x versus y and b versus x, $(q_1, q_2) = (0.4, 1.5)$.	20
Figure 2.14	The phase portraits, Poincaré maps and the bifurcation diagram for the fractional order modified nano Duffing resonator system, x versus y and b versus x, $(q_1, q_2) = (0.5, 1.4)$.	21
Figure 2.15	The phase portraits, Poincaré maps and the bifurcation diagram for the fractional order modified nano Duffing resonator system, x versus y and b versus x, $(q_1, q_2) = (0.6, 1.3)$.	22
Figure 2.16	The phase portraits, Poincaré maps and the bifurcation diagram for the fractional order modified nano Duffing resonator system, x versus y and b versus x, $(q_1, q_2) = (0.8, 1.1)$.	23
Figure 2.17	The phase portraits, Poincaré maps and the bifurcation diagram for the fractional order modified nano Duffing resonator system, x versus y and b versus x, $(q_1, q_2) = (1.9, 0.1)$.	24
Figure 2.18	The phase portraits, Poincaré maps and the bifurcation diagram for the fractional order modified nano Duffing resonator system, x versus y and b versus x, $(q_1, q_2) = (1.8, 0.2)$.	25
Figure 2.19	The phase portraits, Poincaré maps and the bifurcation diagram for the fractional order modified nano Duffing resonator system, x versus y and b versus x, $(q_1, q_2) = (1.2, 0.8)$.	26
Figure 2.20	The phase portraits, Poincaré maps and the bifurcation diagram for the fractional order modified nano Duffing resonator system, x versus y and b versus x, $(q_1, q_2) = (1.1, 0.9)$.	27

Figure 2.21	The phase portraits, Poincaré maps and the bifurcation diagram for the fractional order modified nano Duffing resonator system, x versus y and b versus x, $(q_1, q_2) = (0.2, 1.8)$.	28
Figure 2.22	The phase portraits, Poincaré maps and the bifurcation diagram for the fractional order modified nano Duffing resonator system, x versus y and b versus x, $(q_1, q_2) = (0.8, 1.2)$.	29
Figure 2.23	The phase portraits, Poincaré maps and the bifurcation diagram for the fractional order modified nano Duffing resonator system, x versus y and b versus x, $(q_1, q_2) = (0.9, 1.1)$.	30
Figure 2.24	The phase portraits, Poincaré maps and the bifurcation diagram for the fractional order modified nano Duffing resonator system, x versus y and b versus x, $(q_1, q_2) = (1.2, 0.9)$.	31
Figure 2.25	The phase portraits, Poincaré maps and the bifurcation diagram for the fractional order modified nano Duffing resonator system, x versus y and b versus x, $(q_1, q_2) = (0.2, 1.9)$.	32
Figure 2.26	The phase portraits, Poincaré maps and the bifurcation diagram for the fractional order modified nano Duffing resonator system, x versus y and b versus x, $(q_1, q_2) = (0.9, 1.2)$.	33
Figure 3.1	The phase portrait and Poincaré map of the synchronized fractional order modified nano Duffing resonator systems (11) and (12) with order $q_1 = q_2 = 0.9$ for Case 1.	37
Figure 3.2	The time histories of the errors of the states of the synchronized fractional order modified nano Duffing resonator systems (11) and (12) with order $q_1 = q_2 = 0.9$ for Case 1.	37
Figure 3.3	The phase portrait and Poincaré map of the synchronized fractional order modified nano Duffing resonator systems (11) and (12) with order $q_1 = q_2 = 0.1$ for Case 1.	38
Figure 3.4	The time histories of the errors of the states of the synchronized fractional order modified nano Duffing resonator	38

systems (11) and (12) with order $q_1 = q_2 = 0.1$ for Case 1.

- Figure 3.5 **The phase portrait and Poincaré map of the synchronized fractional order modified nano Duffing resonator systems (11) and (12) with order $q_1 = q_2 = 0.9$ for Case 2.** 39
- Figure 3.6 **The time histories of the errors of the states of the synchronized fractional order modified nano Duffing resonator systems (11) and (12) with order $q_1 = q_2 = 0.9$ for Case 2.** 39
- Figure 3.7 **The phase portrait and Poincaré map of the synchronized fractional order modified nano Duffing resonator systems (11) and (12) with order $q_1 = q_2 = 0.1$ for Case 2.** 40
- Figure 3.8 **The time histories of the errors of the states of the synchronized fractional order modified nano Duffing resonator systems (11) and (12) with order $q_1 = q_2 = 0.1$ for Case 2.** 40
- Figure 3.9 **The phase portrait and Poincaré map of the synchronized fractional order modified nano Duffing resonator systems (11) and (12) with order $q_1 = q_2 = 0.9$ for Case 3.** 41
- Figure 3.10 **The time histories of the errors of the states of the synchronized fractional order modified nano Duffing resonator systems (11) and (12) with order $q_1 = q_2 = 0.9$ for Case 3.** 41
- Figure 3.11 **The phase portrait and Poincaré map of the synchronized fractional order modified nano Duffing resonator systems (11) and (12) with order $q_1 = q_2 = 0.1$ for Case 3.** 42
- Figure 3.12 **The time histories of the errors of the states of the synchronized fractional order modified nano Duffing resonator systems (11) and (12) with order $q_1 = q_2 = 0.1$ for Case 3.** 42
- Figure 3.13 **The phase portrait and Poincaré map of the synchronized fractional order modified nano Duffing resonator systems (11) and (12) with order $q_1 = q_2 = 0.9$ for Case 4.** 43

Figure 3.14	The time histories of the errors of the states of the synchronized fractional order modified nano Duffing resonator systems (11) and (12) with order $q_1 = q_2 = 0.9$ for Case 4.	43
Figure 3.15	The phase portrait and Poincaré map of the synchronized fractional order modified nano Duffing resonator systems (11) and (12) with order $q_1 = q_2 = 0.1$ for Case 4.	44
Figure 3.16	The time histories of the errors of the states of the synchronized fractional order modified nano Duffing resonator systems (11) and (12) with order $q_1 = q_2 = 0.1$ for Case 4.	44
Figure 3.17	The phase portrait and Poincaré map of the synchronized fractional order modified nano Duffing resonator systems (11) and (12) with order $q_1 = q_2 = 0.9$ for Case 5.	45
Figure 3.18	The time histories of the errors of the states of the synchronized fractional order modified nano Duffing resonator systems (11) and (12) with order $q_1 = q_2 = 0.9$ for Case 5.	45
Figure 3.19	The phase portrait and Poincaré map of the synchronized fractional order modified nano Duffing resonator systems (11) and (12) with order $q_1 = q_2 = 0.1$ for Case 5.	46
Figure 3.20	The time histories of the errors of the states of the synchronized fractional order modified nano Duffing resonator systems (11) and (12) with order $q_1 = q_2 = 0.1$ for Case 5.	46
Figure 4.1	The phase portraits and Poincaré maps of the fractional order modified nano Duffing resonator systems (11) without control term.	50
Figure 4.2	The phase portraits and Poincaré maps of the fractional order modified nano Duffing resonator systems (11) with control term $k_1 x_1$, where $k_1 = 10$.	51
Figure 4.3	The phase portraits and Poincaré maps of the fractional order modified nano Duffing resonator systems (11) with control term	52

$k_1 x_1$, where $k_1 = -10$.

Figure 4.4 **The phase portraits and Poincaré maps of the fractional order modified nano Duffing resonator systems (11) with control term $k_2 x_1$, where $k_2 = 10$.** 53

Figure 4.5 **The phase portraits and Poincaré maps of the fractional order modified nano Duffing resonator systems (11) with control term $k_2 x_1$, where $k_2 = -10$.** 54

Figure 4.6 **The phase portraits and Poincaré maps of the fractional order modified nano Duffing resonator systems (11) with control term $k_3 \sin x_1$, where $k_3 = 10$.** 55

Figure 4.7 **The phase portraits and Poincaré maps of the fractional order modified nano Duffing resonator systems (11) with control term $k_3 \sin x_1$, where $k_3 = -10$.** 56

Figure 4.8 **The phase portraits and Poincaré maps of the fractional order modified nano Duffing resonator systems (11) with control term $k_4 \sin x_1$, where $k_4 = 10$.** 57

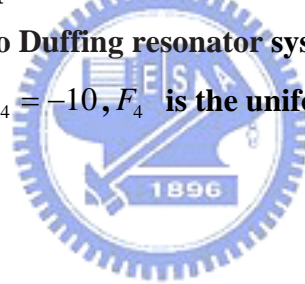
Figure 4.9 **The phase portraits and Poincaré maps of the fractional order modified nano Duffing resonator systems (11) with control term $k_4 \sin x_1$, where $k_4 = -10$.** 58

Figure 5.1 **The phase portraits and Poincaré maps of the fractional order modified nano Duffing resonator systems (11) with control term $k_1 F_1$, where $k_1 = 10$, F_1 is the white noise.** 63

Figure 5.2 **The phase portraits and Poincaré maps of the fractional order modified nano Duffing resonator systems (11) with control term $k_1 F_1$, where $k_1 = -10$, F_1 is the white noise.** 64

Figure 5.3 **The phase portraits and Poincaré maps of the fractional order modified nano Duffing resonator systems (11) with control term $k_2 F_2$, where $k_2 = 10$, F_2 is Rayleigh noise.** 65

Figure 5.4	The phase portraits and Poincaré maps of the fractional order modified nano Duffing resonator systems (11) with control term $k_2 F_2$, where $k_2 = -10$, F_2 is Rayleigh noise.	66
Figure 5.5	The phase portraits and Poincaré maps of the fractional order modified nano Duffing resonator systems (11) with control term $k_3 F_3$, where $k_3 = 10$, F_3 is Rician noise.	67
Figure 5.6	The phase portraits and Poincaré maps of the fractional order modified nano Duffing resonator systems (11) with control term $k_3 F_3$, where $k_3 = -10$, F_3 is Rician noise.	68
Figure 5.7	The phase portraits and Poincaré maps of the fractional order modified nano Duffing resonator systems (11) with control term $k_4 F_4$, where $k_4 = 10$, F_4 is the uniform noise.	69
Figure 5.8	The phase portraits and Poincaré maps of the fractional order modified nano Duffing resonator systems (11) with control term $k_4 F_4$, where $k_4 = -10$, F_4 is the uniform noise.	70



Chapter 1

Introduction

Fractional calculus is a 300-year-old mathematical topic [1-4]. Although it has a long history, the applications of fractional calculus to physics and engineering are just a recent focus of interest. Many systems are known to display fractional order dynamics, such as viscoelastic systems, dielectric polarization [5], electrode electrolyte polarization [6], and electromagnetic waves [7]. More recently, many investigations are devoted to the control [8-12] and dynamics [13-26] of fractional order dynamical systems. In [13], it is shown that the fractional order Chua's circuit of order as low as 2.7 can produce a chaotic attractor. In [14], it is shown that nonautonomous Duffing systems of order less than 2 can still behave in a chaotic manner. In [15], chaotic behaviors of the fractional order "jerk" model is studied, in which chaotic attractor can be obtained with the system order as low as 2.1, and in [16] chaos control of this fractional order chaotic system is investigated. In [17], the fractional order Wien bridge oscillator is studied, where it is shown that limit cycle can be generated for any fractional order, with a proper value of the amplifier gain.

Since the pioneering work by Pecora and Carroll [28], various effective methods for chaos synchronization have been reported [29-63]. However, most of synchronizations can only be realized under the hypotheses that there exists coupling between two chaotic systems. In practice, such as in physical and electrical systems, sometimes it is difficult even impossible to couple two chaotic systems. In comparison with coupled chaotic systems, for synchronization between the uncoupled chaotic systems, there are many advantages [35, 36]. In this thesis, synchronization of two fractional nano Duffing resonator systems whose corresponding parameters are excited by a chaotic signal of a third system is studied.

For continuous time systems, how to design a simple controller that can drive the system from nonchaotic to chaotic, and how to prove that such a controlled system is indeed chaotic in a rigorous mathematical sense, are important and challenging problems for study [64-72].

From [73], we can get the integral order nano Duffing resonator system. One way to

study fractional order systems is through linear approximations. By utilizing frequency domain techniques based on Bode diagrams, one can obtain a linear approximation for the fractional order integrator, the order of which depends on the desired bandwidth and the discrepancy between the actual and the approximate magnitude Bode diagrams. This approach is applied to study the behaviors of the fractional order modified nano Duffing resonator equations in this thesis. We use the approximate linear transfer functions for the fractional integrator of order that varies from 0.1 to 0.9, and study the resulting behavior of the entire system for each case under the effect of different types of nonlinearities. Chaotic behaviors in the fractional order modified nano Duffing resonator equations are studied by phase portraits, Poincaré maps and bifurcation diagrams. It is found that the total system orders for chaos to exist in such systems are 1.8, 1.9, 2.0 and 2.1.

The chaos synchronizations of two uncoupled fractional order modified nano Duffing resonator systems are obtained by replacing their corresponding parameters by the same function of chaotic state variables of a third chaotic system. The method is named parameter excited chaos synchronization which can be successfully obtained for very low total fractional order 0.2. Numerical simulations are illustrated by phase portraits, Poincaré maps and state error plots.

Anti-control of chaos of a fractional order modified nano Duffing resonator system is studied. By using the functions of state variable of a second identical system as the added term, the anti-control of chaos can be obtained. By using the white noise, Rayleigh noise, Rician noise and uniform noise as the added term respectively, the anti-control of chaos can be obtained. Anti-control of chaos can be successfully obtained for very low total fractional order 0.2. Numerical simulations are illustrated by phase portraits and Poincaré maps.

This thesis is organized as follows. Chapter 2 gives the dynamic equation of modified nano Duffing resonator system. The fractional derivative and its approximation are introduced. The system under study is described both in its integer and fractional forms. Numerical simulation results are presented.

In Chapter 3, numerical simulations of synchronization scheme based on driving the corresponding parameters of two chaotic systems by a chaotic signal of a third system are presented.

In Chapter 4, numerical simulations of anti-control scheme based on adding the function of state variables of a second system are presented. In Chapter 5, numerical simulations of anti-control scheme based on adding the white noise, Rayleigh noise, Rician noise and uniform noise as the external term respectively are presented. In Chapter 6, conclusions are drawn.



Chapter 2

Chaos in a Fractional Order Modified Nano Duffing Resonator System

In this chapter, the dynamic equation of modified nano Duffing resonator system is given. The fractional derivative and its approximation are introduced. The system under study is described both in its integer and fractional forms. Numerical simulation results are presented.

2.1 Fractional Derivative and Its Approximation

Two commonly used definitions for the general fractional differintegral are the Grunwald definition and the Riemann-Liouville definition. The Riemann-Liouville definition of the fractional integral is given here as [27]

$$\frac{d^q f(t)}{dt^q} = \frac{1}{\Gamma(-q)} \int_0^t \frac{f(\tau)}{(t-\tau)^{q+1}} d\tau, q < 0 \quad (2.1)$$

where q can have noninteger values, and thus the name fractional differintegral. Notice that the definition is based on integration and more importantly is a convolution integral for $q < 0$. When $q > 0$, then the usual integer n th derivative must be taken of the fractional $(q-n)$ th integral, and yields the fractional derivative of order q as

$$\frac{d^q f}{dt^q} = \frac{d^n}{dt^n} \left[\frac{d^{q-n} f}{dt^{q-n}} \right], \quad q > 0 \text{ and } n \text{ an integer} > q \quad (2.2)$$

This appears so vastly different from the usual intuitive definition of derivative and integral that the reader must abandon the familiar concepts of slope and area and attempt to get some new insight. Fortunately, the basic engineering tool for analyzing linear systems, the Laplace transform, is still applicable and works as one would expect; that is,

$$L \left\{ \frac{d^q f(t)}{dt^q} \right\} = s^q L \{ f(t) \} - \sum_{k=0}^{n-1} s^k \left[\frac{d^{q-1-k} f(t)}{dt^{q-1-k}} \right]_{t=0}, \text{ for all } q \quad (2.3)$$

where n is an integer such that $n - 1 < q < n$. If the initial conditions are considered to be zero, this formula reduces to the more expected and comforting form

$$L\left\{\frac{d^q f(t)}{dt^q}\right\} = s^q L\{f(t)\} \quad (2.4)$$

An efficient method is to approximate fractional operators by using standard integer order operators. In [27], an effective algorithm is developed to approximate fractional order transfer functions. Basically, the idea is to approximate the system behavior in the frequency domain. By utilizing frequency domain techniques based on Bode diagrams, one can obtain a linear approximation of fractional order integrator, the order of which depends on the desired bandwidth and discrepancy between the actual and the approximate magnitude Bode diagrams. In Table 1 of [13], approximations for $\frac{1}{s^q}$ with $q=0.1\sim 0.9$ in steps 0.1 are given, with errors of approximately 2dB. These approximations are used in following simulations.

2.2 A Fractional Order Modified Nano Duffing Resonator System

The famous Duffing system is

$$\ddot{x} + a\dot{x} + x + x^3 = b \cos \omega t \quad (2.5)$$

where a, b are constant parameters

It can be written as two first order ordinary differential equations:

$$\begin{cases} \frac{dx}{dt} = y \\ \frac{dy}{dt} = -x - x^3 - ay + b \cos \omega t \end{cases} \quad (2.6)$$

Consider the following modified nano Duffing resonator system:

$$\begin{cases} \frac{dx}{dt} = y \\ \frac{dy}{dt} = -x - x^3 - ay + bz \\ \frac{dz}{dt} = w \\ \frac{dw}{dt} = -cz - dz^3 \end{cases} \quad (2.7)$$

It becomes an autonomous system with four states where $a, b, c,$ and d are constant parameters of the system. System (2.7) can divide into two parts:

$$\begin{cases} \frac{dx}{dt} = y \\ \frac{dy}{dt} = -x - x^3 - ay + bz \end{cases} \quad (2.8)$$

and

$$\begin{cases} \frac{dz}{dt} = w \\ \frac{dw}{dt} = -cz - dz^3 \end{cases} \quad (2.9)$$

As a nonlinear oscillator, system (2.9) provides the periodic time function bz to system (2.8) as an excitation which produces the chaos in system (2.8). To sum up, system (2.8) can be considered as a nonautonomous system with two states x, y with bz as an excitation which is a given periodic function of time, while system (2.8) and system (2.9) together can be considered as an autonomous system with four states x, y, z, w . We focus on system (2.8), while system (2.9) remains an integral order system.

Now, consider a fractional order modified nano Duffing resonator system. Here, the conventional derivatives in Eq.(2.8) are replaced by the fractional derivatives as follows:

$$\begin{cases} \frac{d^{q_1} x}{dt^{q_1}} = y \\ \frac{d^{q_2} y}{dt^{q_2}} = -x - x^3 - ay + bz \\ \frac{dz}{dt} = w \\ \frac{dw}{dt} = -cz - dz^3 \end{cases} \quad (2.10)$$

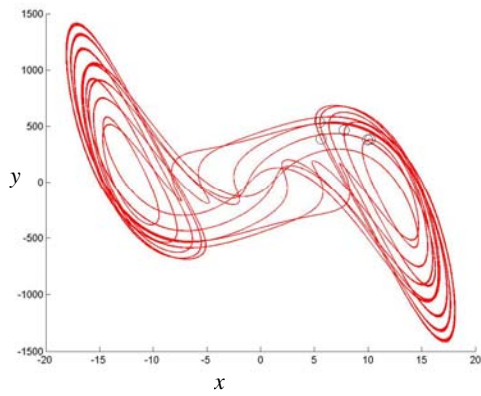
where system parameter b is allowed to be varied, and q_1, q_2 are two fractional order numbers. Simulations are then performed using $q_i (i=1,2)$ varied from 0.1~0.9, respectively. The approximations from Table 1 of [13] are used for the simulations of the appropriate q_i th integrals. When $q_i < 1$, then the approximations are used directly. It should further be noted that approximations used in the simulations for $\frac{1}{s^{q_i}}$, when $q_i > 1$, are obtained by using $1/s$ times the approximation for $\frac{1}{s^{q_i-1}}$ from Table 1 (See

Appendix).

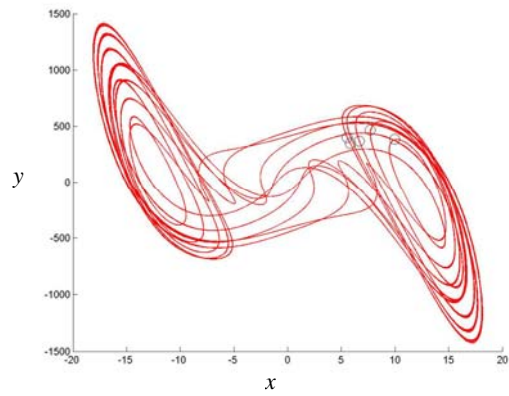
2.3 Simulation Results

In this section, all numerical simulations are run by block diagrams in Simulink environment, using ode45 solver algorithm, where the fractional integrators have been approximated by linear time invariant transfer functions following the procedure in [13]. In so far as the attractor shape is concerned, both procedures gave very similar results. In numerical simulations, three parameters $a = 0.05$, $c = 1$ and $d = 0.3$ are fixed and b is varied. The initial states of the modified Duffing system are $x(0) = 0$, $y(0) = 0$, $z(0) = 10$ and $w(0) = 10$.

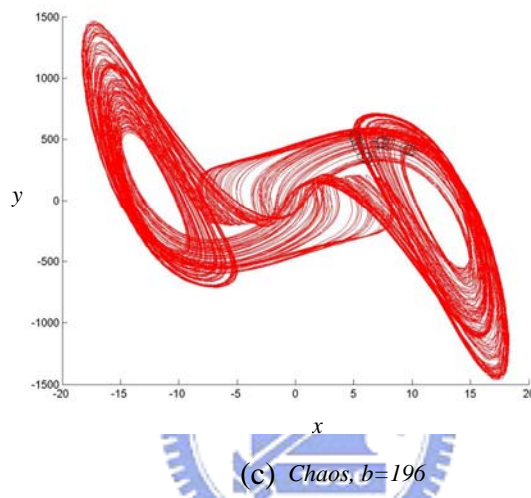
Firstly, when the total order $q_1 + q_2$ is 1.8, chaos is found in the cases: $(q_1, q_2) = (1.5, 0.3)$, $(q_1, q_2) = (1.3, 0.5)$, $(q_1, q_2) = (0.3, 1.5)$, and $(q_1, q_2) = (0.5, 1.3)$. The phase portraits, Poincaré maps and the bifurcation diagrams are showed in Fig.2.1~Fig.2.4. Secondly, when the total order $q_1 + q_2$ is 1.9, chaos is found in the cases: $(q_1, q_2) = (1.8, 0.1)$, $(q_1, q_2) = (1.6, 0.3)$, $(q_1, q_2) = (1.5, 0.4)$, $(q_1, q_2) = (1.4, 0.5)$, $(q_1, q_2) = (1.3, 0.6)$, $(q_1, q_2) = (1.1, 0.8)$, $(q_1, q_2) = (0.1, 1.8)$, $(q_1, q_2) = (0.3, 1.6)$, $(q_1, q_2) = (0.4, 1.5)$, $(q_1, q_2) = (0.5, 1.4)$, $(q_1, q_2) = (0.6, 1.3)$, and $(q_1, q_2) = (0.8, 1.1)$. The phase portraits, Poincaré maps and the bifurcation diagrams are shown in Fig.2.5~Fig.2.16. When the total order $q_1 + q_2$ is 2.0, chaos is found in the cases: $(q_1, q_2) = (1.9, 0.1)$, $(q_1, q_2) = (1.8, 0.2)$, $(q_1, q_2) = (1.2, 0.8)$, $(q_1, q_2) = (1.1, 0.9)$, $(q_1, q_2) = (0.2, 1.8)$, $(q_1, q_2) = (0.8, 1.2)$, and $(q_1, q_2) = (0.9, 1.1)$. The phase portraits, Poincaré maps and the bifurcation diagrams are shown in Fig.2.17~Fig.2.23. Finally, when the total order $q_1 + q_2$ is 2.1, chaos is found in the cases: $(q_1, q_2) = (1.2, 0.9)$, $(q_1, q_2) = (0.2, 1.9)$, and $(q_1, q_2) = (1.2, 0.9)$. The phase portraits, Poincaré maps and the bifurcation diagrams are showed in Fig.2.24~Fig.2.26. It can be seen that when q_1 is larger, the range of y state is also larger.



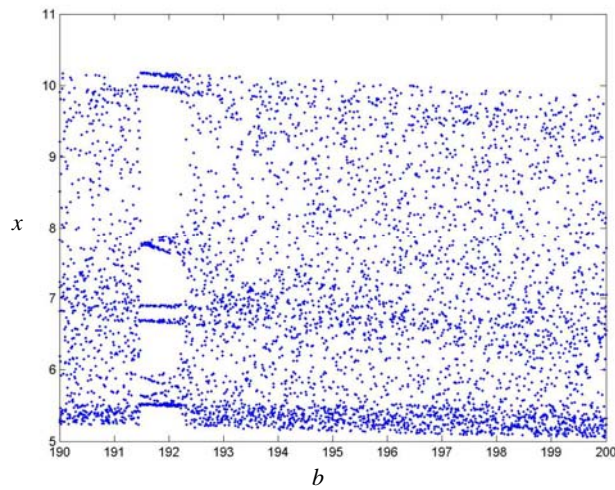
(a) *Period 5, $b=191.6$*



(b) *Period 5, $b=191.8$*

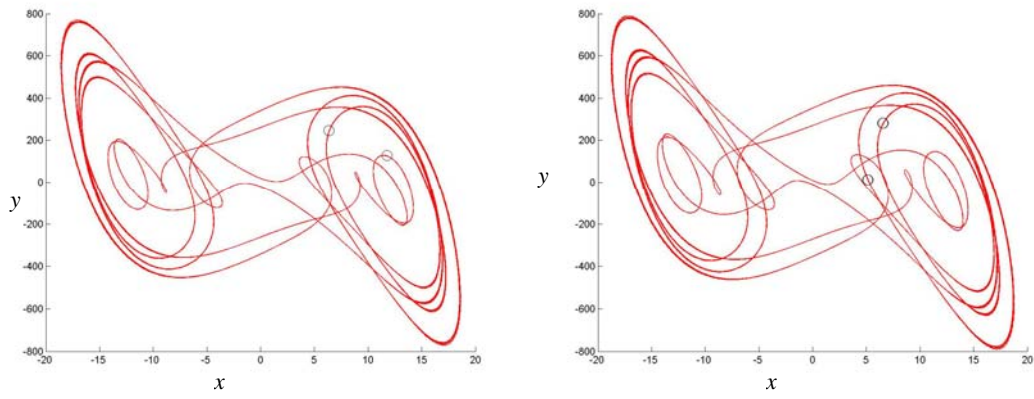


(c) *Chaos, $b=196$*



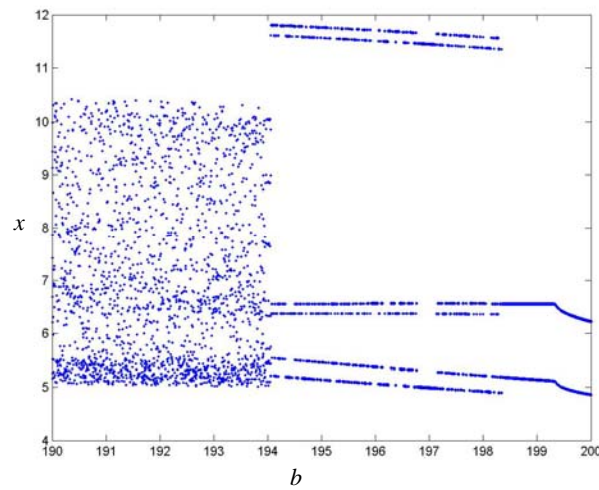
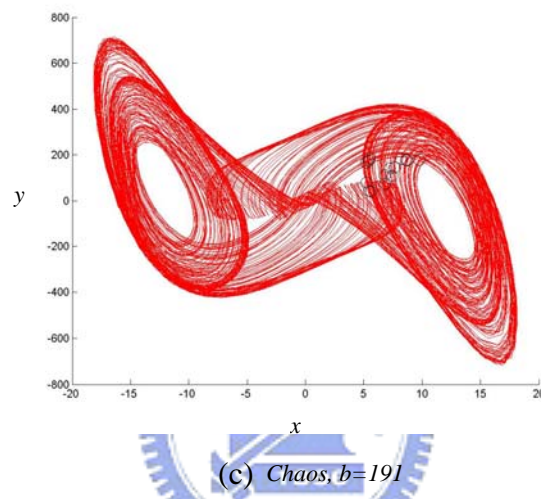
(d)

Fig. 2.1 The phase portraits, Poincaré maps and the bifurcation diagram for the fractional order modified nano Duffing resonator system, x versus y and b versus x , $(q_1, q_2) = (1.5, 0.3)$.



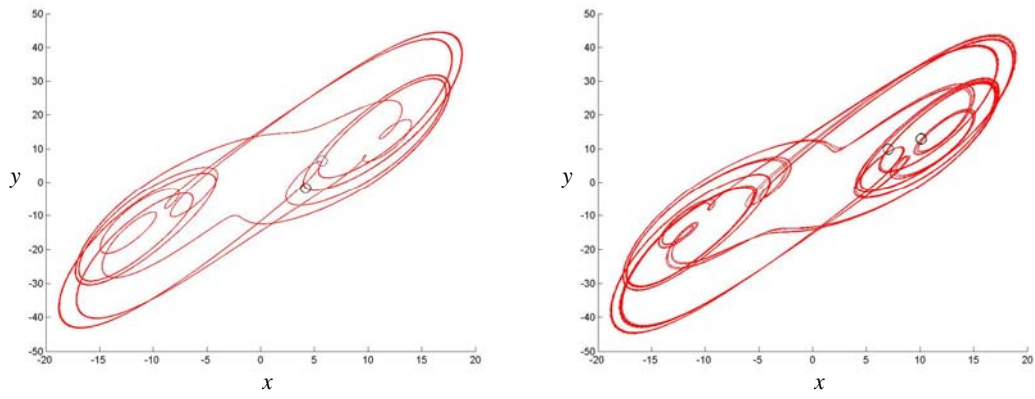
(a) Period 5, $b=195$

(b) Period 5, $b=199$



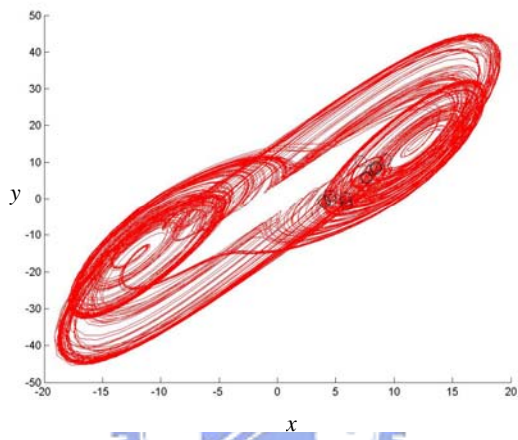
(d)

Fig. 2.2 The phase portraits, Poincaré maps and the bifurcation diagram for the fractional order modified nano Duffing resonator system, x versus y and b versus x , $(q_1, q_2)=(1.3, 0.5)$.

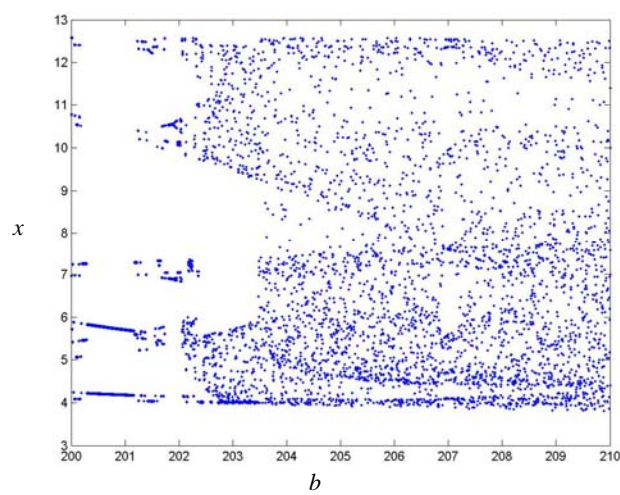


(a) *Period 2, b=201*

(b) *Period 5, b=202*

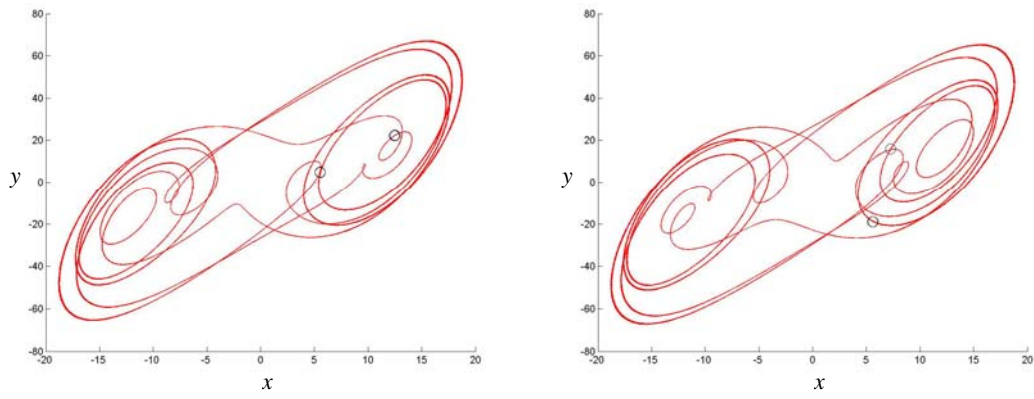


(c) *Chaos, b=206*



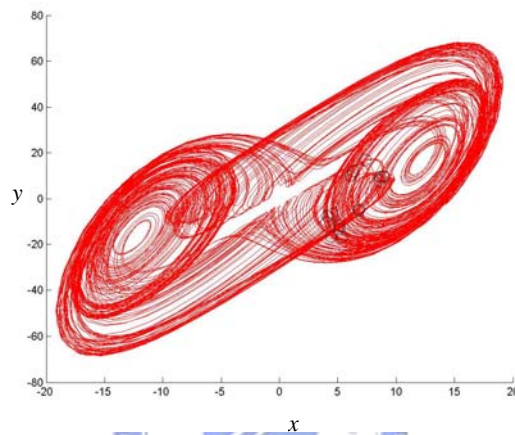
(d)

Fig. 2.3 The phase portraits, Poincaré maps and the bifurcation diagram for the fractional order modified nano Duffing resonator system, x versus y and b versus x , $(q_1, q_2) = (0.3, 1.5)$.

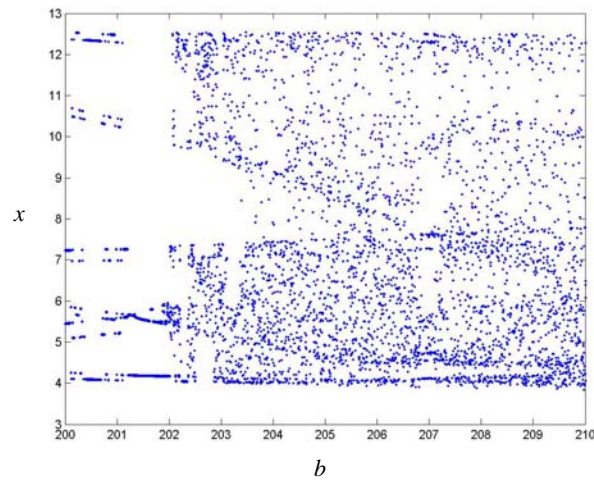


(a) *Period 2, $b=200.9$*

(b) *Period 2, $b=201.2$*

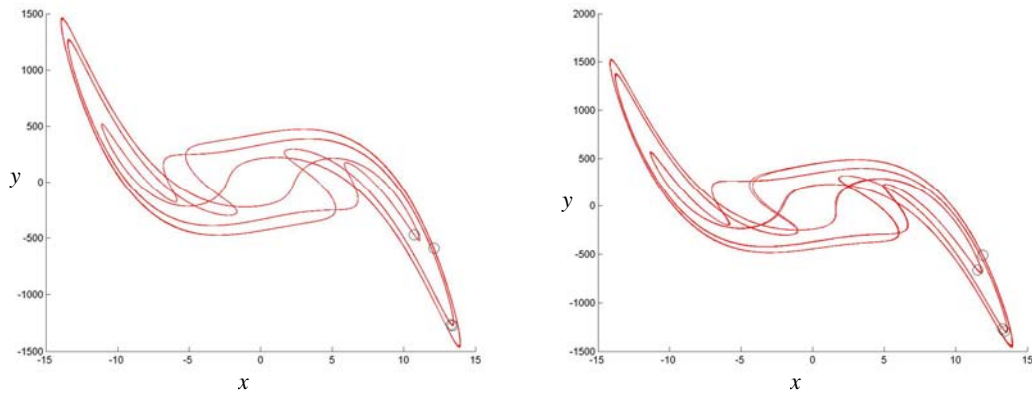


(c) *Chaos, $b=206$*



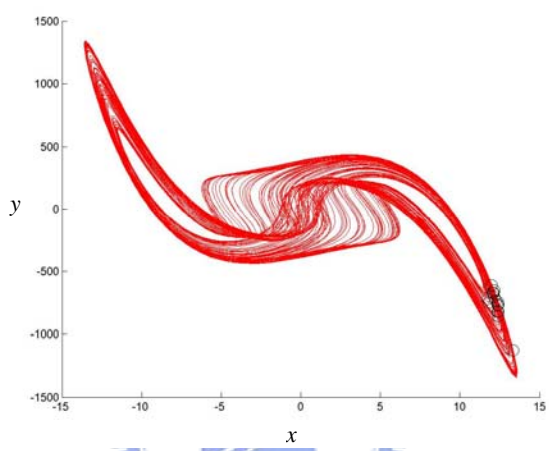
(d)

Fig. 2.4 The phase portraits, Poincaré maps and the bifurcation diagram for the fractional order modified nano Duffing resonator system, x versus y and b versus x , $(q_1, q_2) = (0.5, 1.3)$.

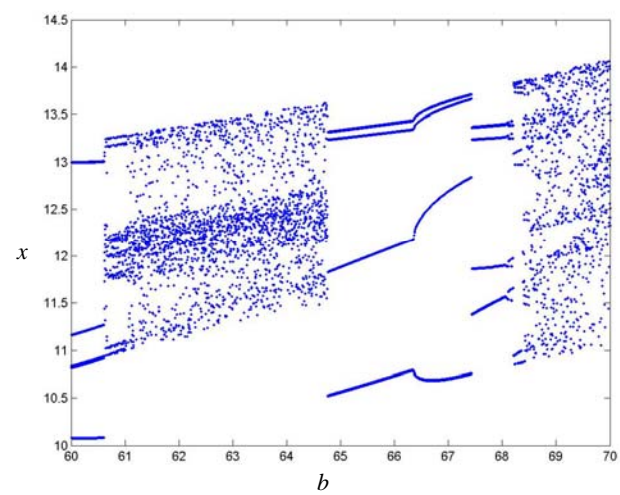


(a) *Period 4, b=66*

(b) *Period 6, b=68.1*

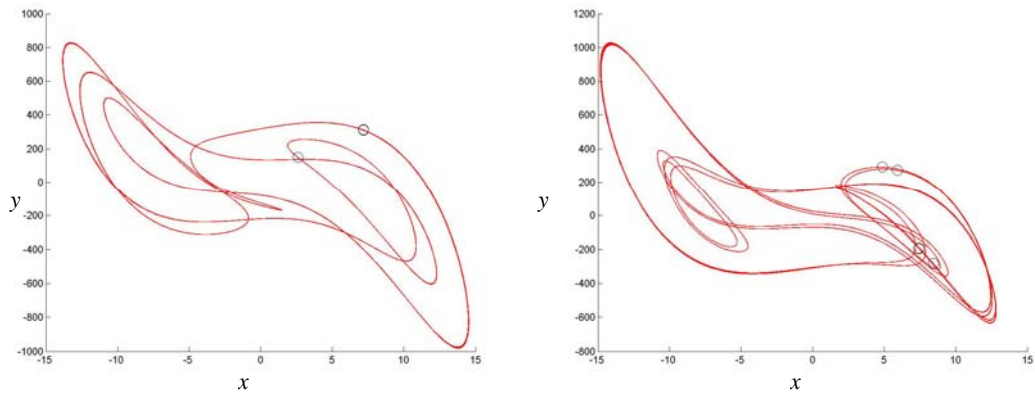


(c) *Chaos, b=63*



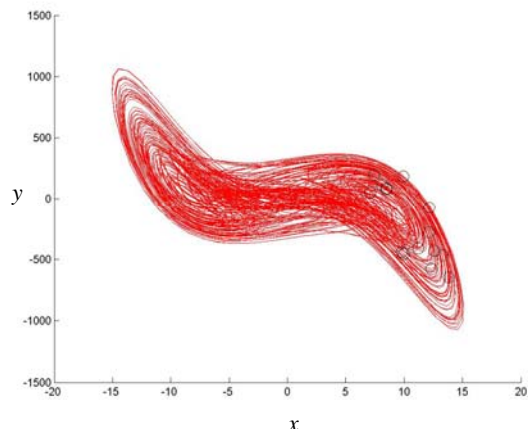
(d)

Fig. 2.5 The phase portraits, Poincaré maps and the bifurcation diagram for the fractional order modified nano Duffing resonator system, x versus y and b versus x , $(q_1, q_2) = (1.8, 0.1)$.

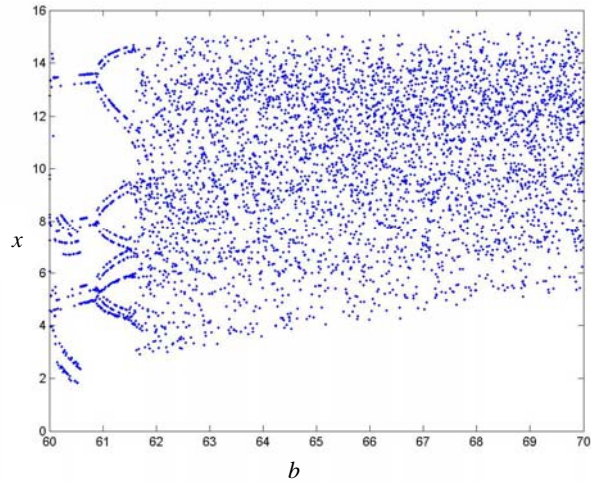


(a) *Period 2, b=60.5*

(b) *Period 4, b=61*

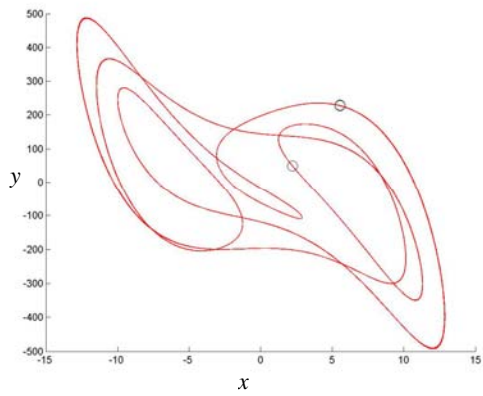


(c) *Chaos, b=65*

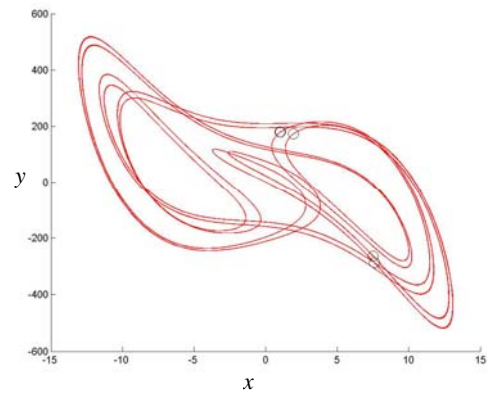


(d)

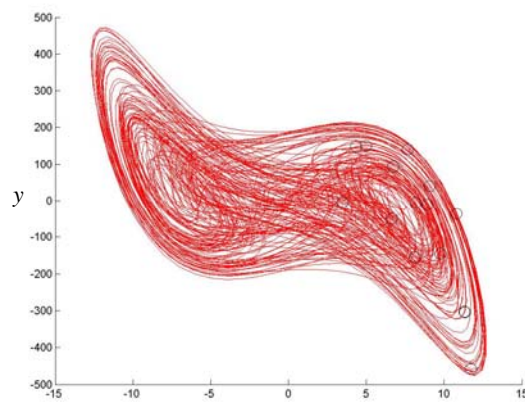
Fig. 2.6 The phase portraits, Poincaré maps and the bifurcation diagram for the fractional order modified nano Duffing resonator system, x versus y and b versus x , $(q_1, q_2) = (1.6, 0.3)$.



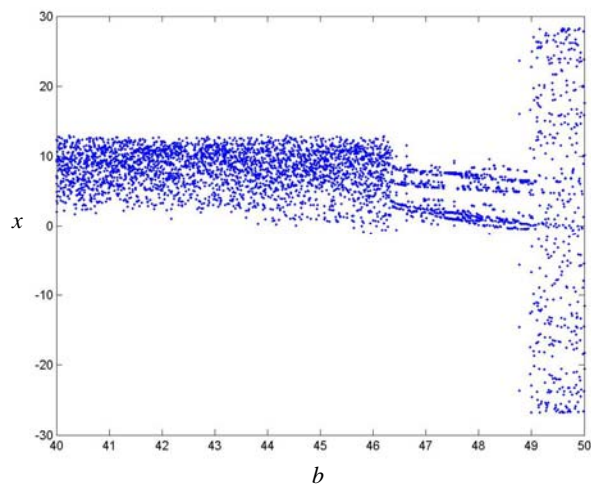
(a) *Period 2, $b=47.1$*



(b) *Period 4, $b=47.5$*

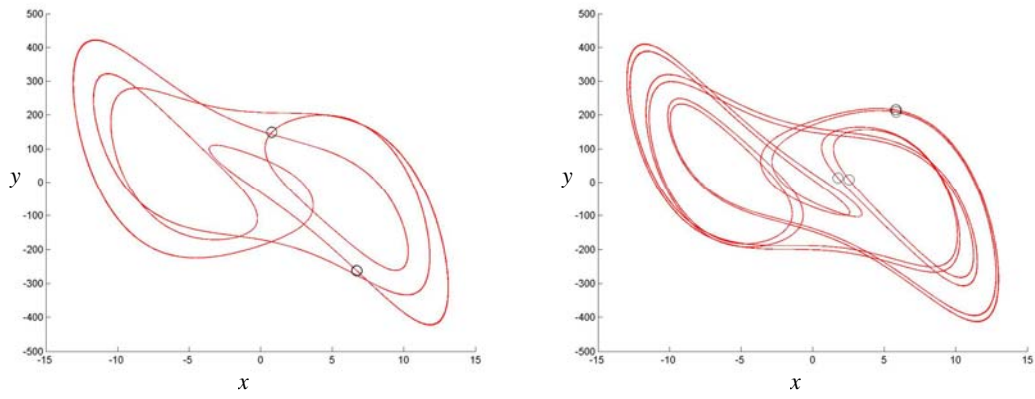


(c) *Chaos, $b=42$*



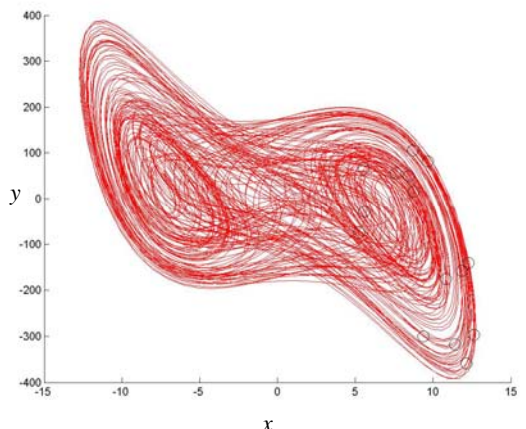
(d)

Fig. 2.7 The phase portraits, Poincaré maps and the bifurcation diagram for the fractional order modified nano Duffing resonator system, x versus y and b versus x , $(q_1, q_2) = (1.5, 0.4)$.

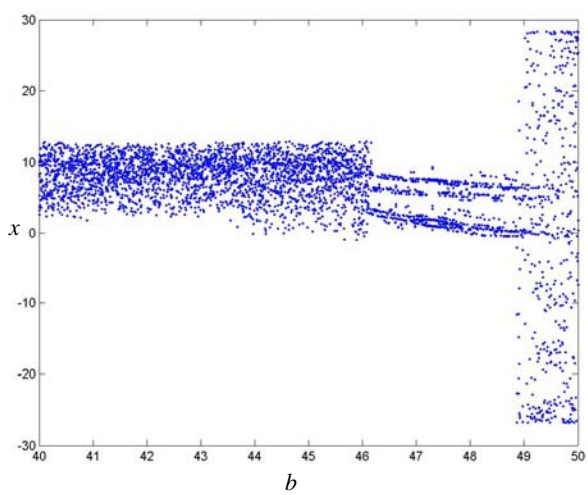


(a) *Period 2, $b=48$*

(b) *Period 4, $b=47.1$*

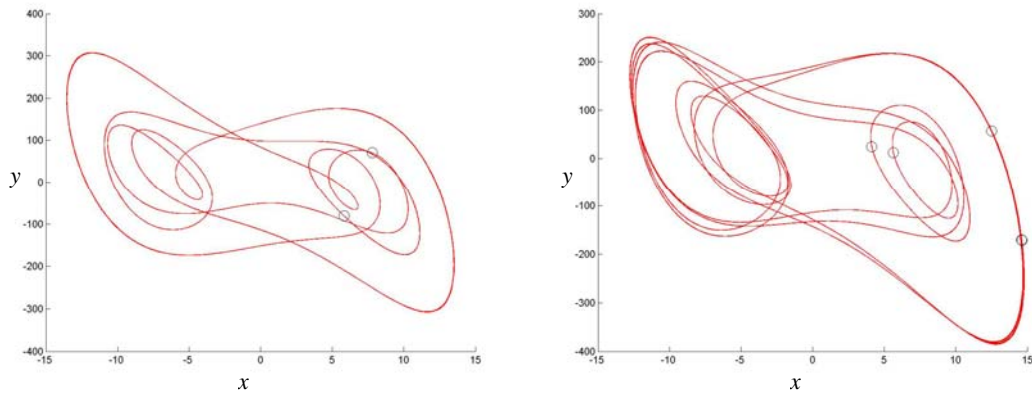


(c) *Chaos, $b=42$*



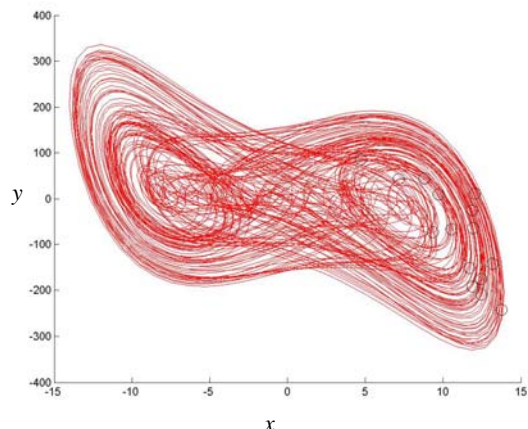
(d)

Fig. 2.8 The phase portraits, Poincaré maps and the bifurcation diagram for the fractional order modified nano Duffing resonator system, x versus y and b versus x , $(q_1, q_2) = (1.4, 0.5)$.

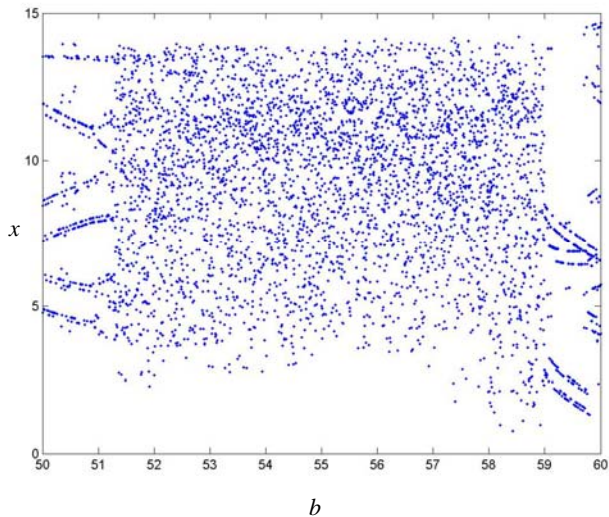


(a) *Period 2, $b=50.5$*

(b) *Period 4, $b=59.9$*

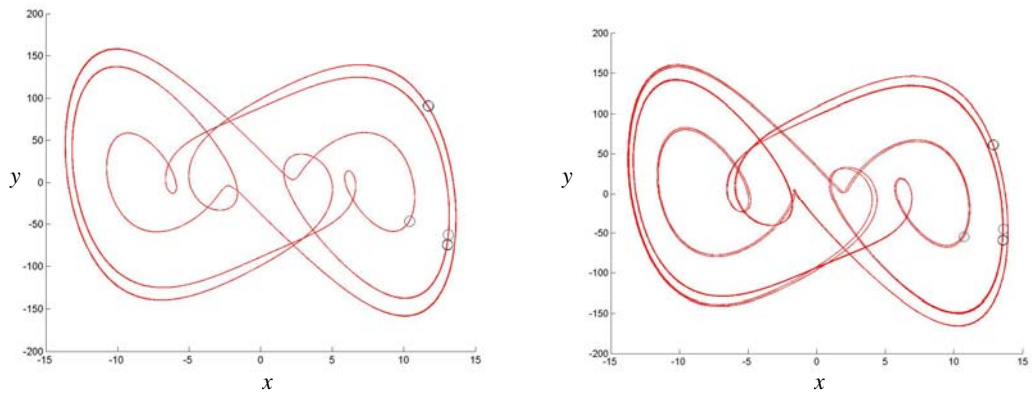


(c) *Chaos, $b=55$*



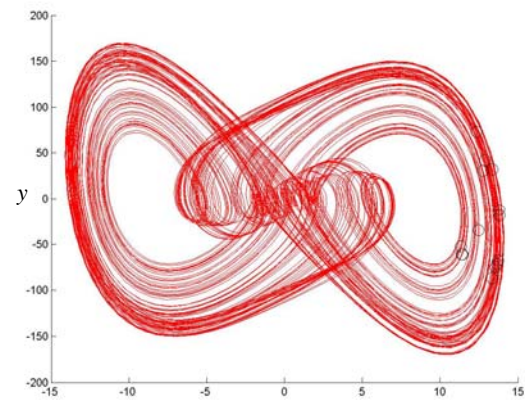
(d)

Fig. 2.9 The phase portraits, Poincaré maps and the bifurcation diagram for the fractional order modified nano Duffing resonator system, x versus y and b versus x , $(q_1, q_2) = (1.3, 0.6)$.

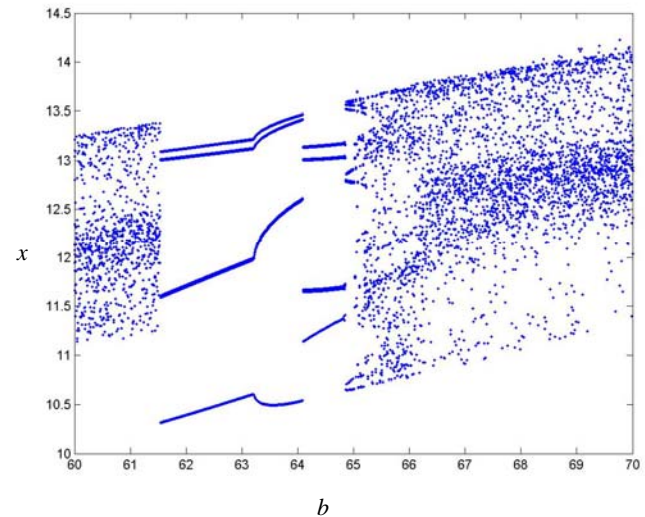


(a) *Period 4, $b=62$*

(b) *Period 5, $b=64.9$*

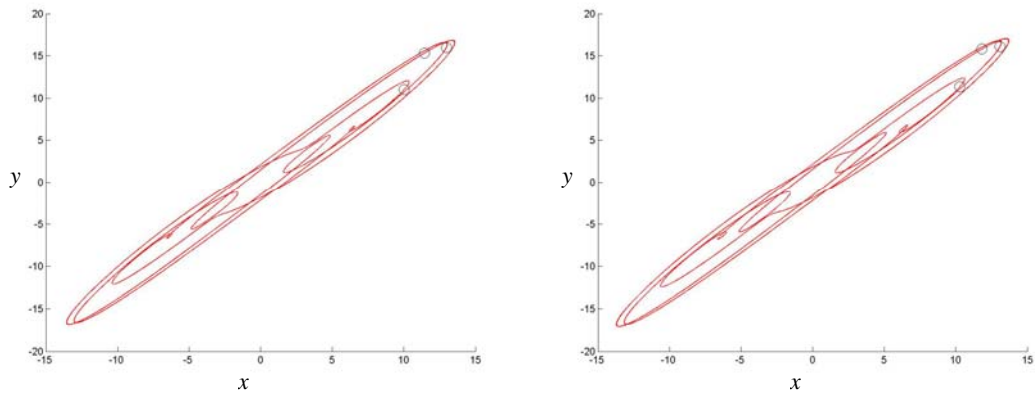


(c) *Chaos, $b=67$*



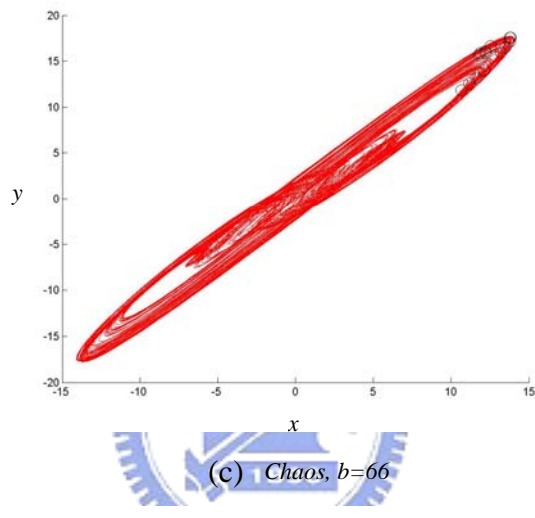
(d)

Fig. 2.10 The phase portraits, Poincaré maps and the bifurcation diagram for the fractional order modified nano Duffing resonator system, x versus y and b versus x , $(q_1, q_2) = (1.1, 0.8)$.

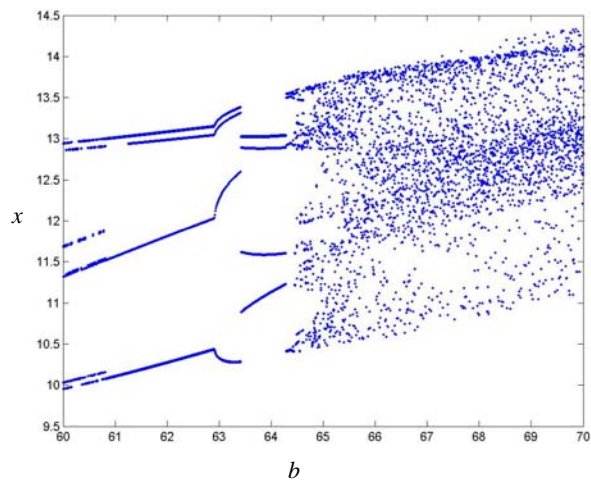


(a) *Period 3, $b=60.5$*

(b) *Period 4, $b=62$*

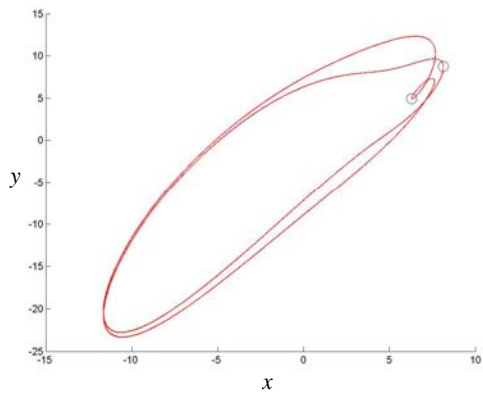


(c) *Chaos, $b=66$*

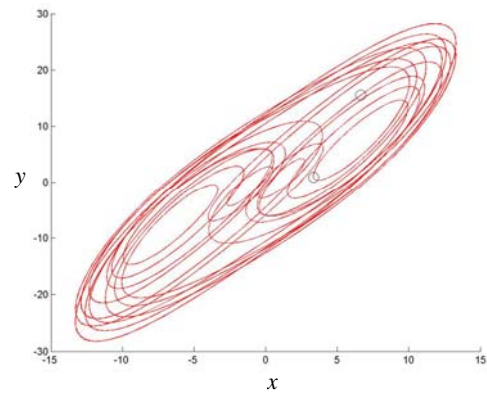


(d)

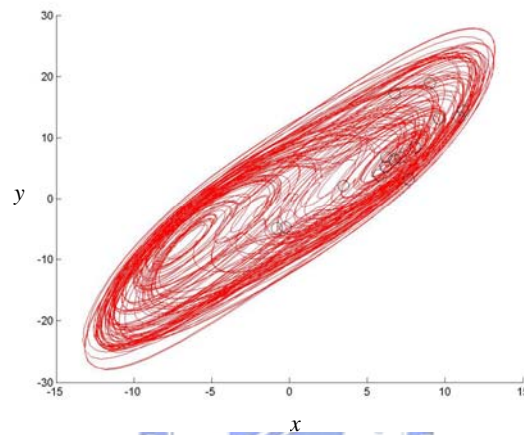
Fig. 2.11 The phase portraits, Poincaré maps and the bifurcation diagram for the fractional order modified nano Duffing resonator system, x versus y and b versus x , $(q_1, q_2) = (0.1, 1.8)$.



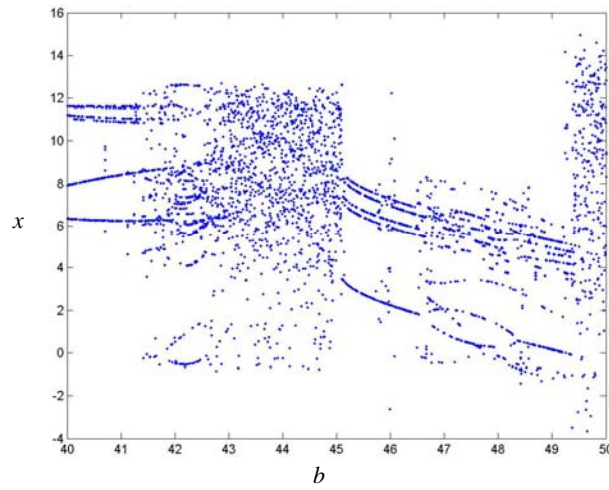
(a) *Period 4, $b=40.4$*



(b) *Period 5, $b=47.2$*

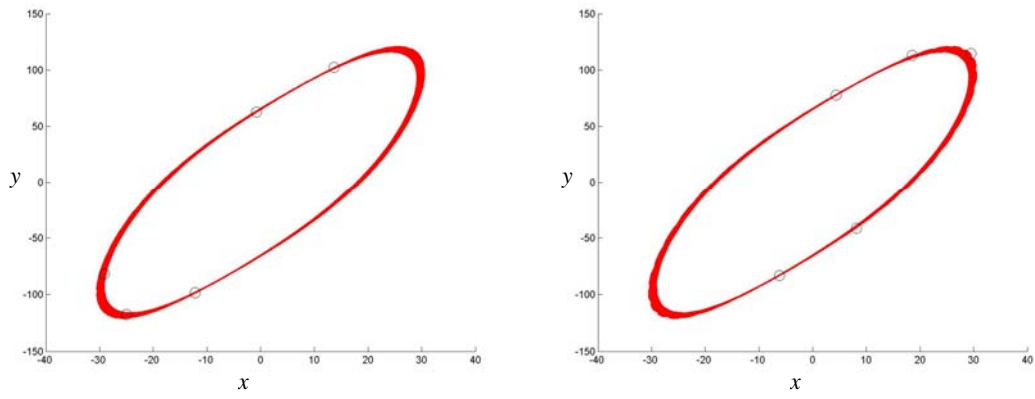


(c) *Chaos, $b=44$*



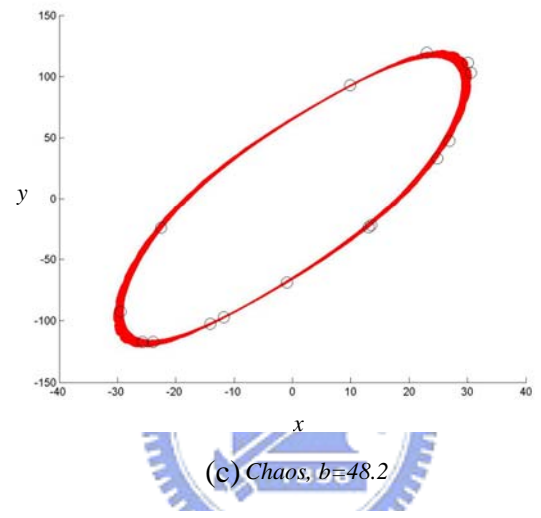
(d)

Fig. 2.12 The phase portraits, Poincaré maps and the bifurcation diagram for the fractional order modified nano Duffing resonator system, x versus y and b versus x , $(q_1, q_2) = (0.3, 1.6)$.

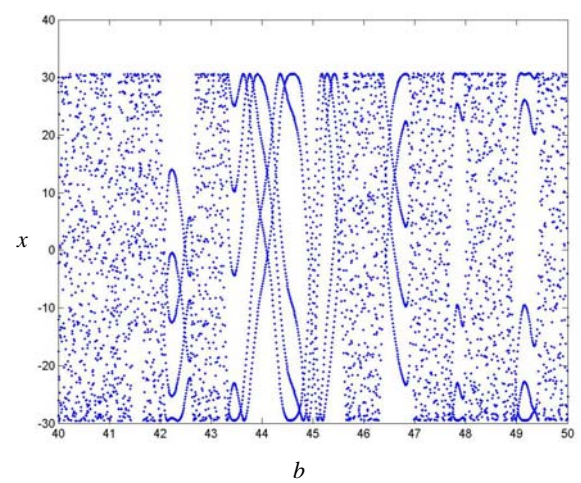


(a) *Period 5, $b=42.2$*

(b) *Period 5, $b=44$*

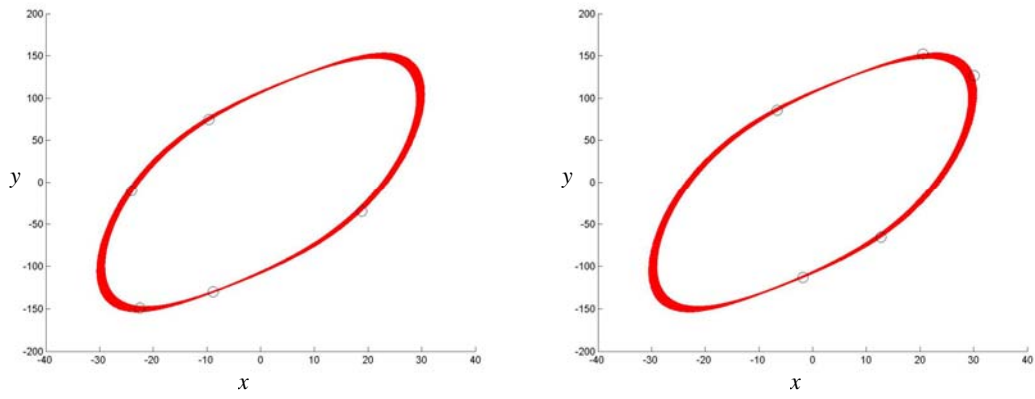


(c) *Chaos, $b=48.2$*



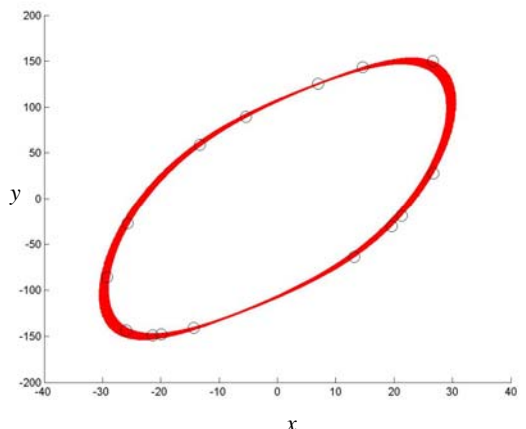
(d)

Fig. 2.13 The phase portraits, Poincaré maps and the bifurcation diagram for the fractional order modified nano Duffing resonator system, x versus y and b versus x , $(q_1, q_2) = (0.4, 1.5)$.

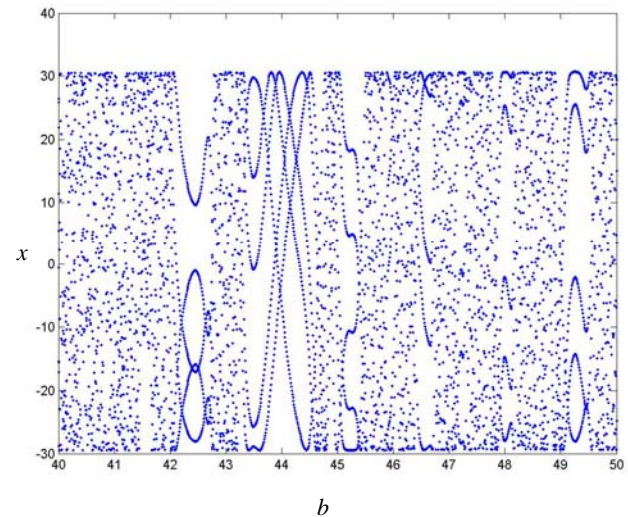


(a) Period 5, $b=42.2$

(b) Period 5, $b=44$

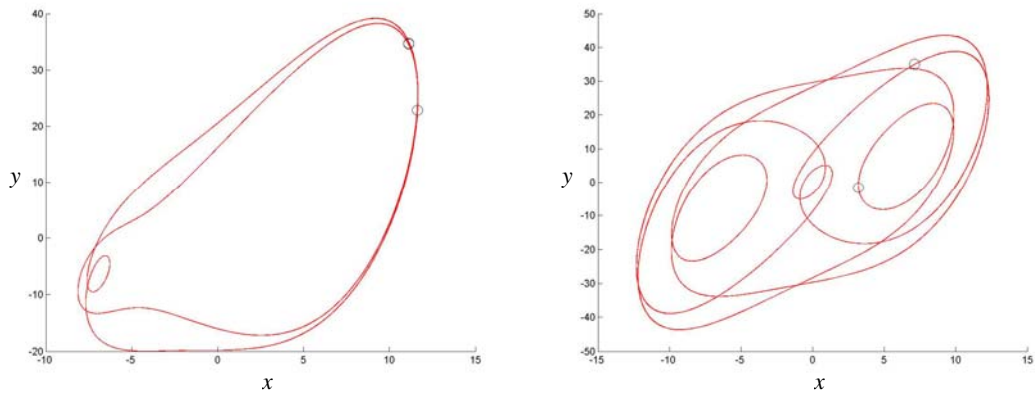


(c) Chaos, $b=45.8$



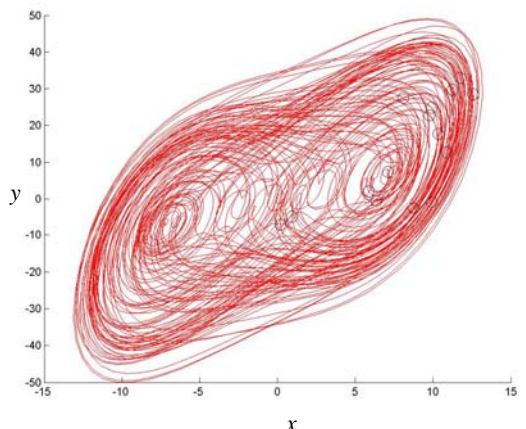
(d)

Fig. 2.14 The phase portraits, Poincaré maps and the bifurcation diagram for the fractional order modified nano Duffing resonator system, x versus y and b versus x , $(q_1, q_2) = (0.5, 1.4)$.

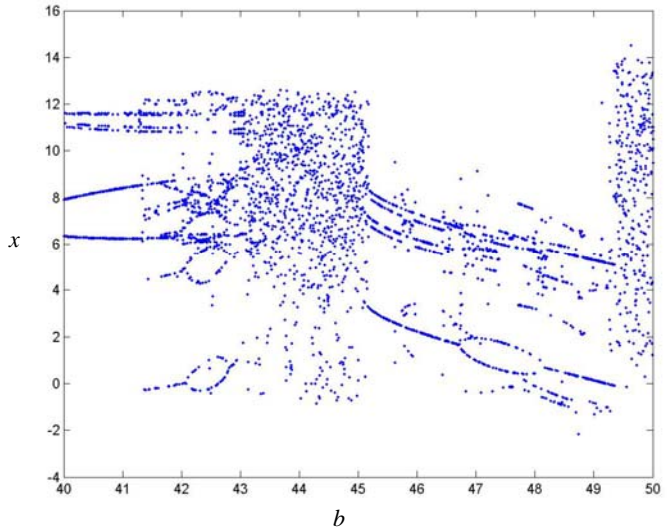


(a) *Period 2, $b=40.4$*

(b) *Period 4, $b=45.2$*

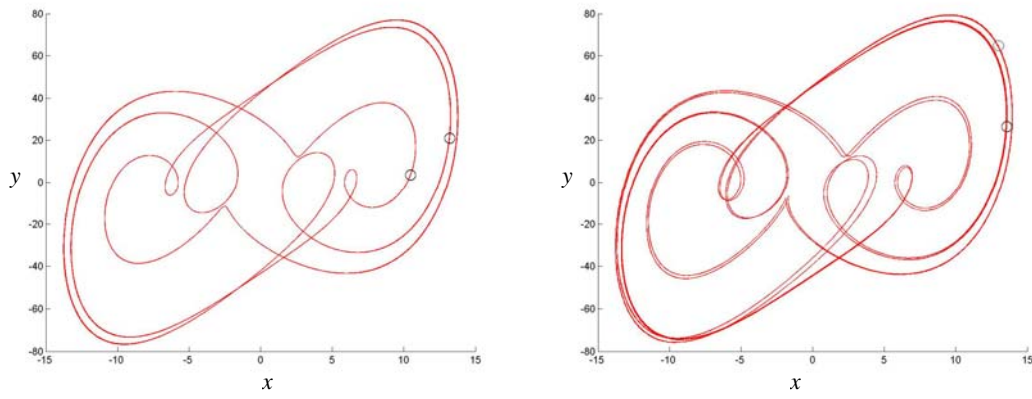


(c) *Chaos, $b=44$*



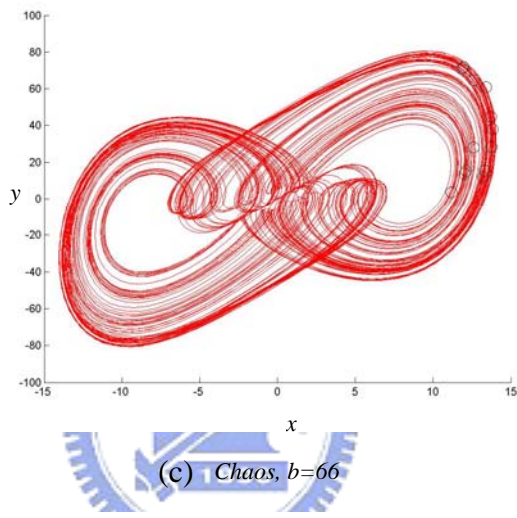
(d)

Fig. 2.15 The phase portraits, Poincaré maps and the bifurcation diagram for the fractional order modified nano Duffing resonator system, x versus y and b versus x , $(q_1, q_2) = (0.6, 1.3)$.

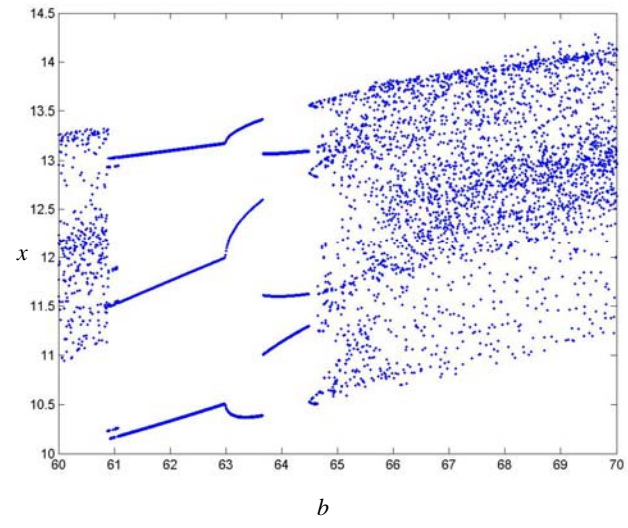


(a) *Period 3, $b=63$*

(b) *Period 4, $b=64.7$*

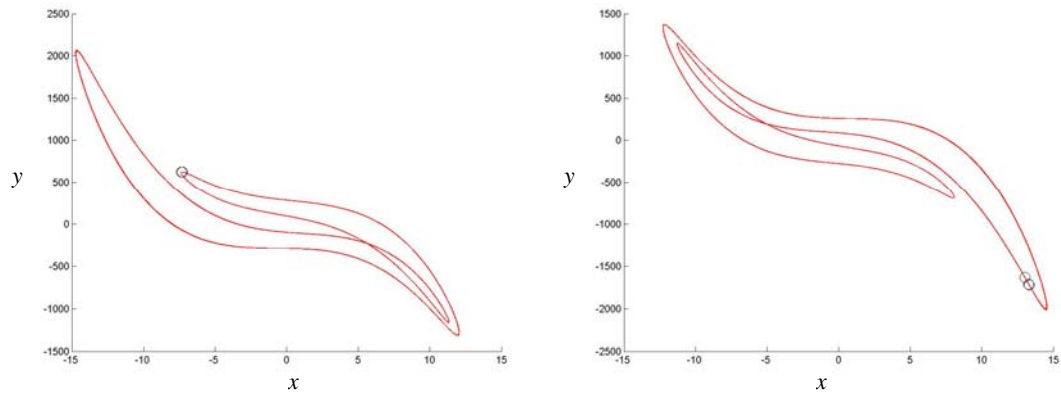


(c) *Chaos, $b=66$*



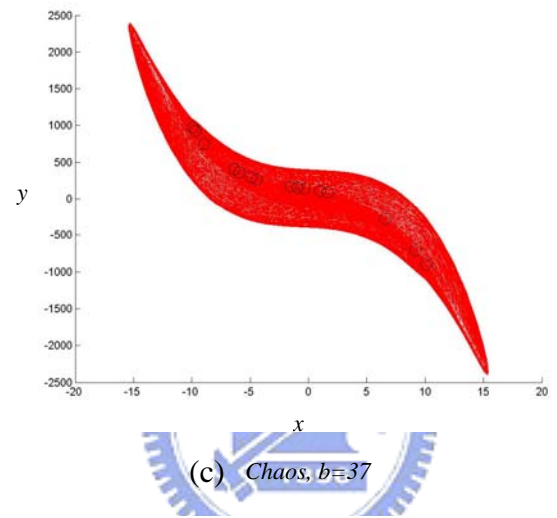
(d)

Fig. 2.16 The phase portraits, Poincaré maps and the bifurcation diagram for the fractional order modified nano Duffing resonator system, x versus y and b versus x , $(q_1, q_2) = (0.8, 1.1)$.

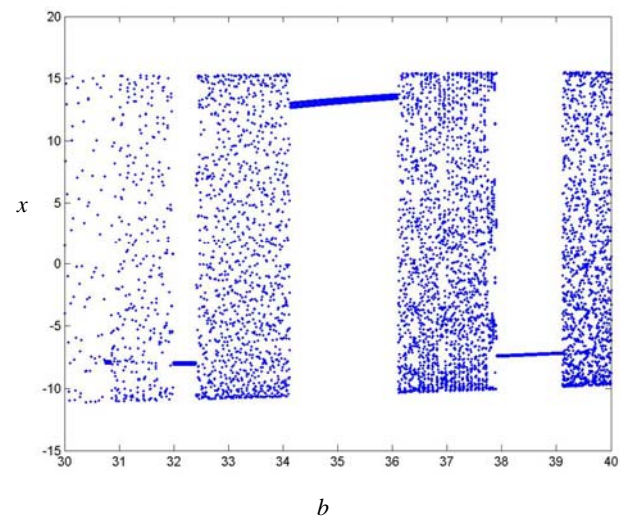


(a) *Period 1, $b=38.5$*

(b) *Period 2, $b=35$*

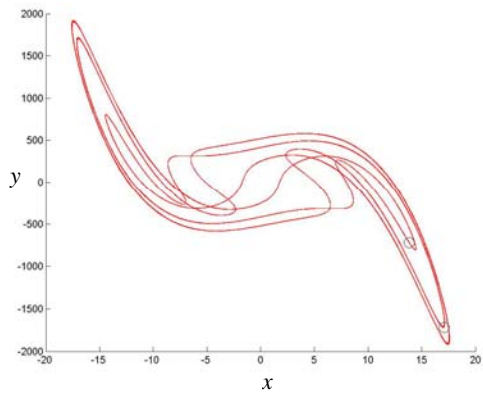


(c) *Chaos, $b=37$*

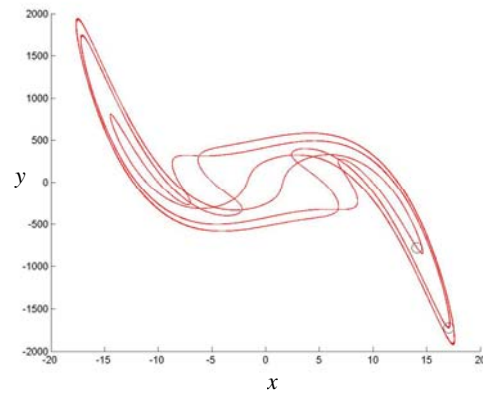


(d)

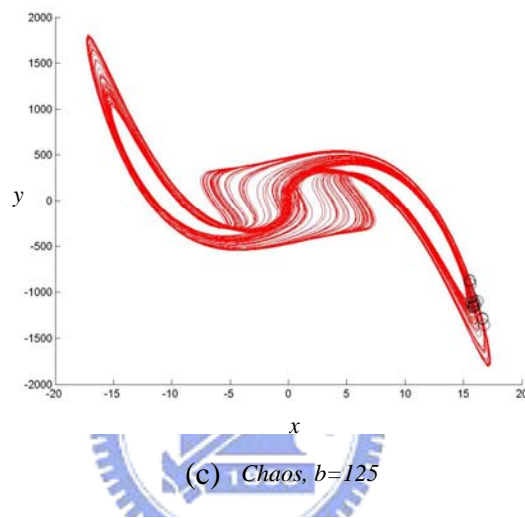
Fig. 2.17 The phase portraits, Poincaré maps and the bifurcation diagram for the fractional order modified nano Duffing resonator system, x versus y and b versus x , $(q_1, q_2) = (1.9, 0.1)$.



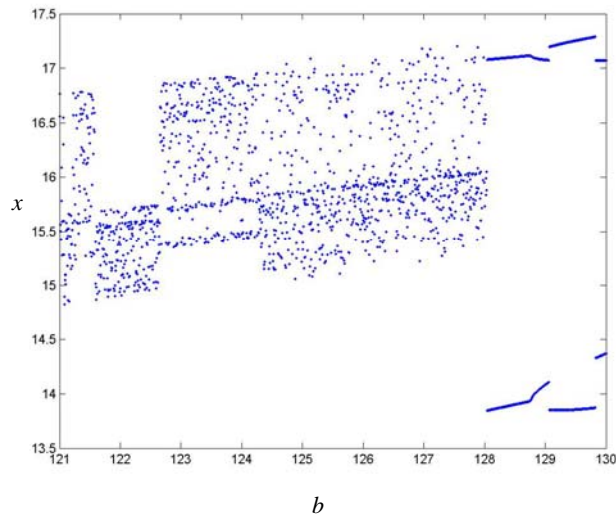
(a) *Period 2, $b=128.1$*



(b) *Period 2, $b=129.05$*

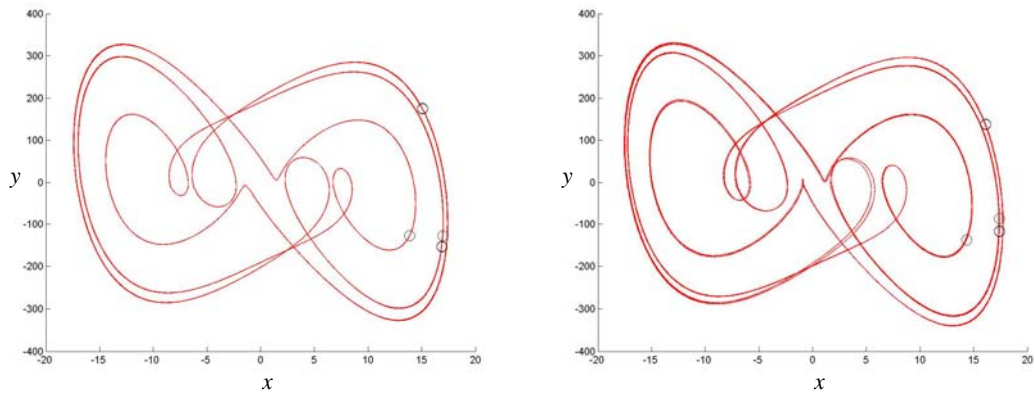


(c) *Chaos, $b=125$*



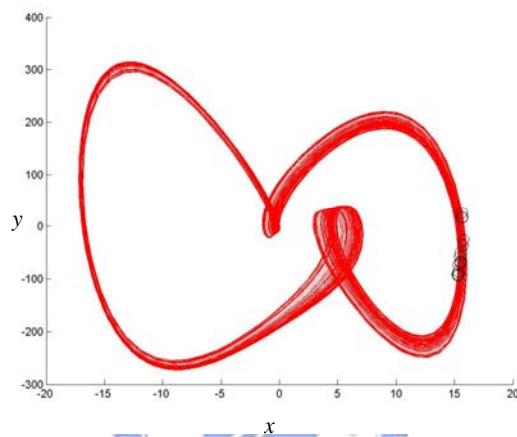
(d)

Fig. 2.18 The phase portraits, Poincaré maps and the bifurcation diagram for the fractional order modified nano Duffing resonator system, x versus y and b versus x , $(q_1, q_2) = (1.8, 0.2)$.

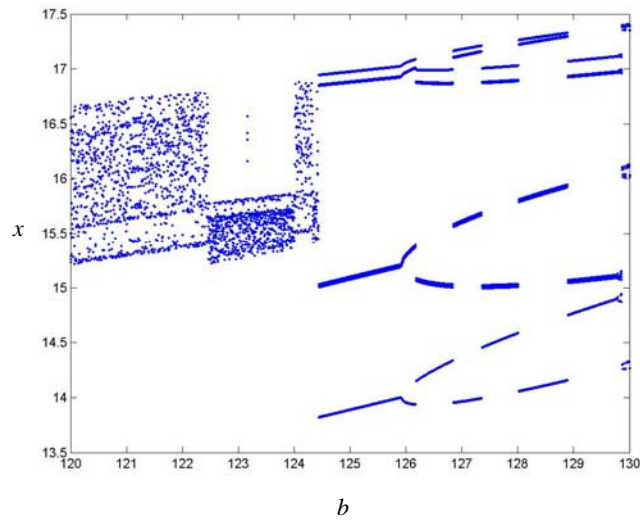


(a) Period 5, $b=125$

(b) Period 6, $b=129$

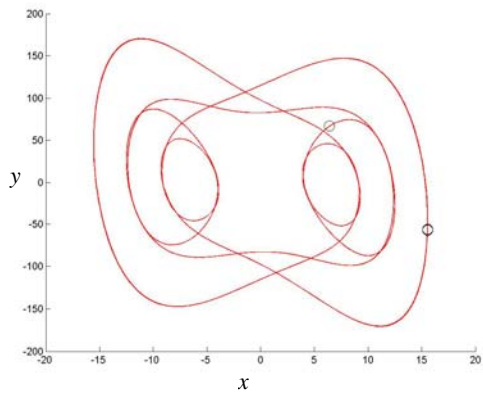


(c) Chaos, $b=123$

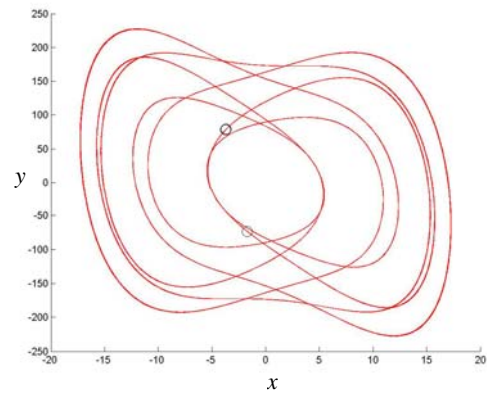


(d)

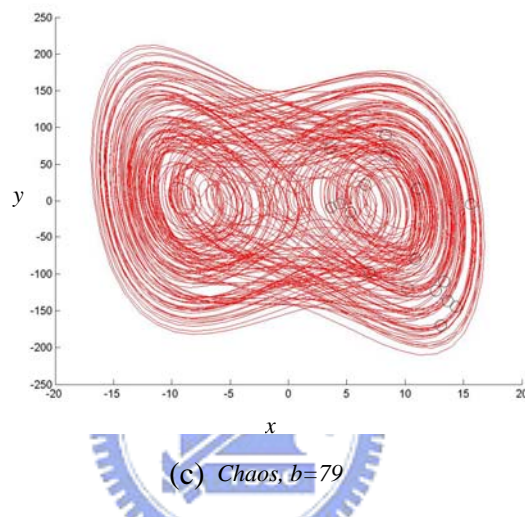
Fig. 2.19 The phase portraits, Poincaré maps and the bifurcation diagram for the fractional order modified nano Duffing resonator system, x versus y and b versus x , $(q_1, q_2) = (1.2, 0.8)$.



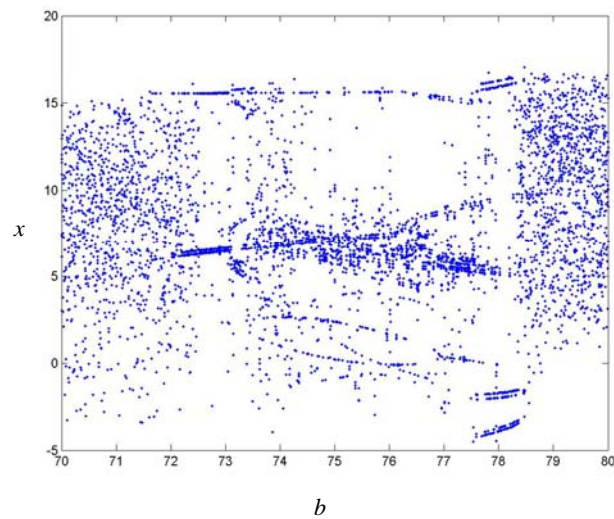
(a) *Period 3, $b=72.8$*



(b) *Period 5, $b=78.01$*

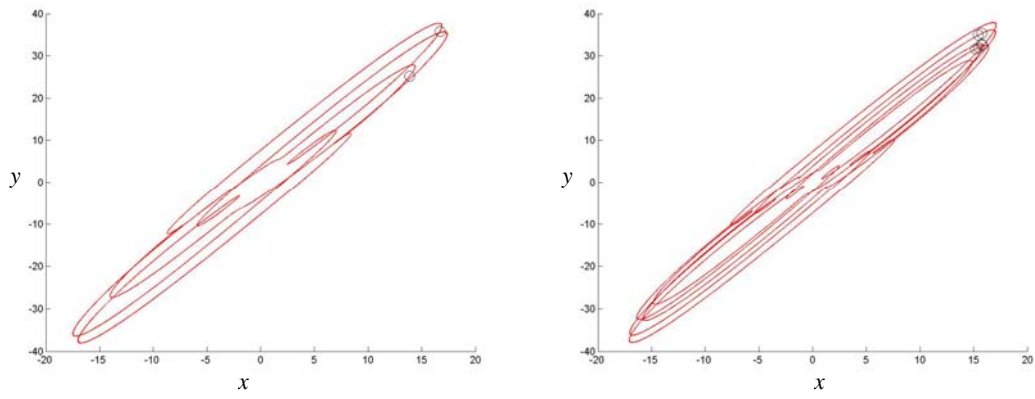


(c) *Chaos, $b=79$*



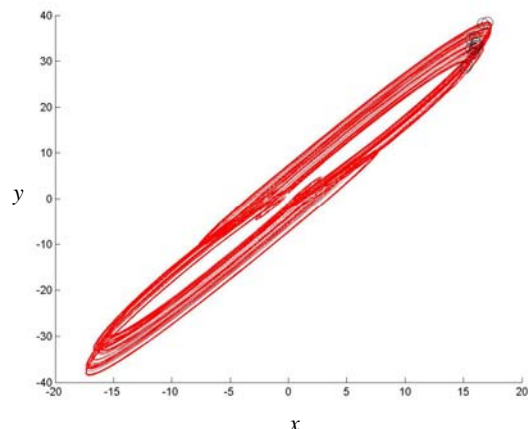
(d)

Fig. 2.20 The phase portraits, Poincaré maps and the bifurcation diagram for the fractional order modified nano Duffing resonator system, x versus y and b versus x , $(q_1, q_2) = (1.1, 0.9)$.

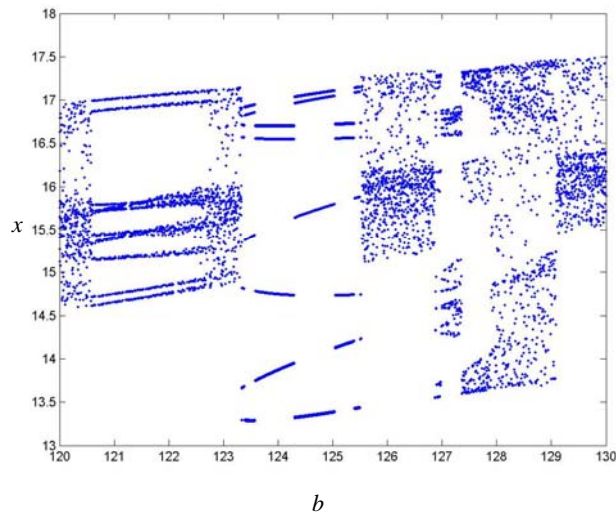


(a) *Period 4, $b=124$*

(b) *Period 6, $b=121$*

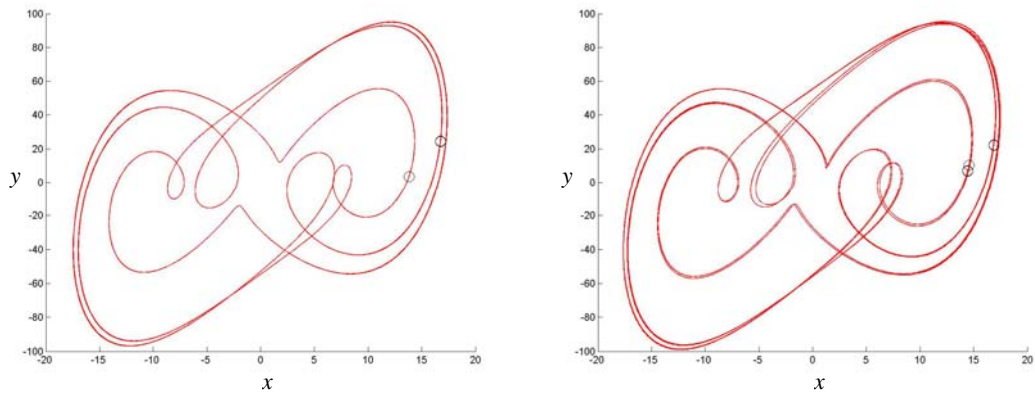


(c) *Chaos, $b=126$*



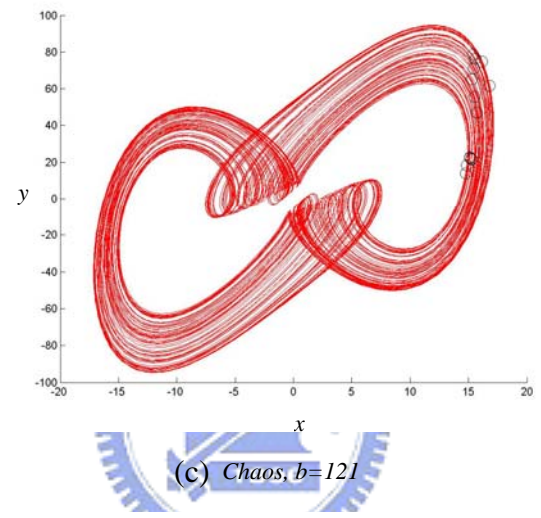
(d)

Fig. 2.21 The phase portraits, Poincaré maps and the bifurcation diagram for the fractional order modified nano Duffing resonator system, x versus y and b versus x , $(q_1, q_2) = (0.2, 1.8)$.

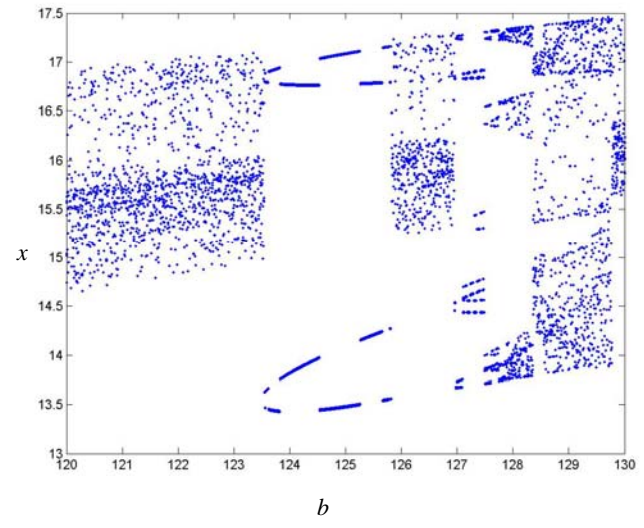


(a) Period 4, $b=124$

(b) Period 5, $b=127.2$

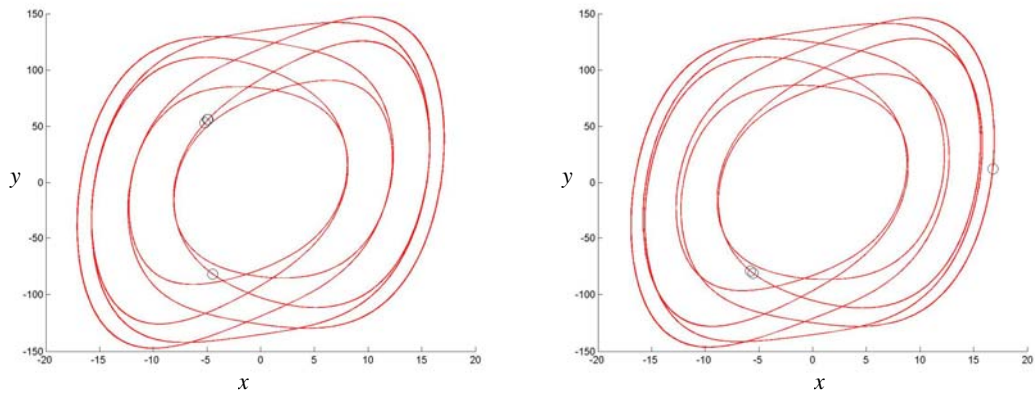


(c) Chaos, $b=121$



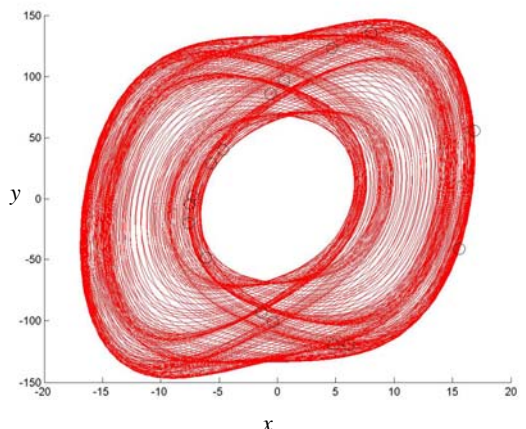
(d)

Fig. 2.22 The phase portraits, Poincaré maps and the bifurcation diagram for the fractional order modified nano Duffing resonator system, x versus y and b versus x , $(q_1, q_2) = (0.8, 1.2)$.

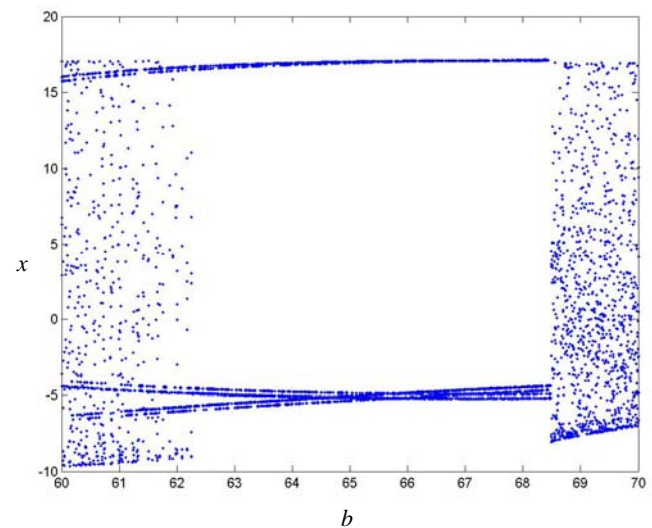


(a) *Period 4, b=68*

(b) *Period 5, b=63*

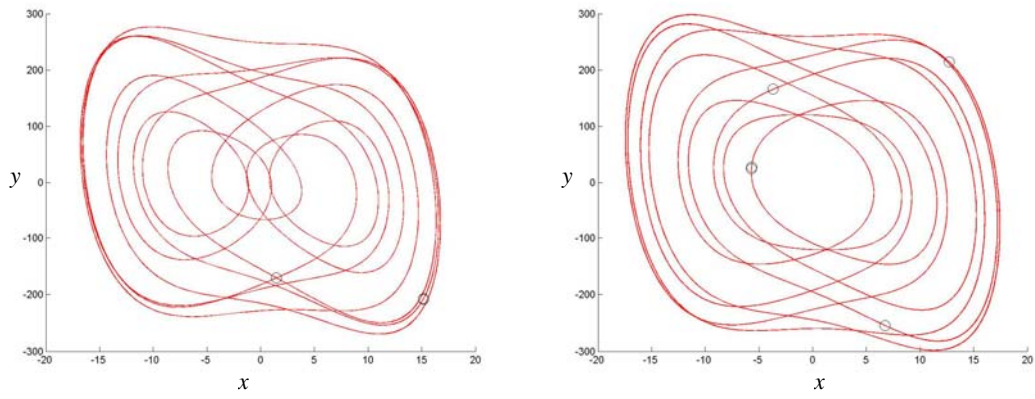


(c) *Chaos, b=69*



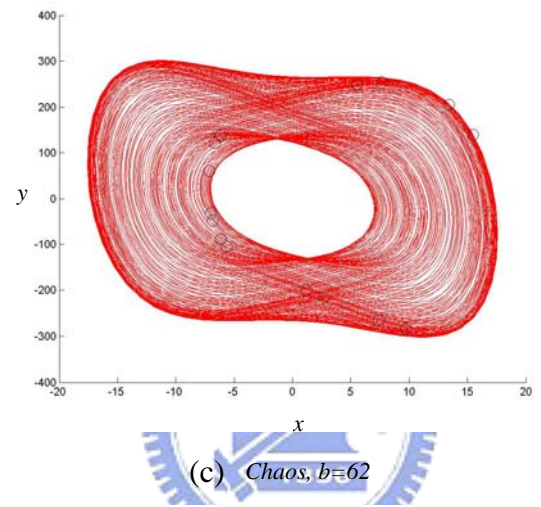
(d)

Fig. 2.23 The phase portraits, Poincaré maps and the bifurcation diagram for the fractional order modified nano Duffing resonator system, x versus y and b versus x , $(q_1, q_2) = (0.9, 1.1)$.

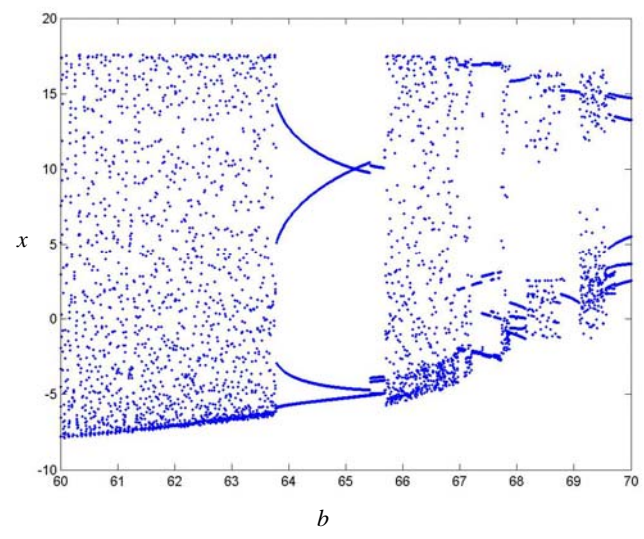


(a) *Period 2, $b=68.9$*

(b) *Period 5, $b=64$*

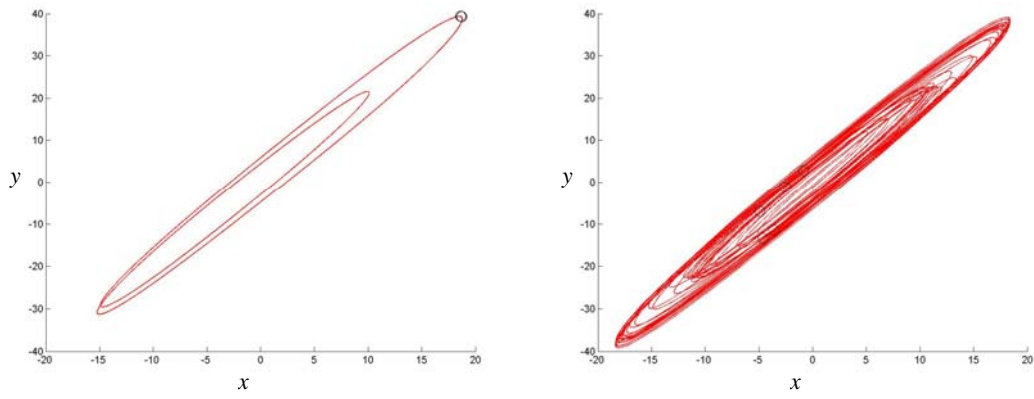


(c) *Chaos, $b=62$*



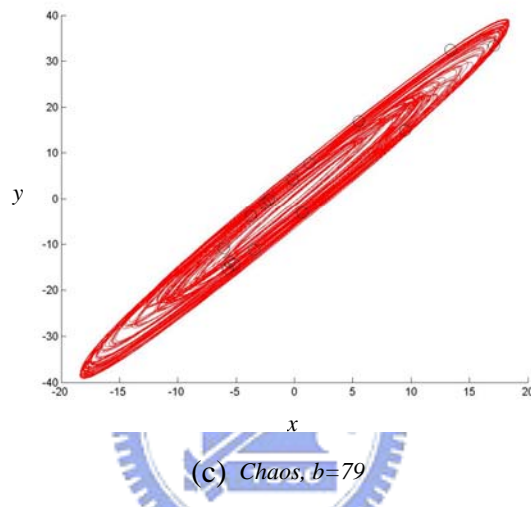
(d)

Fig. 2.24 The phase portraits, Poincaré maps and the bifurcation diagram for the fractional order modified nano Duffing resonator system, x versus y and b versus x , $(q_1, q_2) = (1.2, 0.9)$.

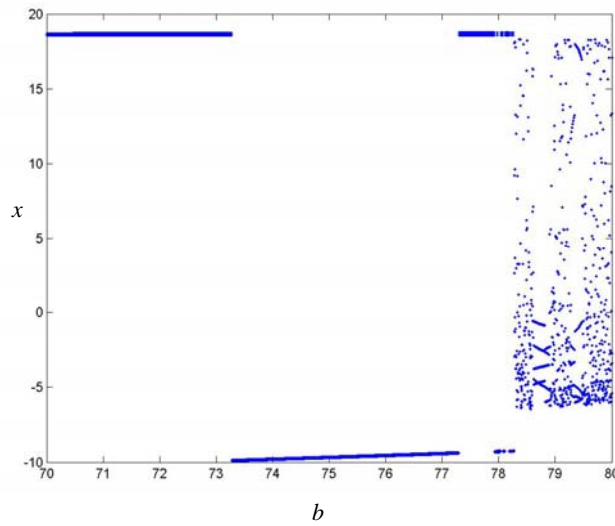


(a) *Period 2, $b=72$*

(b) *Period 5, $b=78.8$*

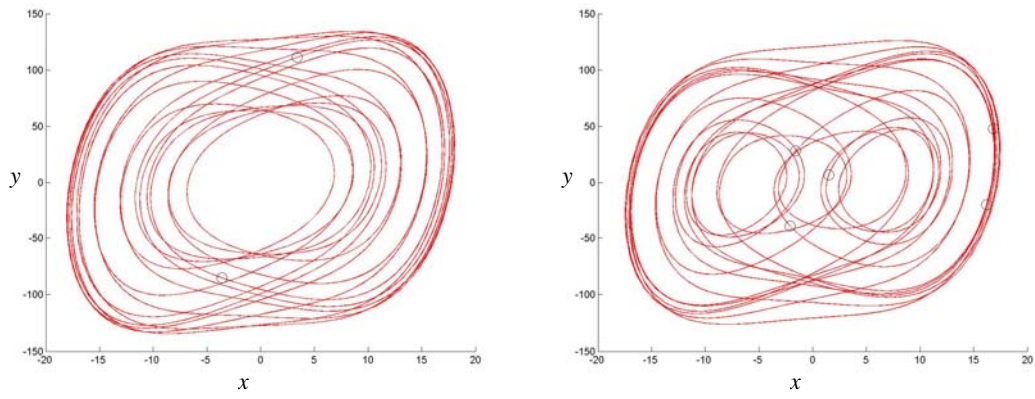


(c) *Chaos, $b=79$*



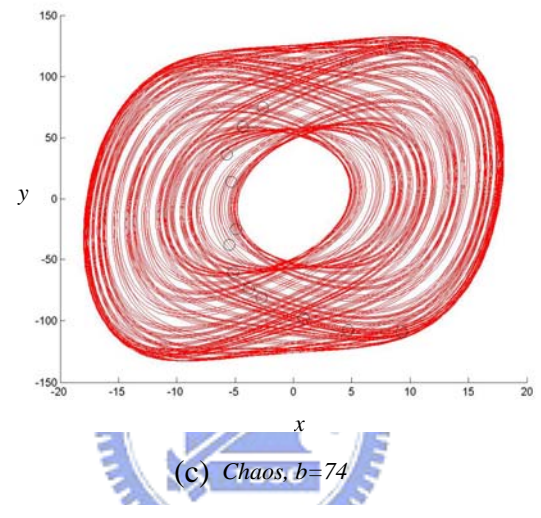
(d)

Fig. 2.25 The phase portraits, Poincaré maps and the bifurcation diagram for the fractional order modified nano Duffing resonator system, x versus y and b versus x , $(q_1, q_2) = (0.2, 1.9)$.

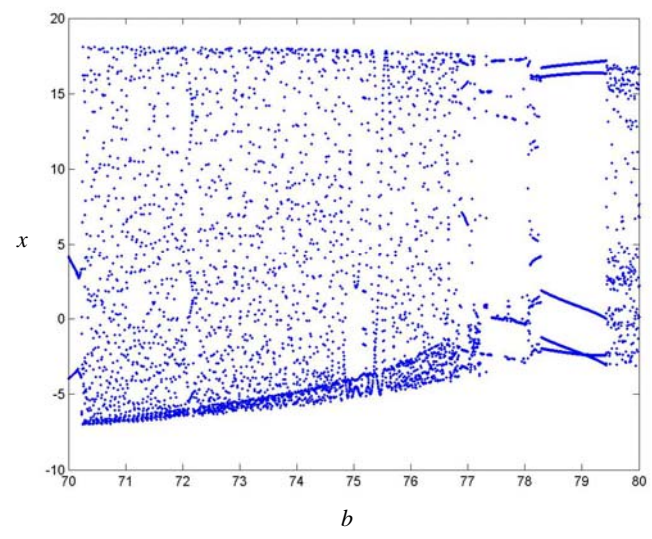


(a) *Period 2, $b=70.1$*

(b) *Period 5, $b=78.5$*



(c) *Chaos, $b=74$*



(d)

Fig. 2.26 The phase portraits, Poincaré maps and the bifurcation diagram for the fractional order modified nano Duffing resonator system, x versus y and b versus x , $(q_1, q_2) = (0.9, 1.2)$.

Chapter 3

Chaos Synchronization of Fractional Order Modified Nano Duffing Resonator Systems with Parameters Excited by a Chaotic Signal

3.1 Preliminaries

The chaos synchronizations of two uncoupled fractional order modified nano Duffing resonator systems are obtained by replacing their corresponding parameters by the same function of chaotic state variables of a third chaotic system in this chapter. The method is named parameter excited chaos synchronization which can be successfully obtained for very low total fractional order 0.2.

3.2 Numerical Simulations for Chaos Synchronization with Parameter Driven by a Chaotic Signal

In this section, two chaotic fractional order modified nano Duffing resonator systems

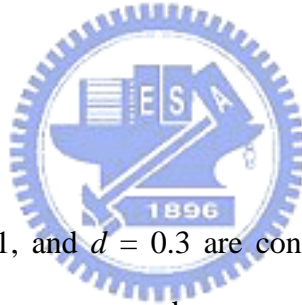
$$\left\{ \begin{array}{l} \frac{d^{q_1} x_1}{dt^{q_1}} = y_1 \\ \frac{d^{q_2} y_1}{dt^{q_2}} = -x_1 - x_1^3 - ay_1 + bz_1 \\ \frac{dz_1}{dt} = w_1 \\ \frac{dw_1}{dt} = -cz_1 - dz_1^3 \end{array} \right. \quad (3.1)$$

and

$$\begin{cases} \frac{d^{q_1} x_2}{dt^{q_1}} = y_2 \\ \frac{d^{q_2} y_2}{dt^{q_2}} = -x_2 - x_2^3 - ay_2 + bz_2 \\ \frac{dz_2}{dt} = w_2 \\ \frac{dw_2}{dt} = -cz_2 - dz_2^3 \end{cases} \quad (3.2)$$

where q_1 and q_2 are the fractional orders, are synchronized by replacing corresponding parameters by the same function of chaotic states of chaotic modified nano Duffing resonator system

$$\begin{cases} \frac{dx}{dt} = y \\ \frac{dy}{dt} = -x - x^3 - ay + bz \\ \frac{dz}{dt} = w \\ \frac{dw}{dt} = -cz - dz^3 \end{cases} \quad (3.3)$$



where $a = 0.05$, $b = 53$, $c = 1$, and $d = 0.3$ are constant parameters of the system. Define the error states as $e_1 = x_1 - x_2$ and $e_2 = y_1 - y_2$ in system (3.1) and (3.2). The synchronization scheme is to replace the corresponding parameters b in system (3.1) and (3.2) by the same function of chaotic states of system (3.3) such that $\|e(t)\| \rightarrow 0$ as $t \rightarrow \infty$. In following simulations, for various derivative orders q_1 and q_2 , we replace the system parameter b in system (3.1) and (3.2) by x , y , x^2 , y^2 , xy where x and y are state variables in system (3.3). Simulations are performed under $q_1 = q_2 = 0.1 \sim 0.9$ in steps of 0.1. In our numerical simulations, four parameters $a = 0.05$, $b = 53$, $c = 1$ and $d = 0.3$ of system (3.3) are fixed. The initial states of system (13) are $x(0) = 3$, $y(0) = 4$, $z(0) = 1$ and $w(0) = 0$. The numerical simulations are carried out by MATLAB.

Case 1: The parameters $a = 0.05$, $c = 1$ and $d = 0.3$ of system (3.1) and (3.2) are fixed. The parameter b of system (3.1) and (3.2) is replaced by the same x , where x is the state variable of system (3.3). All synchronizations for $q_1 = q_2 = 0.1 \sim 0.9$ are successfully obtained. For saving space, only results for $q_1 = q_2 = 0.1$ and 0.9 are shown in Fig. 3.1 ~ 3.4.

Case 2: The parameters $a = 0.05$, $c = 1$ and $d = 0.3$ of system (3.1) and (3.2) are fixed. The parameter b of system (3.1) and (3.2) is replaced by the same y , where y is the state variable of system (3.3). All synchronizations for $q_1 = q_2 = 0.1 \sim 0.9$ are successfully obtained. For saving space, only results for $q_1 = q_2 = 0.1$ and 0.9 are shown in Fig. 3.5 ~ 3.8.

Case 3: The parameters $a = 0.05$, $c = 1$ and $d = 0.3$ of system (3.1) and (3.2) are fixed. The parameter b of system (3.1) and (3.2) is replaced by the same x^2 , where x is the state variable of system (3.3). All synchronizations for $q_1 = q_2 = 0.1 \sim 0.9$ are successfully obtained. For saving space, only results for $q_1 = q_2 = 0.1$ and 0.9 are shown in Fig. 3.9 ~ 3.12.

Case 4: The parameters $a = 0.05$, $c = 1$ and $d = 0.3$ of system (3.1) and (3.2) are fixed. The parameter b of system (3.1) and (3.2) is replaced by the same y^2 , where y is the state variable of system (3.3). All synchronizations for $q_1 = q_2 = 0.1 \sim 0.9$ are successfully obtained. For saving space, only results for $q_1 = q_2 = 0.1$ and 0.9 are shown in Fig. 3.13 ~ 3.16.

Case 5: The parameters $a = 0.05$, $c = 1$ and $d = 0.3$ of system (3.1) and (3.2) are fixed. The parameter b of system (3.1) and (3.2) is replaced by the same xy , where x and y are the state variables of system (3.3). All synchronizations for $q_1 = q_2 = 0.1 \sim 0.9$ are successfully obtained. For saving space, only results for $q_1 = q_2 = 0.1$ and 0.9 are shown in Fig. 3.17 ~ 3.20.

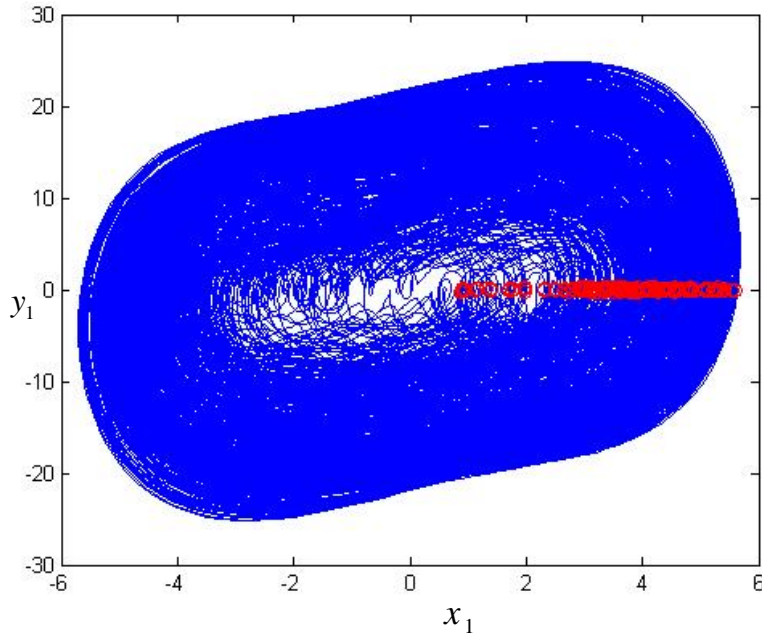


Fig. 3.1 The phase portrait and Poincaré map of the synchronized fractional order modified nano Duffing resonator systems (11) and (12) with order $q_1 = q_2 = 0.9$ for Case 1.

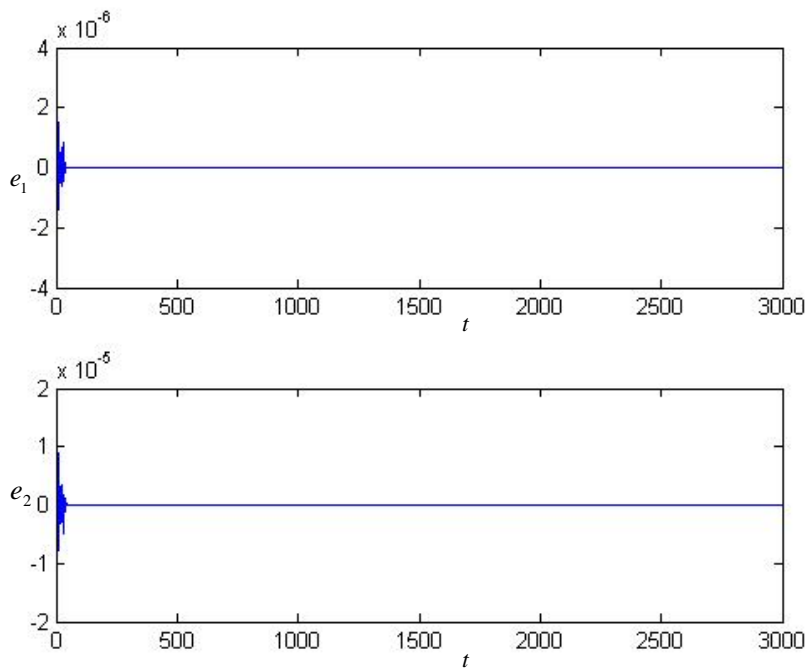


Fig. 3.2 The time histories of the errors of the states of the synchronized fractional order modified nano Duffing resonator systems (11) and (12) with order $q_1 = q_2 = 0.9$ for Case 1.

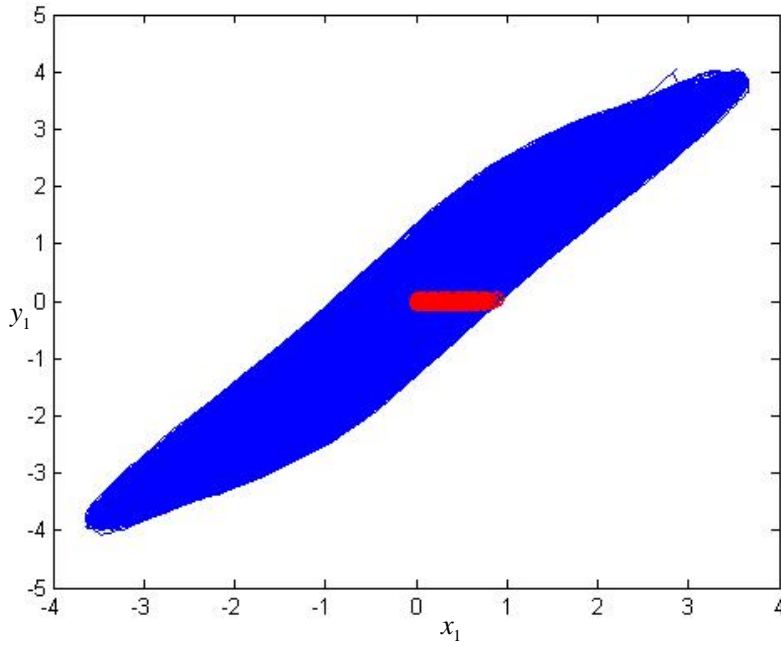


Fig. 3.3 The phase portrait and Poincaré map of the synchronized fractional order modified nano Duffing resonator systems (11) and (12) with order $q_1 = q_2 = 0.1$ for Case 1.

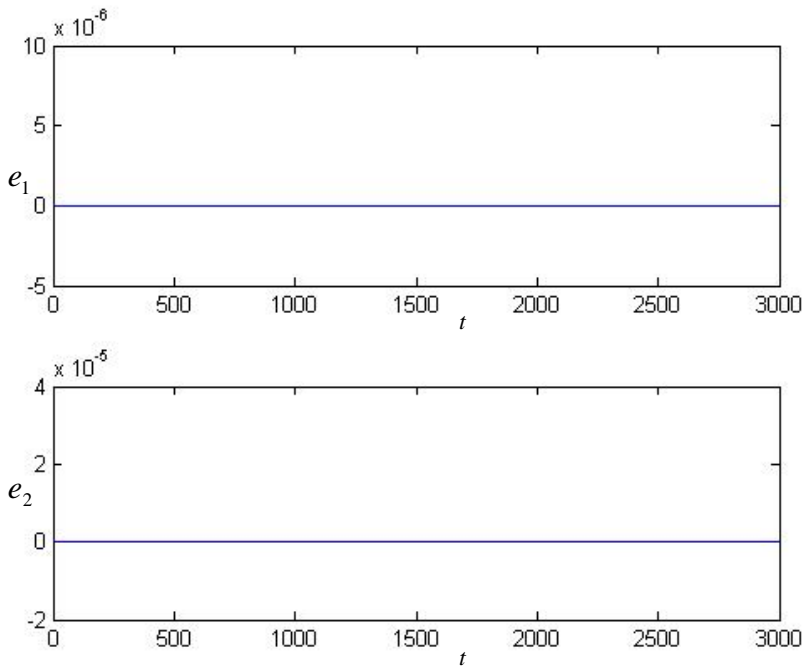


Fig. 3.4 The time histories of the errors of the states of the synchronized fractional order modified nano Duffing resonator systems (11) and (12) with order $q_1 = q_2 = 0.1$ for Case 1.

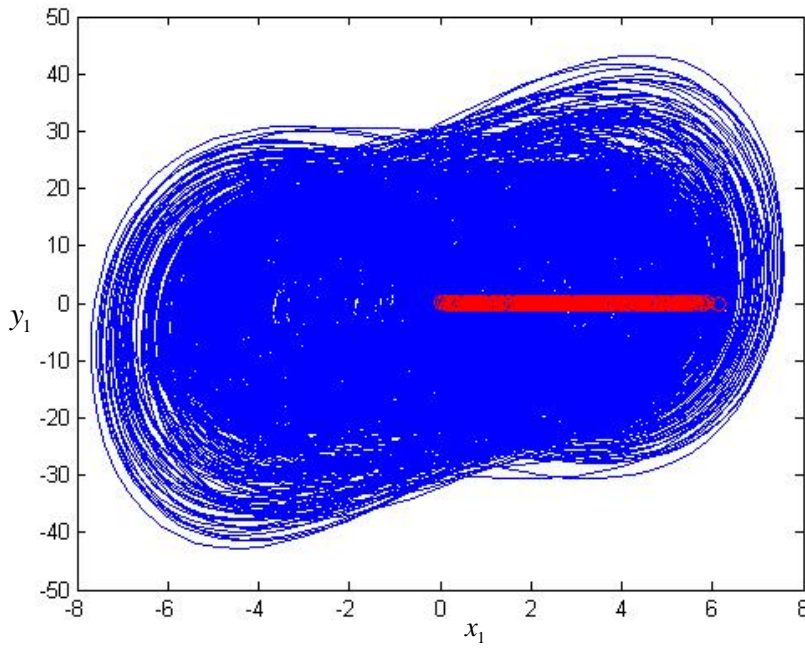


Fig. 3.5 The phase portrait and Poincaré map of the synchronized fractional order modified nano Duffing resonator systems (11) and (12) with order $q_1 = q_2 = 0.9$ for Case 2.

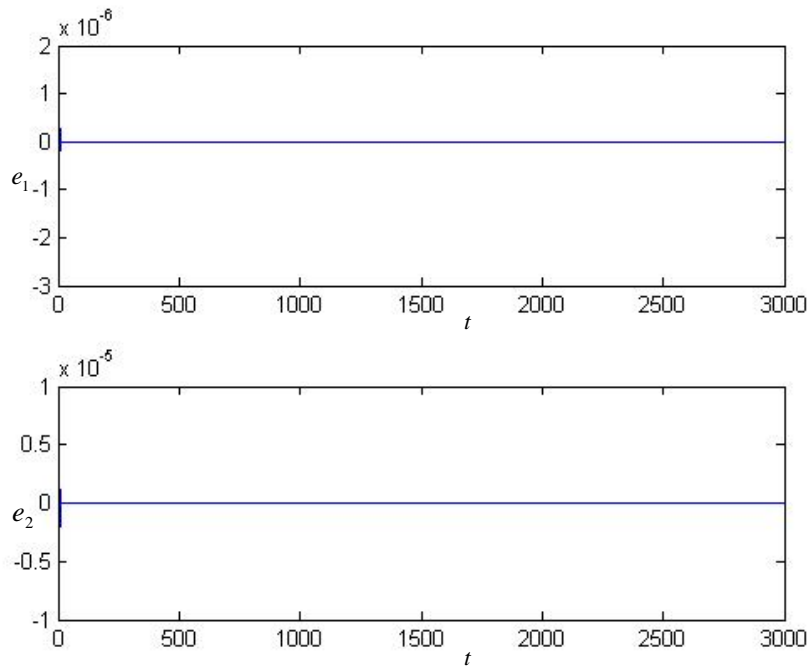


Fig. 3.6 The time histories of the errors of the states of the synchronized fractional order modified nano Duffing resonator systems (11) and (12) with order $q_1 = q_2 = 0.9$ for Case 2.

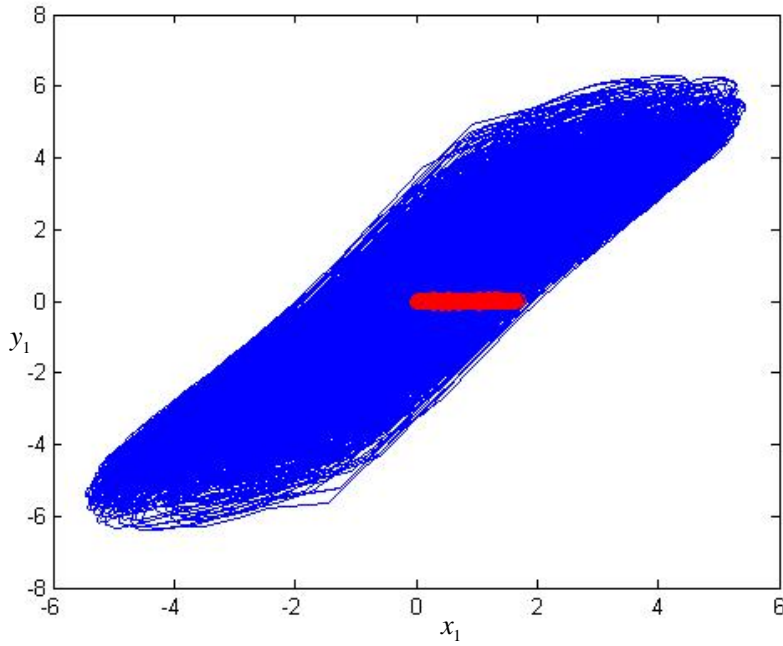


Fig. 3.7 The phase portrait and Poincaré map of the synchronized fractional order modified nano Duffing resonator systems (11) and (12) with order $q_1 = q_2 = 0.1$ for Case 2.

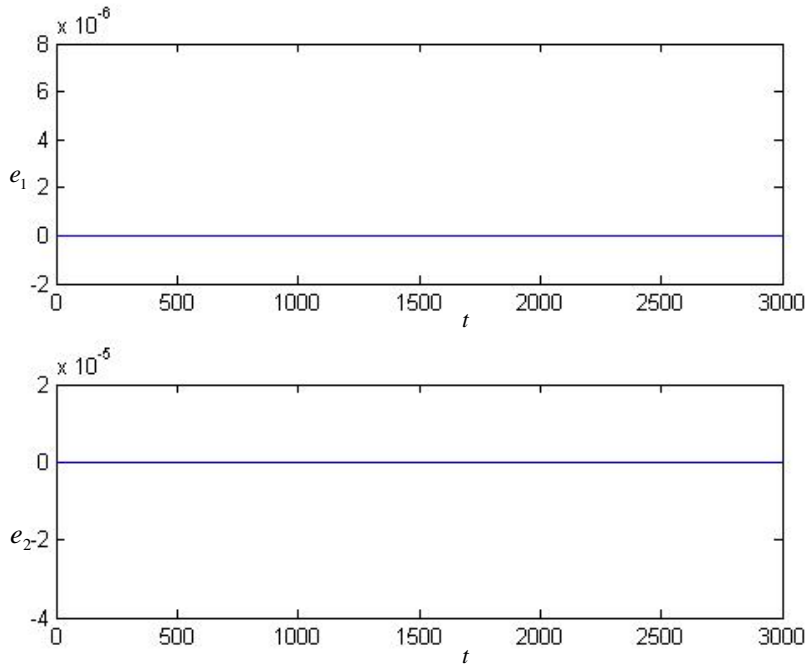


Fig. 3.8 The time histories of the errors of the states of the synchronized fractional order modified nano Duffing resonator systems (11) and (12) with order $q_1 = q_2 = 0.1$ for Case 2.

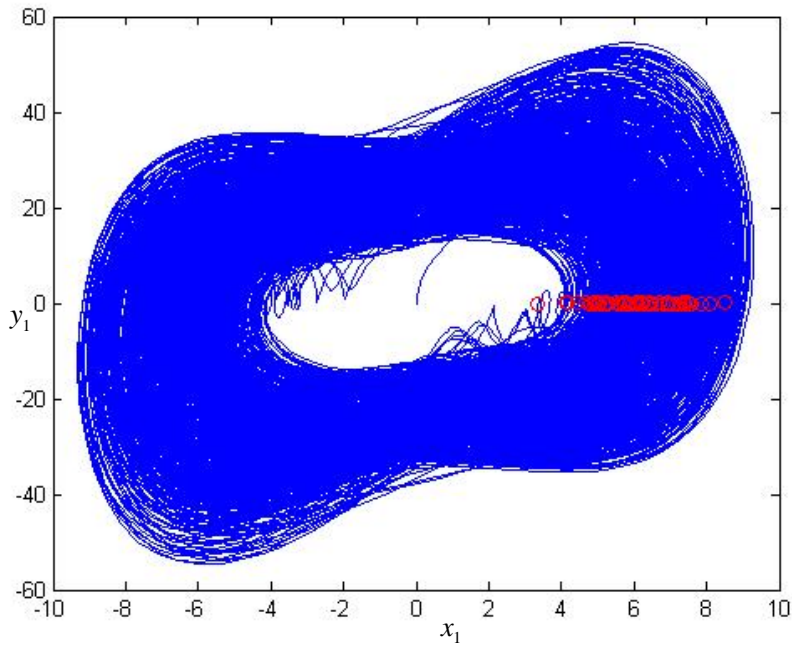


Fig. 3.9 The phase portrait and Poincaré map of the synchronized fractional order modified nano Duffing resonator systems (11) and (12) with order $q_1 = q_2 = 0.9$ for Case 3.

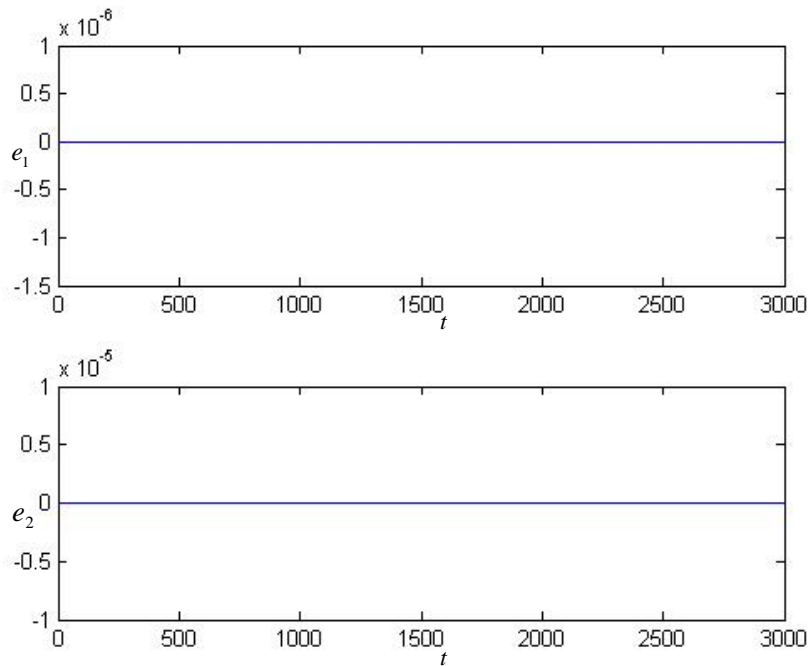


Fig. 3.10 The time histories of the errors of the states of the synchronized fractional order modified nano Duffing resonator systems (11) and (12) with order $q_1 = q_2 = 0.9$ for Case 3.

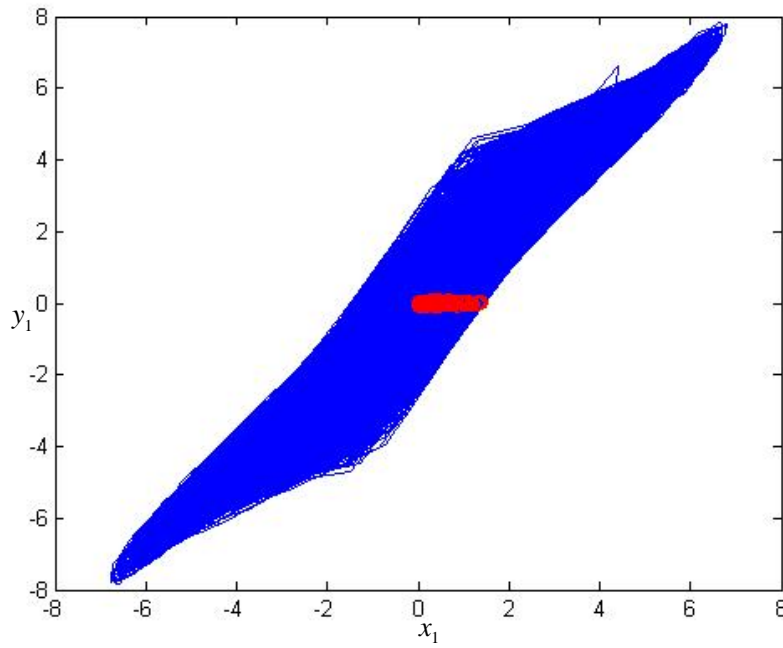


Fig. 3.11 The phase portrait and Poincaré map of the synchronized fractional order modified nano Duffing resonator systems (11) and (12) with order $q_1 = q_2 = 0.1$ for Case 3.

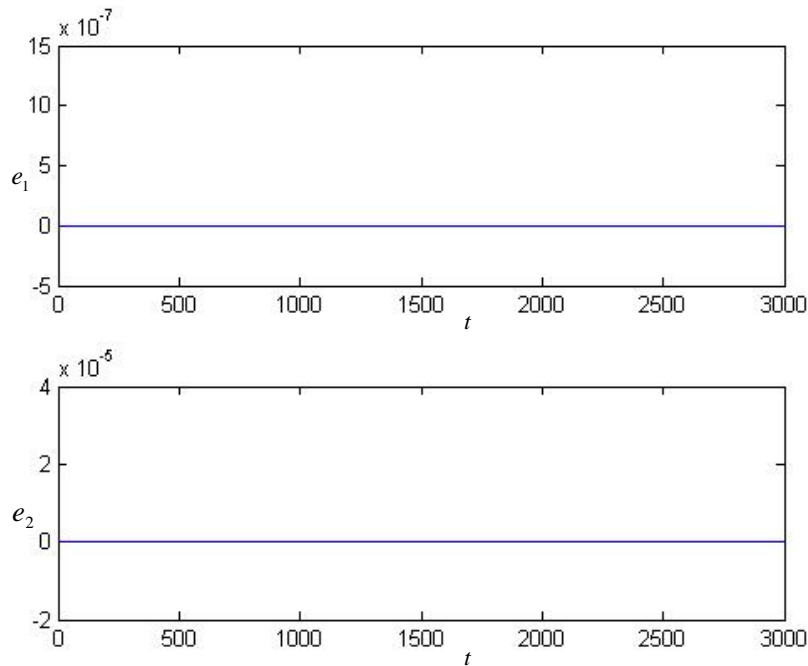


Fig. 3.12 The time histories of the errors of the states of the synchronized fractional order modified nano Duffing resonator systems (11) and (12) with order $q_1 = q_2 = 0.1$ for Case 3.

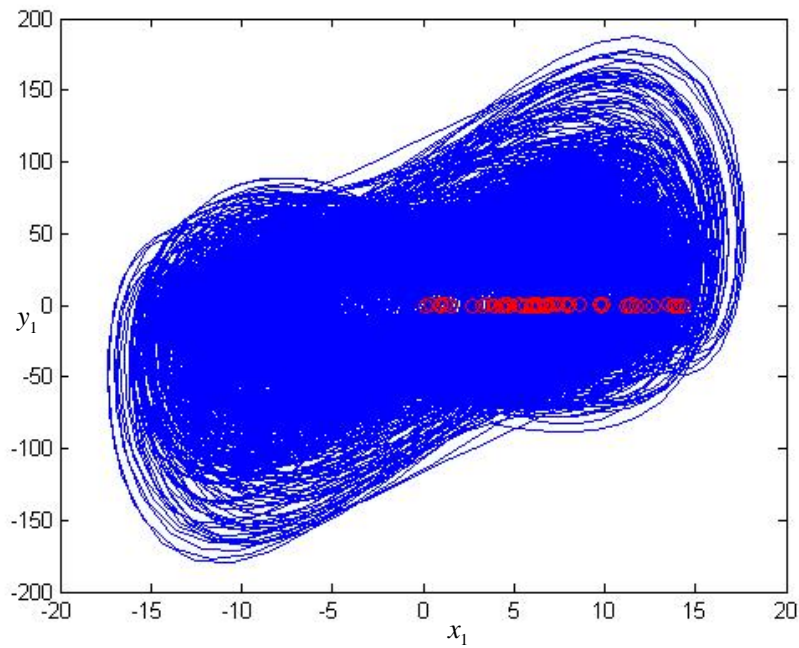


Fig. 3.13 The phase portrait and Poincaré map of the synchronized fractional order modified nano Duffing resonator systems (11) and (12) with order $q_1 = q_2 = 0.9$ for Case 4.

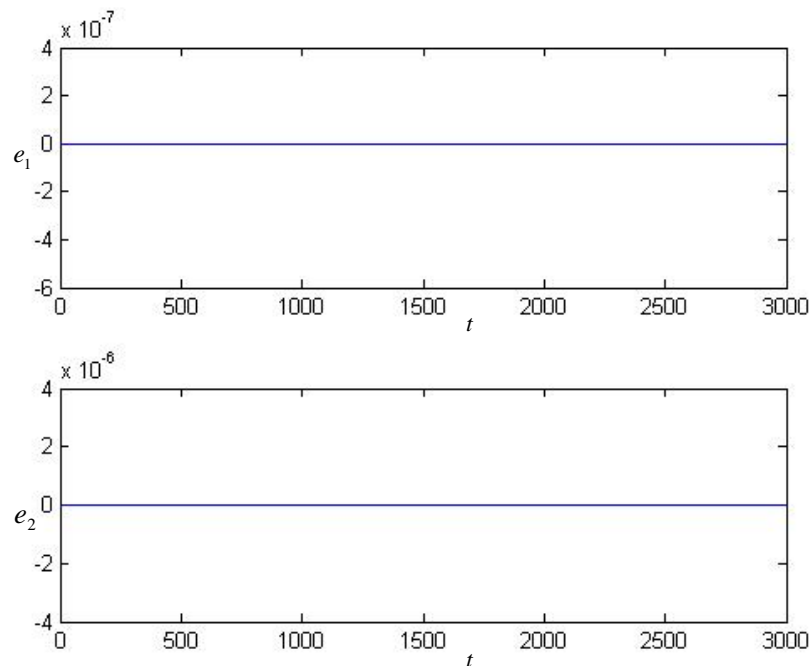


Fig. 3.14 The time histories of the errors of the states of the synchronized fractional order modified nano Duffing resonator systems (11) and (12) with order $q_1 = q_2 = 0.9$ for Case 4.

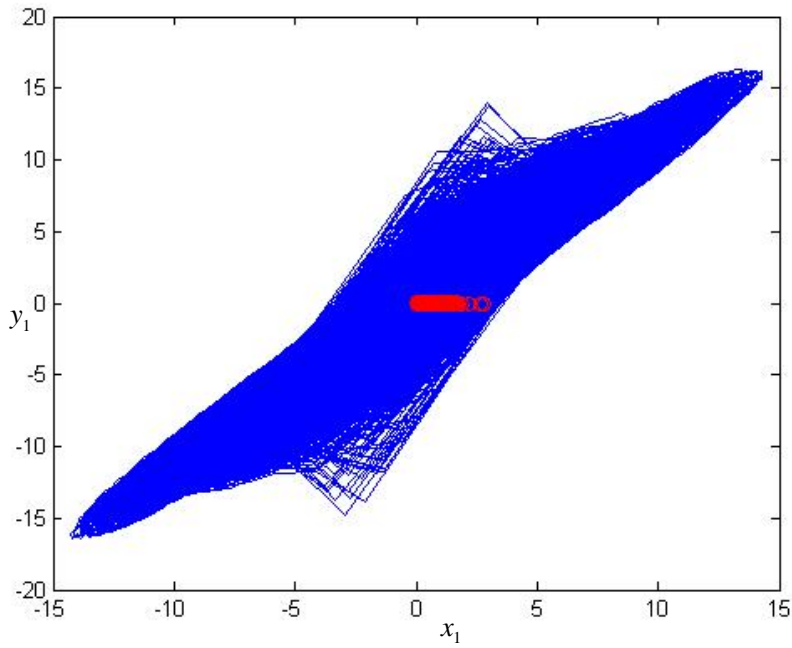


Fig. 3.15 The phase portrait and Poincaré map of the synchronized fractional order modified nano Duffing resonator systems (11) and (12) with order $q_1 = q_2 = 0.1$ for Case 4.

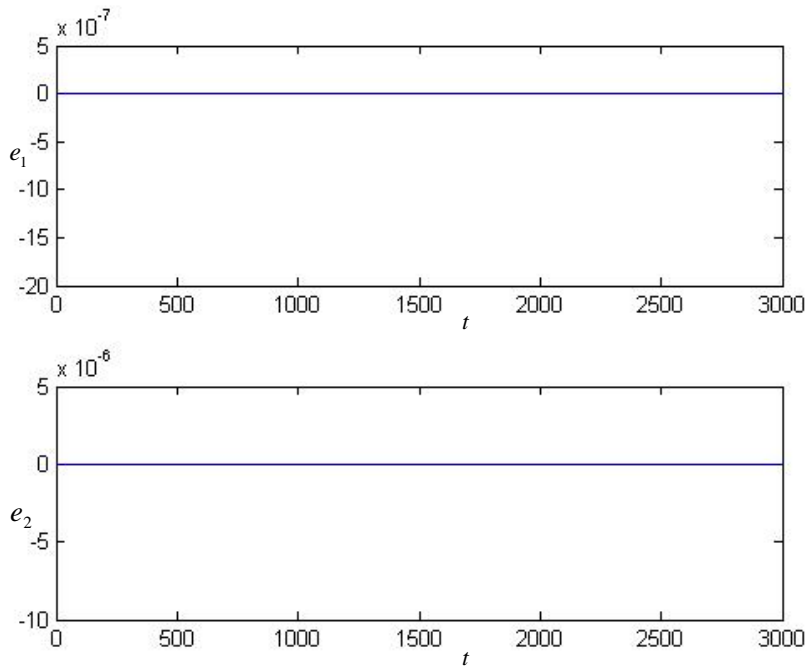


Fig. 3.16 The time histories of the errors of the states of the synchronized fractional order modified nano Duffing resonator systems (11) and (12) with order $q_1 = q_2 = 0.1$ for Case 4.

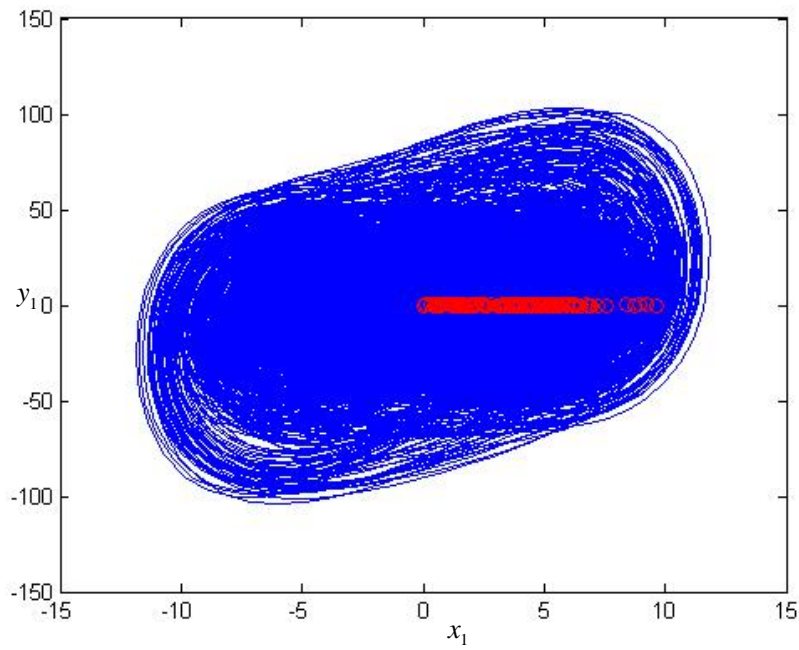


Fig. 3.17 The phase portrait and Poincaré map of the synchronized fractional order modified nano Duffing resonator systems (11) and (12) with order $q_1 = q_2 = 0.9$ for Case 5.

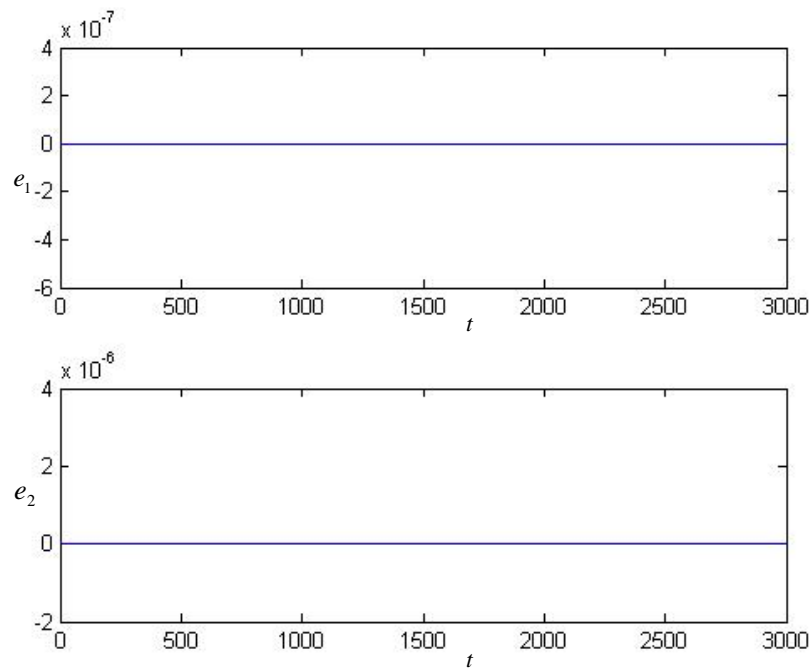


Fig. 3.18 The time histories of the errors of the states of the synchronized fractional order modified nano Duffing resonator systems (11) and (12) with order $q_1 = q_2 = 0.9$ for Case 5.

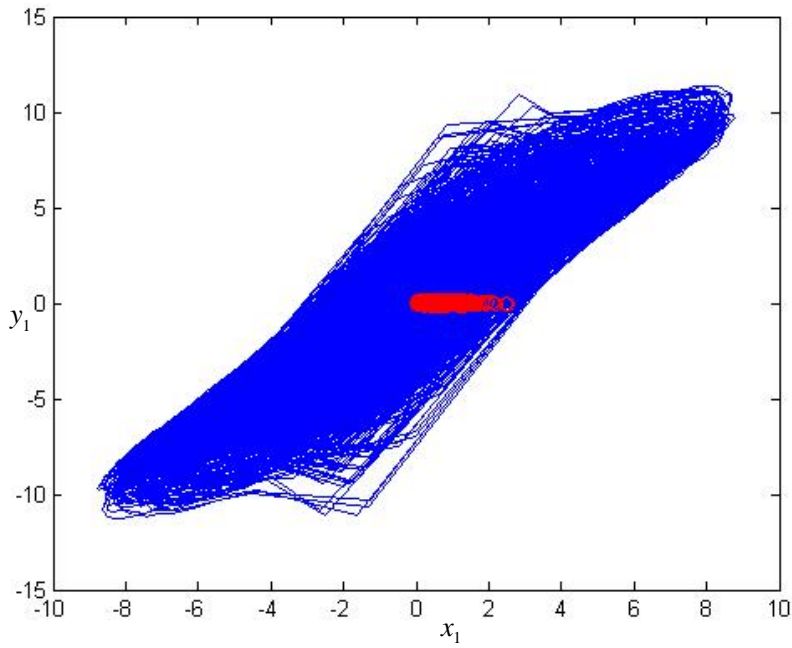


Fig. 3.19 The phase portrait and Poincaré map of the synchronized fractional order modified nano Duffing resonator systems (11) and (12) with order $q_1 = q_2 = 0.1$ for Case 5.

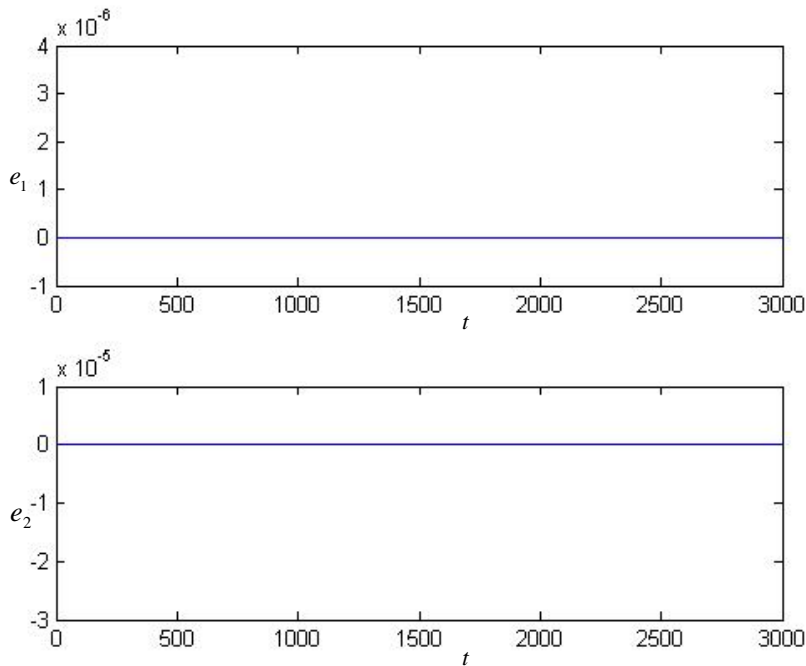


Fig. 3.20 The time histories of the errors of the states of the synchronized fractional order modified nano Duffing resonator systems (11) and (12) with order $q_1 = q_2 = 0.1$ for Case 5.

Chapter 4

Anti-control of Chaos of a Fractional Order Modified Nano Duffing Resonator System

In this chapter, anti-control of chaos is applied by adding various external terms. By using the functions of state variables of a second system as the external terms, the anti-control of chaos can be obtained. Anti-control of chaos can be successfully obtained for very low total fractional order 0.2.

4.1 Regular Dynamics of a Fractional Modified Nano Duffing Resonator System

In this section, consider the fractional order modified nano Duffing resonator system

$$\begin{cases} \frac{d^{q_1} x}{dt^{q_1}} = y \\ \frac{d^{q_2} y}{dt^{q_2}} = -x - x^3 - ay + bz \\ \frac{dz}{dt} = w \\ \frac{dw}{dt} = -cz - dz^3 \end{cases} \quad (4.1)$$



where $a=0.05$, $b=10$, $c=1$ and $d=0.3$, q_1 and q_2 are the fractional orders, and the initial condition is $x(0) = 0$, $y(0) = 0$, $z(0) = 10$ and $w(0) = 10$. It can be obtained that the motion is periodic for $q_1 = q_2 = 0.1 \sim 0.9$. For saving space, only results for $q_1 = q_2 = 0.1, 0.5$ and 0.9 are shown in Fig.4.1.

4.2 Anti-control of Chaos

Creating chaos is called anti-control of chaos at times [74]. In this section, addition of a state of another identical system and addition of a periodic sinusoidal

function of a state of another identical system enhance the existing chaos of the originally system effectively. The results are demonstrated by numerical results, i.e. phase portrait and Poincaré map.

Now, consider a second identical modified nano Duffing resonator system:

$$\begin{cases} \frac{dx_1}{dt} = y_1 \\ \frac{dy_1}{dt} = -x_1 - x_1^3 - ay_1 + bz_1 \\ \frac{dz_1}{dt} = w_1 \\ \frac{dw_1}{dt} = -cz_1 - dz_1^3 \end{cases} \quad (4.2)$$

where $a = 0.05$, $b = 10$, $c = 1$, and $d = 0.3$ are constant parameters of the system, and the initial condition is $x_1(0) = 3$, $y_1(0) = 4$, $z_1(0) = 1$ and $w_1(0) = 0$.

In order to induce chaotic phenomena of the fractional modified nano Duffing resonator system (4.1), kx_1 and $k \sin x_1$ are added to system (4.1) respectively, where k is a constant.



4.2.1 Adding the term kx_1

First, we add an external term k_1x_1 to the first equation of (4.1). Second, we add an external term k_2x_1 to the second equation of (4.1). The strengths k_1 and k_2 are either positive or negative. For anti-control of chaos all simulations for $q_1 = q_2 = 0.1 \sim 0.9$ are obtained successfully. For saving space, only results for $q_1 = q_2 = 0.1, 0.5$ and 0.9 are shown as Fig. 4.2-4.5. It can be seen that when total order is larger, the range of y state is also larger.

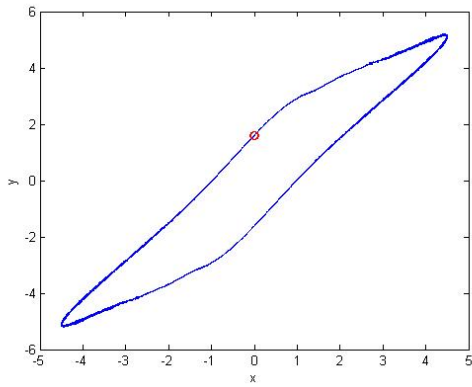
From above numerical results, it is shown that whether k_1 and k_2 are either positive or negative, the chaotization effects are similar.

4.2.2 Adding the term $k \sin x_1$

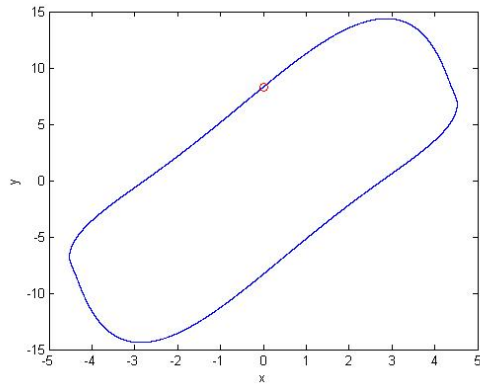
First, we add an external term $k_3 \sin x_1$ to the first equation of (4.1). Second, we add an external term $k_4 \sin x_1$ to the second equation of (4.1). The strengths k_3 and k_4 are either positive or negative. For anti-control of chaos all simulations for $q_1 = q_2 = 0.1 \sim 0.9$ are obtained successfully. For saving space, only results for $q_1 = q_2 = 0.1, 0.5$ and 0.9 are shown as Fig. 4.6-4.9.

From above numerical results, it is also shown that whether k_3 and k_4 are positive or negative, the chaotization effects are similar. It can be seen that when total order is larger, the range of y state is also larger.

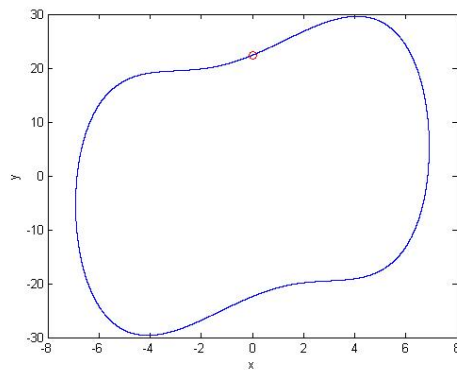




(a) $q_1 = q_2 = 0.1$

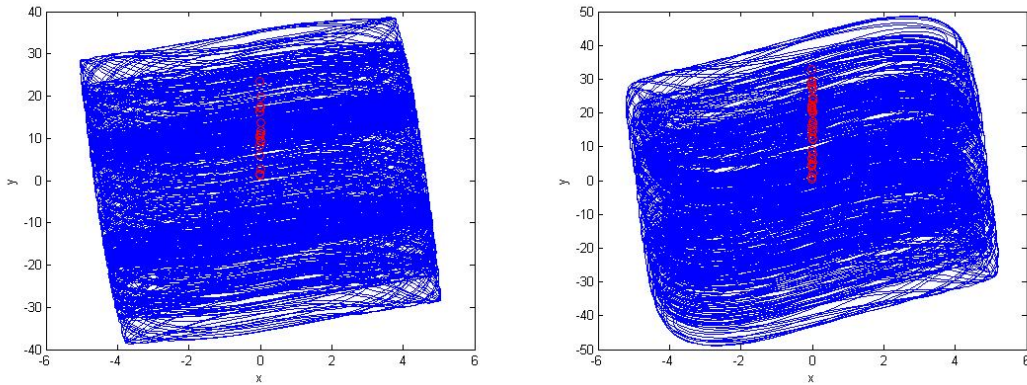


(b) $q_1 = q_2 = 0.5$



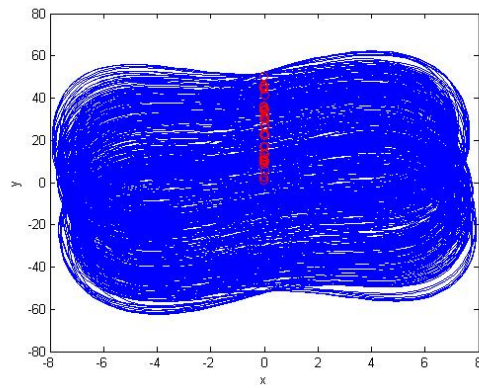
(c) $q_1 = q_2 = 0.9$

Fig. 4.1 The phase portraits and Poincaré maps of the fractional order modified nano Duffing resonator systems (11) without control term.



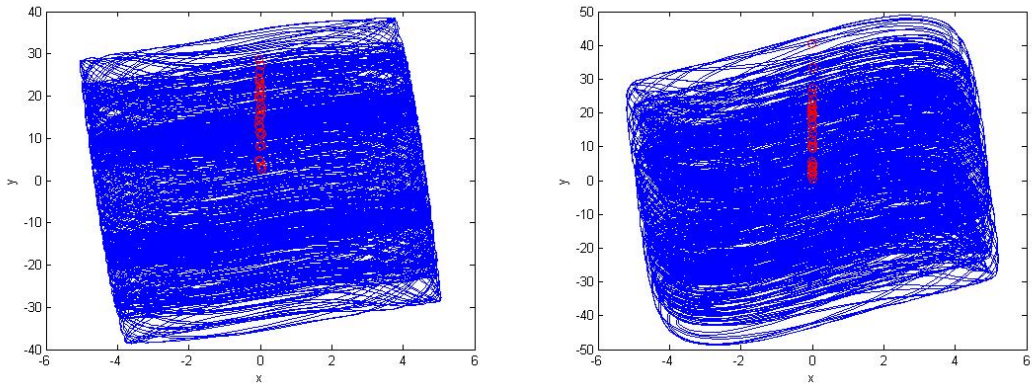
(a) $q_1 = q_2 = 0.1$

(b) $q_1 = q_2 = 0.5$



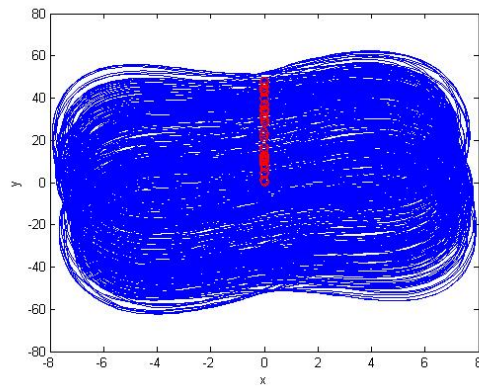
(c) $q_1 = q_2 = 0.9$

Fig. 4.2 The phase portraits and Poincaré maps of the fractional order modified nano Duffing resonator systems (11) with control term $k_1 x_1$, where $k_1 = 10$.



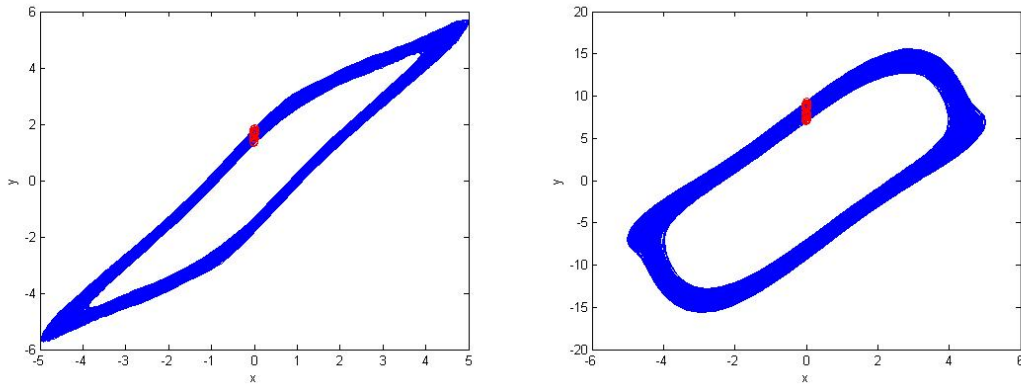
(a) $q_1 = q_2 = 0.1$

(b) $q_1 = q_2 = 0.5$



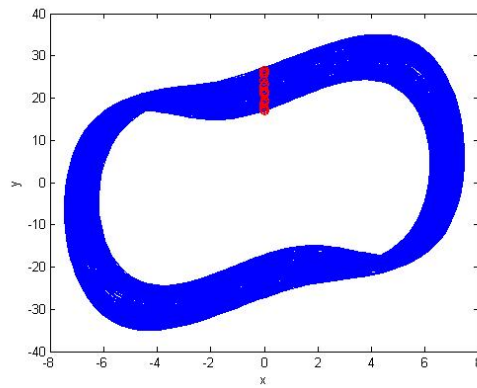
(c) $q_1 = q_2 = 0.9$

Fig. 4.3 The phase portraits and Poincaré maps of the fractional order modified nano Duffing resonator systems (11) with control term $k_1 x_1$, where $k_1 = -10$.



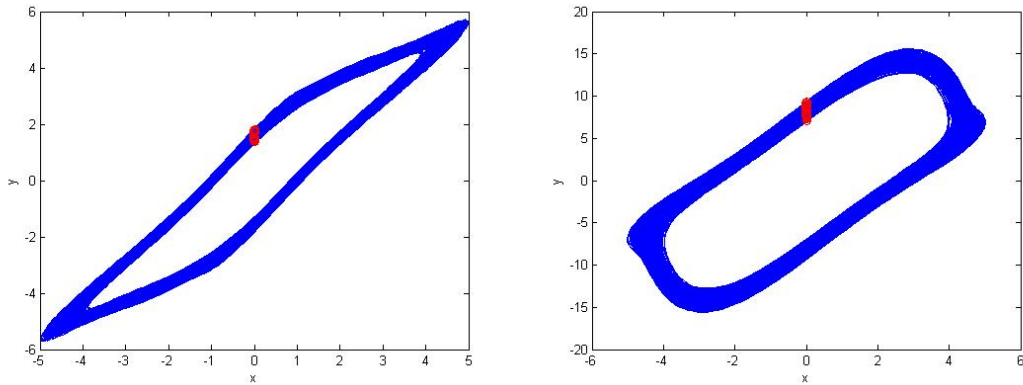
(a) $q_1 = q_2 = 0.1$

(b) $q_1 = q_2 = 0.5$



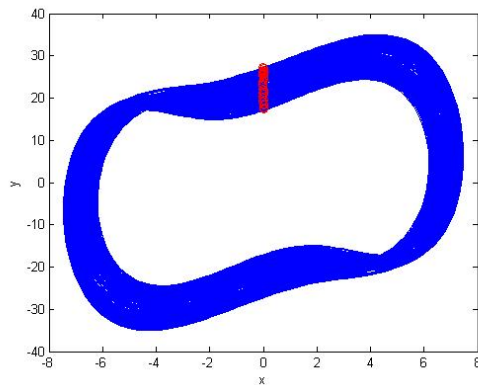
(c) $q_1 = q_2 = 0.9$

Fig. 4.4 The phase portraits and Poincaré maps of the fractional order modified nano Duffing resonator systems (11) with control term $k_2 x_1$, where $k_2 = 10$.



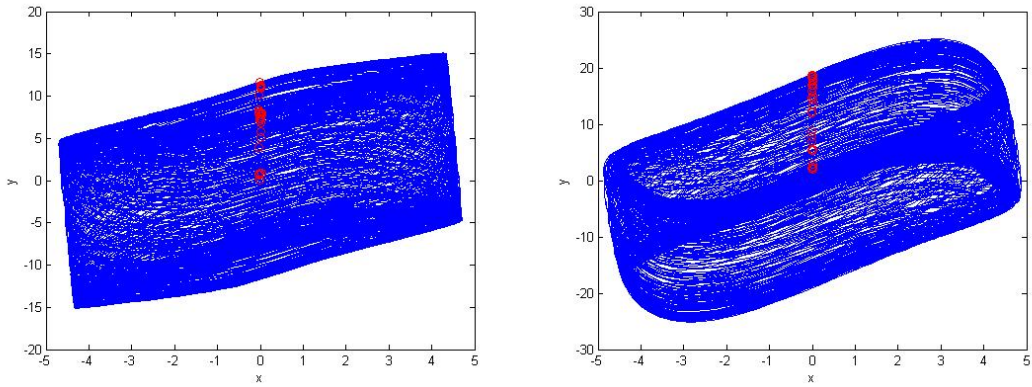
(a) $q_1 = q_2 = 0.1$

(b) $q_1 = q_2 = 0.5$



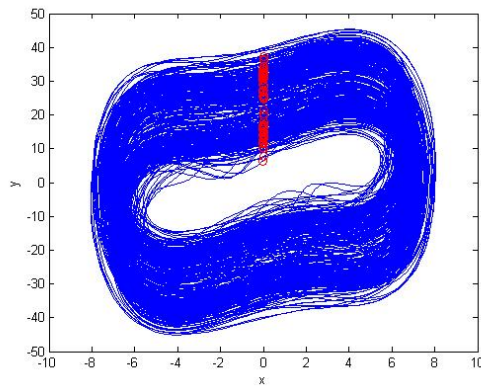
(c) $q_1 = q_2 = 0.9$

Fig. 4.5 The phase portraits and Poincaré maps of the fractional order modified nano Duffing resonator systems (11) with control term $k_2 x_1$, where $k_2 = -10$.



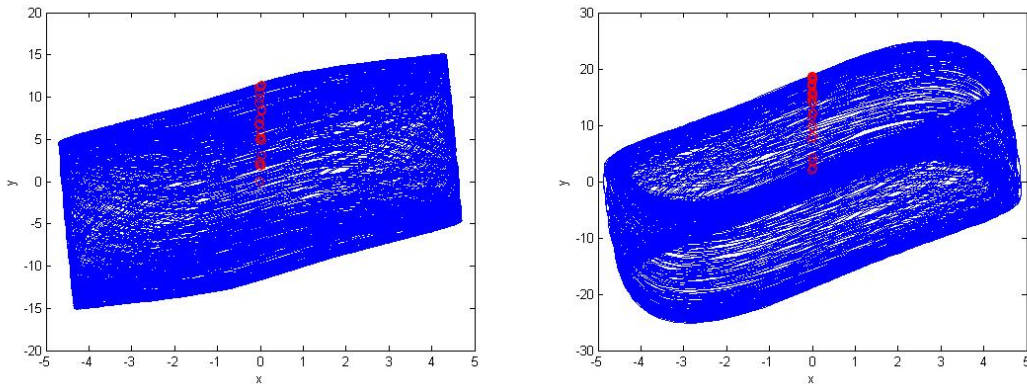
(a) $q_1 = q_2 = 0.1$

(b) $q_1 = q_2 = 0.5$



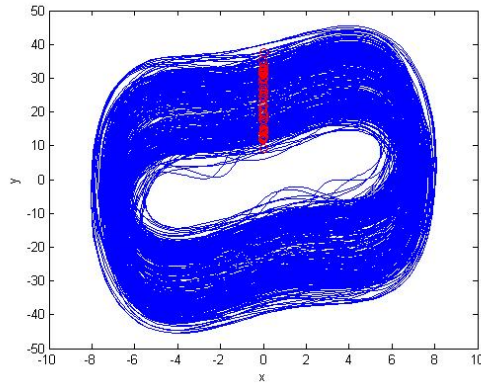
(c) $q_1 = q_2 = 0.9$

Fig. 4.6 The phase portraits and Poincaré maps of the fractional order modified nano Duffing resonator systems (11) with control term $k_3 \sin x_1$, where $k_3 = 10$.



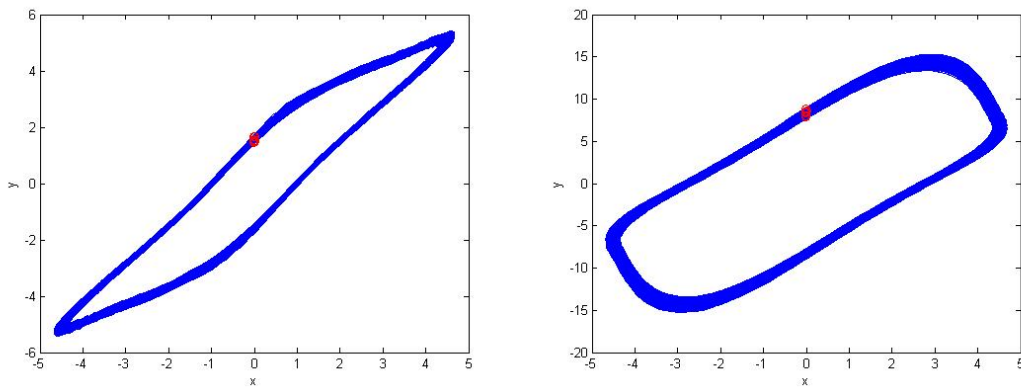
(a) $q_1 = q_2 = 0.1$

(b) $q_1 = q_2 = 0.5$



(c) $q_1 = q_2 = 0.9$

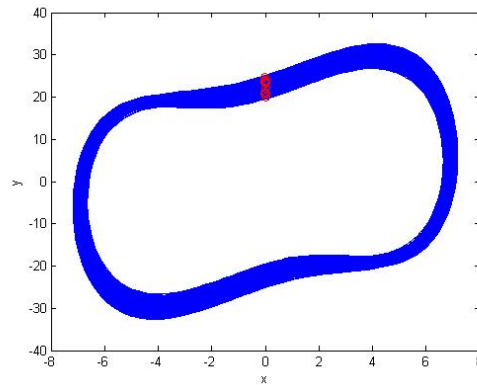
Fig. 4.7 The phase portraits and Poincaré maps of the fractional order modified nano Duffing resonator systems (11) with control term $k_3 \sin x_1$, where $k_3 = -10$.



(a) $q_1 = q_2 = 0.1$

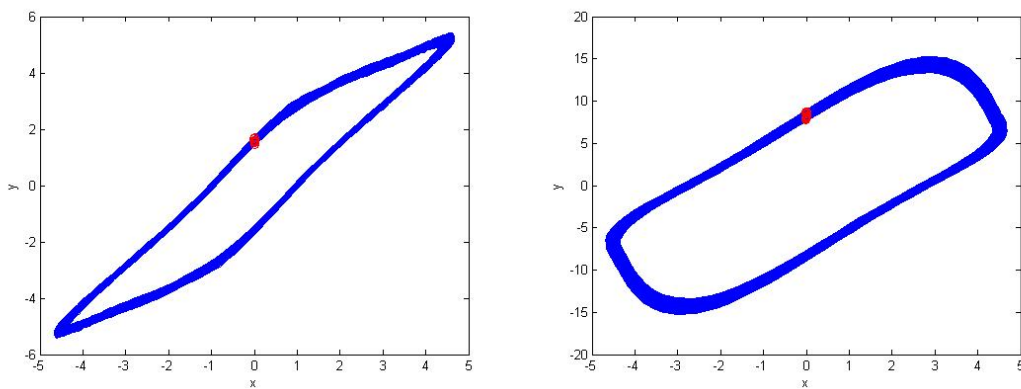


(b) $q_1 = q_2 = 0.5$



(c) $q_1 = q_2 = 0.9$

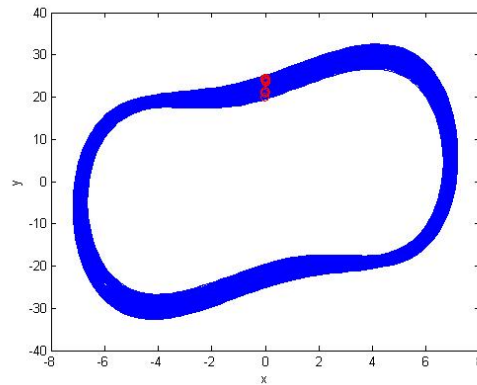
Fig. 4.8 The phase portraits and Poincaré maps of the fractional order modified nano Duffing resonator systems (11) with control term $k_4 \sin x_1$, where $k_4 = 10$.



(a) $q_1 = q_2 = 0.1$



(b) $q_1 = q_2 = 0.5$



(c) $q_1 = q_2 = 0.9$

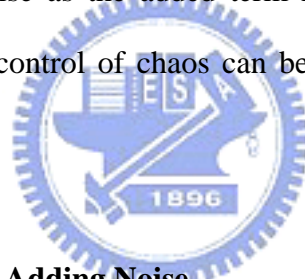
Fig. 4.9 The phase portraits and Poincaré maps of the fractional order modified nano Duffing resonator systems (11) with control term $k_4 \sin x_1$, where $k_4 = -10$.

Chapter 5

Anti-control of Chaos of a Fractional Order Modified Nano Duffing Resonator System by Adding Noise

5.1 Preliminaries

In this chapter, anti-control of chaos of a fractional order modified nano Duffing resonator system is studied by adding noise. By using the white noise, Rayleigh noise, Rician noise and uniform noise as the added term respectively, the anti-control of chaos can be obtained. Anti-control of chaos can be successfully obtained for very low total fractional order 0.2.



5.2 Anti-control of Chaos by Adding Noise

In this section, addition of the white noise, Rayleigh noise, Rician noise and uniform noise as the external term respectively are presented, which can enhance the existing chaos of the originally system. All numerical simulations are run by block diagrams in Simulink environment. The results are demonstrated by numerical results, i.e. phase portraits and Poincaré maps.

5.2.1 Adding the white noise

We add an external term $k_1 F_1$ to the second equation of (4.1), where F_1 is the white noise. The strength k_1 is either positive or negative.

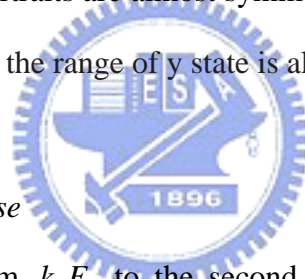
The probability density function of n-dimensional Gaussian noise is

$$f(x) = ((2\pi)^n \det K)^{-\frac{1}{2}} \exp(-(x - \mu)^T K^{-1} (x - \mu) / 2) \quad (5.1)$$

where x is a length- n vector, K is the n -by- n covariance matrix, μ is the mean value vector, and the superscript T indicates matrix transpose. The Simulink Communications toolbox provides the Gaussian Noise Generator block. The initial seed, the mean value and the variance in the simulation must be specified. We take the initial seed 41, the mean value 1 and the variance 1 in the simulation.

For anti-control of chaos, all simulations for $q_1 = q_2 = 0.1 \sim 0.9$ are obtained successfully. For saving space, only results for $q_1 = q_2 = 0.1, 0.5$ and 0.9 are shown as Fig. 5.1-5.2.

From above numerical results, it is shown that when k_1 is either positive or negative, the chaotic phase portraits are almost symmetric to the origin. It can be seen that when total order is larger, the range of y state is also larger.



5.2.2 Adding the Rayleigh noise

We add an external term $k_2 F_2$ to the second equation of (4.1), where F_2 is Rayleigh noise. The strength k_2 is either positive or negative.

The Rayleigh probability density function is given by

$$f(x) = \begin{cases} \frac{x}{\sigma^2} e^{-\frac{x^2}{2\sigma^2}} & x \geq 0 \\ 0 & x < 0 \end{cases} \quad (5.2)$$

where σ^2 is known as the fading envelope of the Rayleigh distribution. The Simulink Communications toolbox provides the Rayleigh Noise Generator block. The initial seed and the sigma parameter in the simulation must be specified. We specify the initial seed 47 and the sigma parameter 5 in the simulation.

For anti-control of chaos, all simulations for $q_1 = q_2 = 0.1 \sim 0.9$ are obtained successfully. For saving space, only results for $q_1 = q_2 = 0.1, 0.5$ and 0.9 are shown as

Fig. 5.3-5.4.

From above numerical results, it is also shown that when k_2 is either positive or negative, the chaotic phase portraits are almost symmetric to the origin. It can be seen that when total order is larger, the range of y state is also larger.

5.2.3 Adding the Rician noise

We add an external term $k_3 F_3$ to the second equation of (4.1), where F_3 is Rician noise. The strength k_3 is either positive or negative.

The Rician probability density function is given by

$$f(x) = \begin{cases} \frac{x}{\sigma^2} I_0\left(\frac{mx}{\sigma^2}\right) e^{-\frac{x^2+m^2}{2\sigma^2}} & x \geq 0 \\ 0 & x < 0 \end{cases} \quad (5.3)$$

where σ is the standard deviation of the Gaussian distribution that underlies the Rician distribution noise, $m^2 = m_I^2 + m_Q^2$, where m_I and m_Q are the mean values of two independent Gaussian components, and I_0 is the modified 0th-order Bessel function of the first kind given by

$$I_0(y) = \frac{1}{2\pi} \int_{-\pi}^{\pi} e^{y \cos t} dt \quad (5.4)$$

Note that m and σ are not the mean value and standard deviation for the Rician noise. The Simulink Communications toolbox provides the Rician Noise Generator block. The initial seed, Rician K-factor and the sigma parameter must be specified in the simulation. We specify the initial seed 59, Rician K-factor 10 and the sigma parameter 5 in the simulation.

For anti-control of chaos, all simulations for $q_1 = q_2 = 0.1 \sim 0.9$ are obtained successfully. For saving space, only results for $q_1 = q_2 = 0.1, 0.5$ and 0.9 are shown as

Fig. 5.5-5.6.

From above numerical results, it is also shown that when k_3 is either positive or negative, the chaotic phase portraits are almost symmetric to the origin. It can be seen that when total order is larger, the range of y state is also larger.

5.2.4 Adding the Uniform noise

We add an external term $k_4 F_4$ to the second equation of (4.1), where F_4 is the uniform noise. The strength k_4 is either positive or negative.

The probability density function of uniform noise is given by

$$f(x) = \begin{cases} \frac{1}{b-a} & \text{if } a \leq x \leq b \\ 0 & \text{otherwise} \end{cases} \quad (5.5)$$

The mean of this density function is given by $\mu = \frac{a+b}{2}$ and its variance by

$$\sigma^2 = \frac{(b-a)^2}{12}.$$

The Simulink Communications toolbox provides the Uniform Noise Generator block. The initial seed, the noise lower bound and the noise upper bound must be specified in the simulation. We specify the initial seed 31, the noise lower bound 0 and the noise upper bound 5 in the simulation.

For anti-control of chaos, all simulations for $q_1 = q_2 = 0.1 \sim 0.9$ are obtained successfully. For saving space, only results for $q_1 = q_2 = 0.1, 0.5$ and 0.9 are shown as Fig. 5.7-5.8.

From above numerical results, it is shown that when k_4 is either positive or negative, the chaotic phase portraits are almost symmetric to the origin. It can be seen that when total order is larger, the range of y state is also larger.

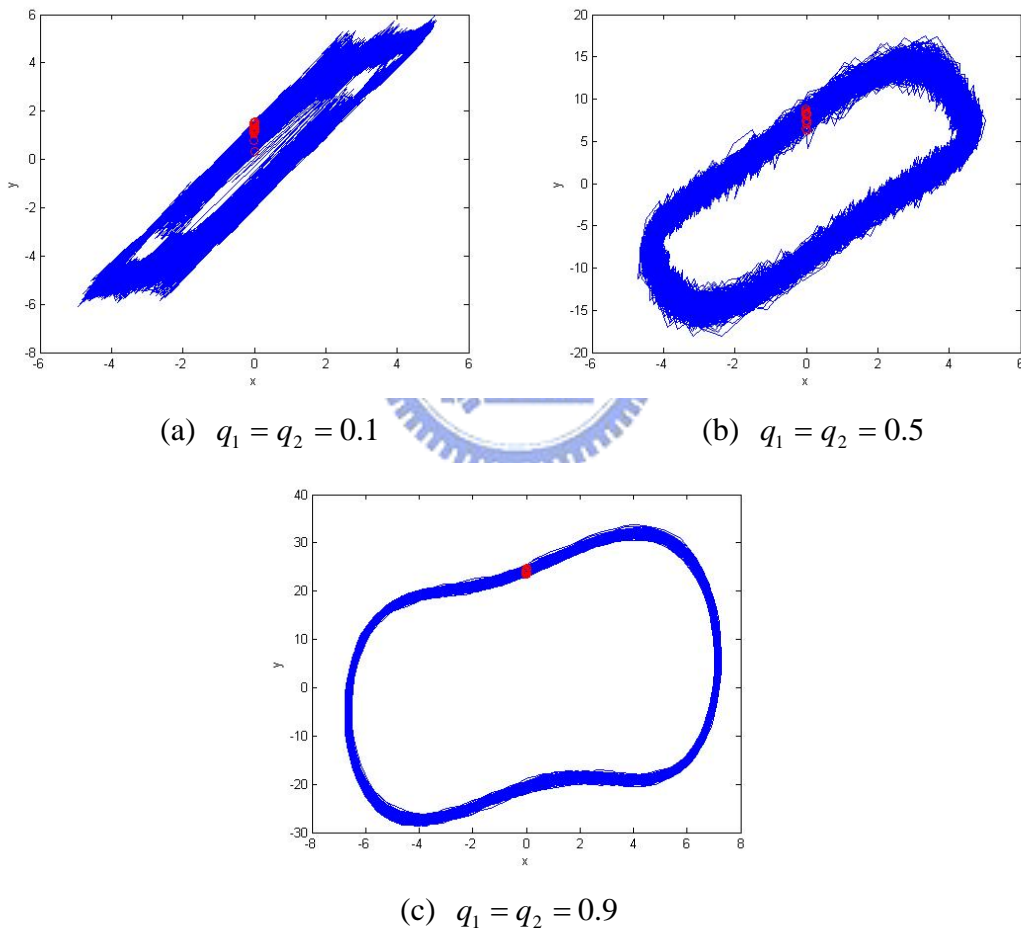


Fig. 5.1 The phase portraits and Poincaré maps of the fractional order modified nano Duffing resonator systems (11) with control term $k_1 F_1$, where $k_1 = 10$, F_1 is the white noise.

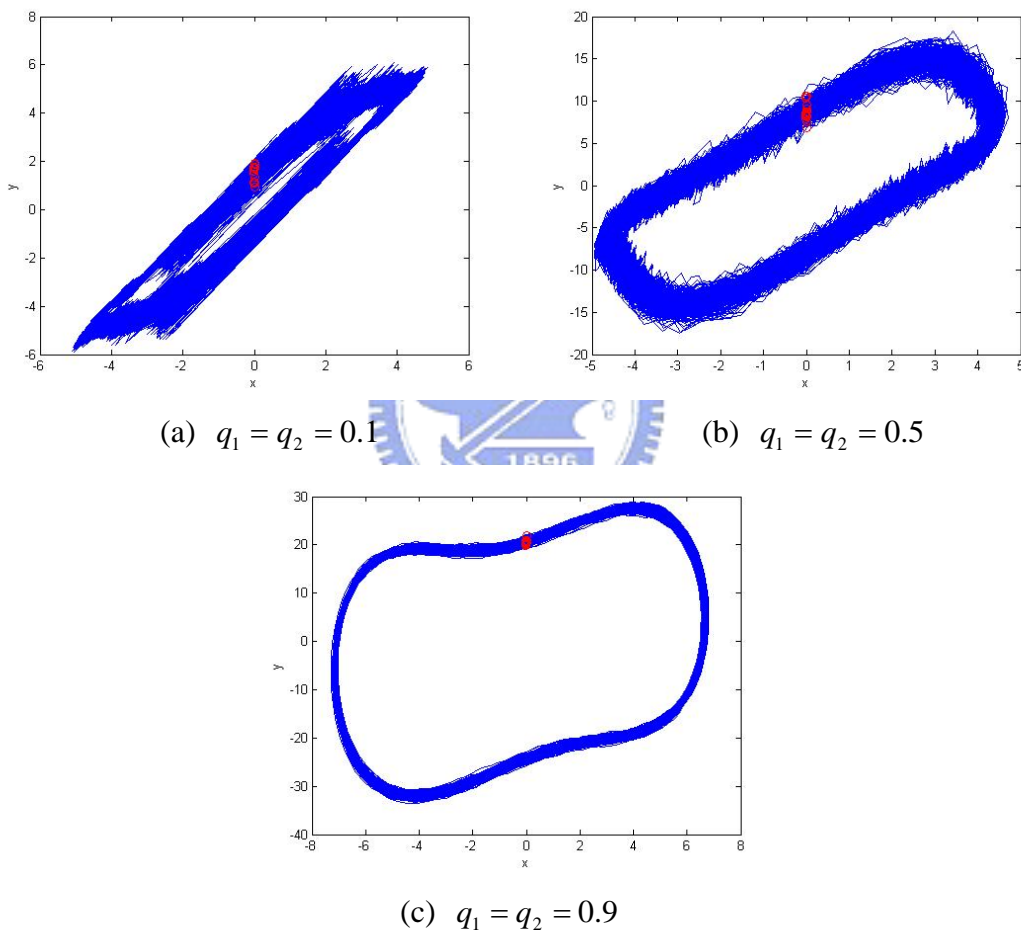
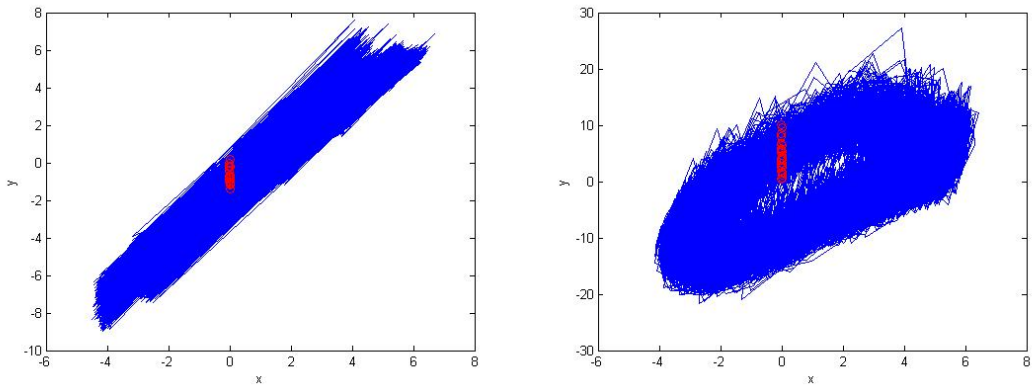
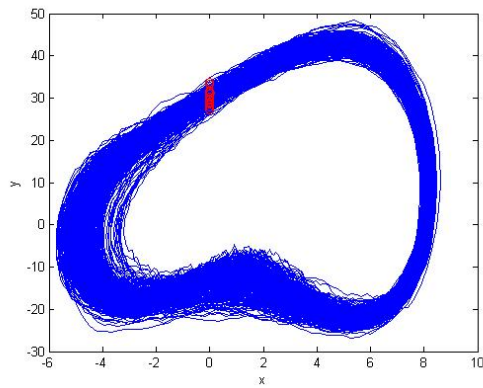


Fig. 5.2 The phase portraits and Poincaré maps of the fractional order modified nano Duffing resonator systems (11) with control term $k_1 F_1$, where $k_1 = -10$, F_1 is the white noise.



(a) $q_1 = q_2 = 0.1$

(b) $q_1 = q_2 = 0.5$



(c) $q_1 = q_2 = 0.9$

Fig. 5.3 The phase portraits and Poincaré maps of the fractional order modified nano Duffing resonator systems (11) with control term $k_2 F_2$, where $k_2 = 10$, F_2 is Rayleigh noise.

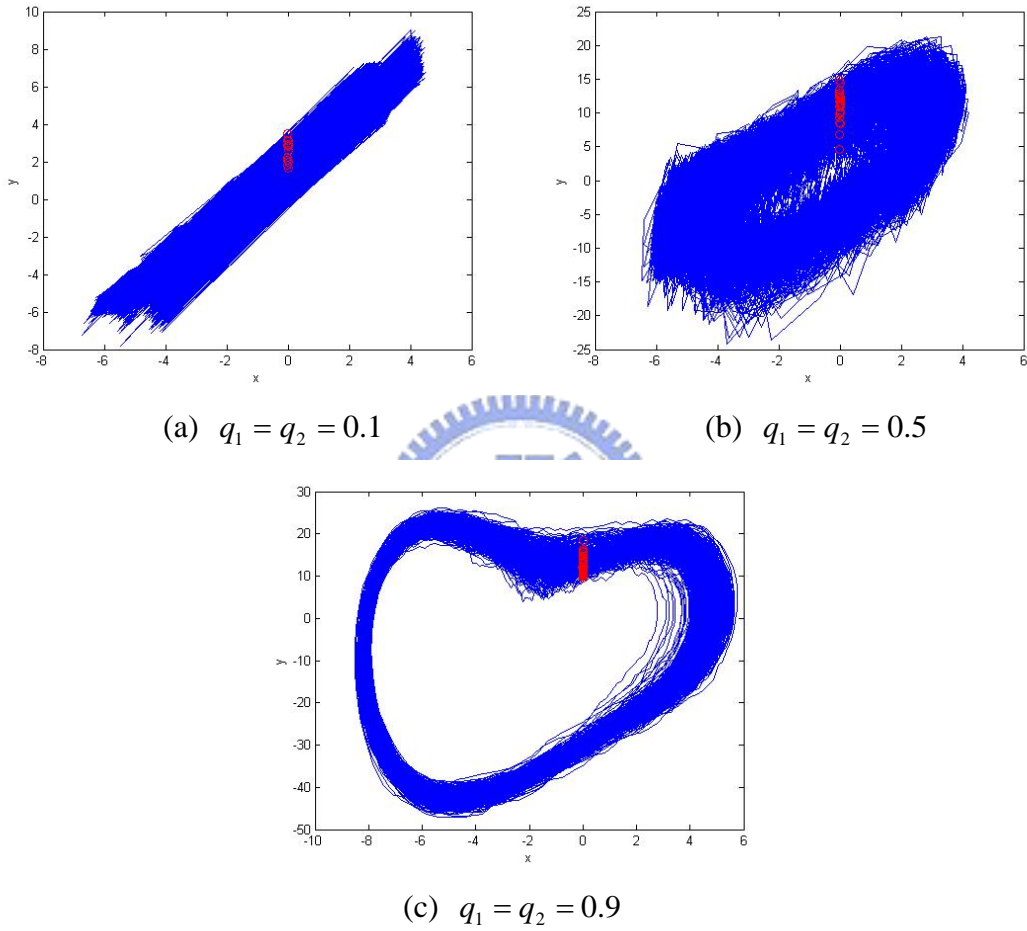
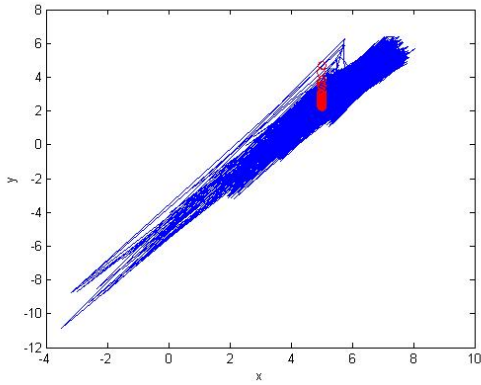
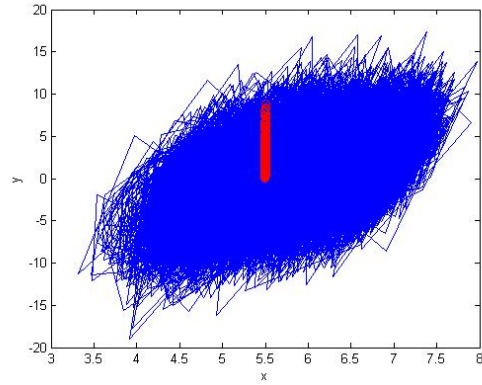


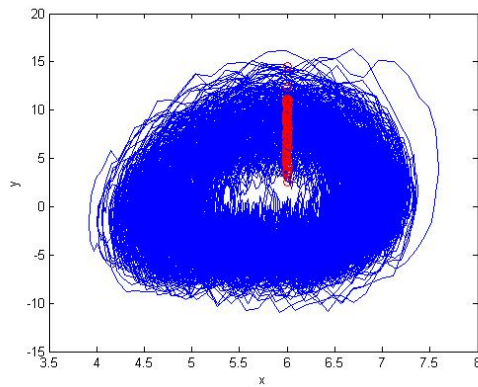
Fig. 5.4 The phase portraits and Poincaré maps of the fractional order modified nano Duffing resonator systems (11) with control term $k_2 F_2$, where $k_2 = -10$, F_2 is Rayleigh noise.



(a) $q_1 = q_2 = 0.1$

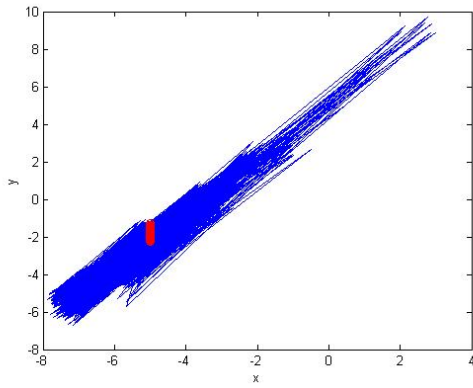


(b) $q_1 = q_2 = 0.5$

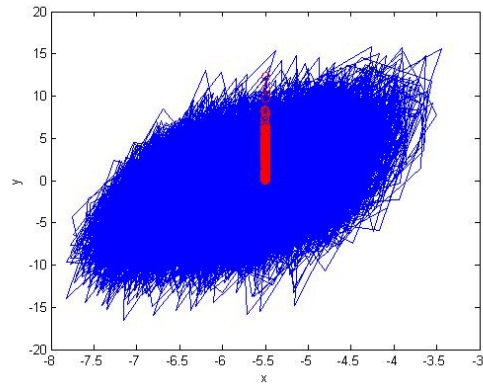


(c) $q_1 = q_2 = 0.9$

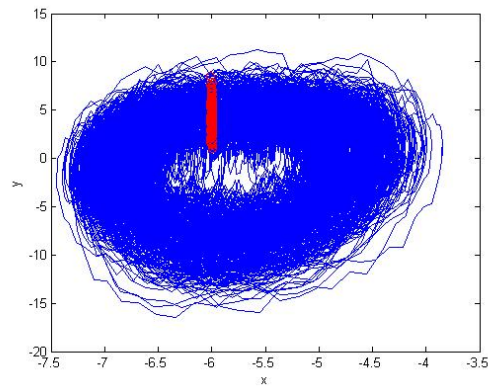
Fig. 5.5 The phase portraits and Poincaré maps of the fractional order modified nano Duffing resonator systems (11) with control term $k_3 F_3$, where $k_3 = 10$, F_3 is Rician noise.



(a) $q_1 = q_2 = 0.1$

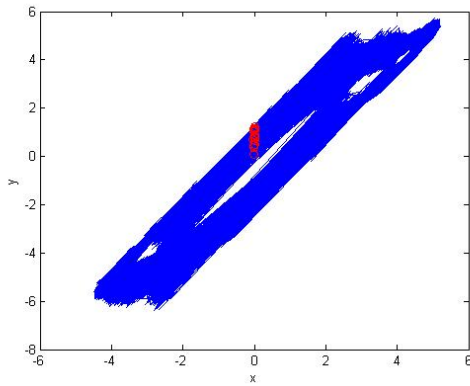


(b) $q_1 = q_2 = 0.5$

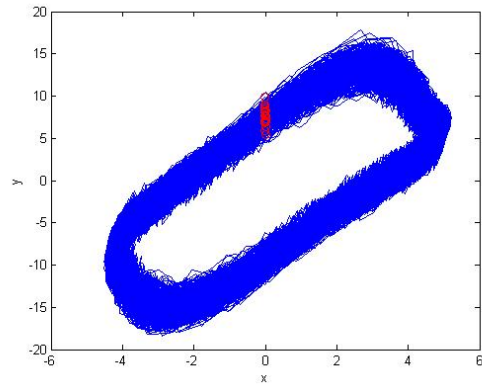


(c) $q_1 = q_2 = 0.9$

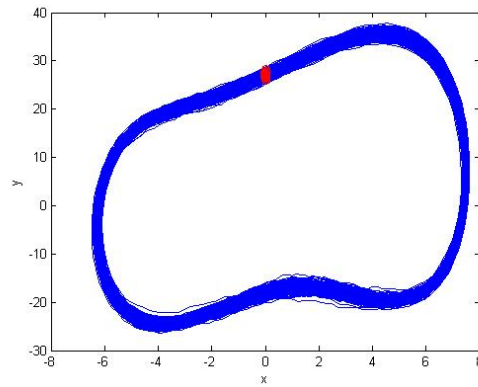
Fig. 5.6 The phase portraits and Poincaré maps of the fractional order modified nano Duffing resonator systems (11) with control term $k_3 F_3$, where $k_3 = -10$, F_3 is Rician noise.



(a) $q_1 = q_2 = 0.1$



(b) $q_1 = q_2 = 0.5$



(c) $q_1 = q_2 = 0.9$

Fig. 5.7 The phase portraits and Poincaré maps of the fractional order modified nano Duffing resonator systems (11) with control term $k_4 F_4$, where $k_4 = 10$, F_4 is the uniform noise.

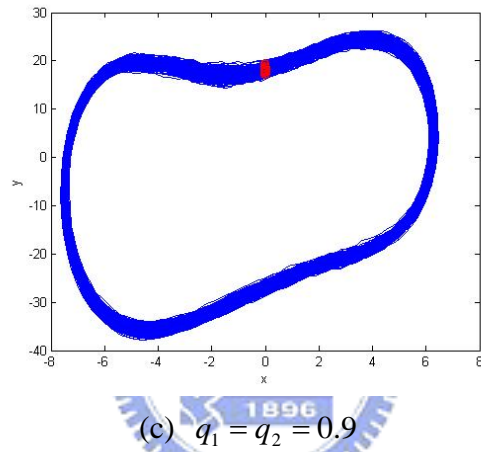
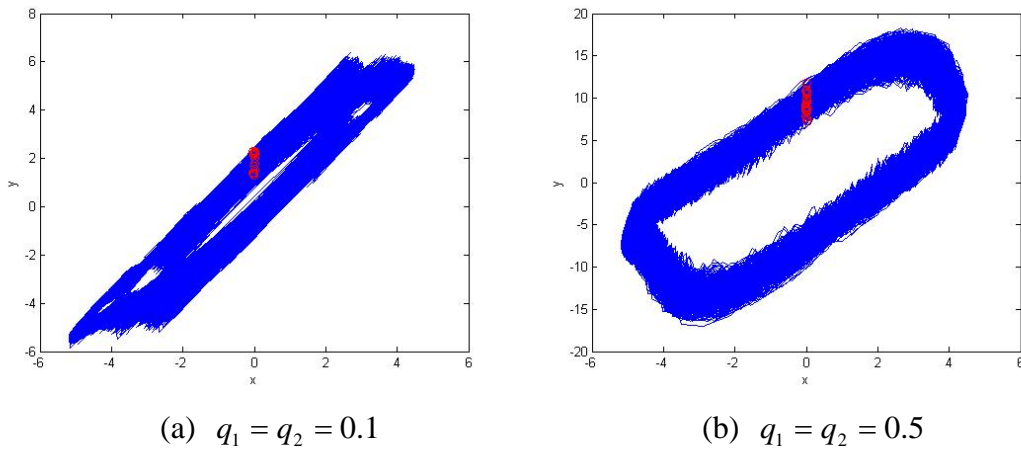


Fig. 5.8 The phase portraits and Poincaré maps of the fractional order modified nano Duffing resonator systems (11) with control term $k_4 F_4$, where $k_4 = -10$, F_4 is the uniform noise.

Chapter 6

Conclusions

In this thesis we have studied the chaos in the fractional order modified nano Duffing resonator system by phase portraits, Poincaré maps and bifurcation diagrams in Chapter 2. The total orders of the system for the existence of chaos are 1.8, 1.9, 2.0 and 2.1.

In Chapter 3, The chaos synchronizations of two uncoupled fractional order modified nano Duffing resonator systems are obtained by replacing their corresponding parameters by the same function of chaotic state variables of a third chaotic system. The method is named parameter excited chaos synchronization which can be successfully obtained for very low total fractional order 0.2. Numerical simulations are illustrated by phase portraits, Poincaré maps and state error plots.

In Chapter 4 and 5, anti-control of chaos of a fractional order modified nano Duffing resonator system is studied. By using the functions of state variable of a second identical system as the added term, the anti-control of chaos can be obtained. By using the white noise, Rayleigh noise, Rician noise and uniform noise as the added term respectively, the anti-control of chaos can be obtained. Anti-control of chaos can be successfully obtained for very low total fractional order 0.2. Numerical simulations are illustrated by phase portraits and Poincaré maps.

REFERENCES

- [1] He, G.L.; Zhou, S.P., "What is the exact condition for fractional integrals and derivatives of Besicovitch functions to have exact box dimension?", *Chaos, Solitons and Fractals* 2005;26:867-79.
- [2] Yao, K.; Su, W.Y.; Zhou, S.P., "On the connection between the order of fractional calculus and the dimensions of a fractal function". *Chaos, Solitons and Fractals* 2005;23: 621-9.
- [3] Guy, Jumarie, "Fractional master equation: non-standard analysis and Liouville–Riemann derivative". *Chaos, Solitons and Fractals* 2001;12: 2577-87.
- [4] Elwakil, S. A.; Zahran, M. A., "Fractional Integral Representation of Master Equation". *Chaos, Solitons and Fractals* 1999;10: 1545-8.
- [5] Sun, H.H., Abdelwahad A.A., Onaral B., *IEEE Trans. Autom. Control* 1984;29: 441.
- [6] Ichise, M., Nagayanagi, Y., Kojima, T., *Electroanal J., Chem.* 1971;33:253.
- [7] Heaviside, O., *Electromagnetic Theory*, Chelsea, New York, 1971.
- [8] Oustaloup, A., Levron, F., Nanot, F., Mathieu, B., "Frequency band complex non integer differentiator: characterization and synthesis". *IEEE Trans CAS-I* 2000;47:25–40.
- [9] Chen, Y.Q., Moore, K., "Discretization schemes for fractional-order differentiators and integrators". *IEEE Trans CAS-I* 2002;49:363–7.
- [10] Hartley, T.T., Lorenzo, C.F., "Dynamics and control of initialized fractional-order systems". *Nonlinear Dyn* 2002;29:201–33.
- [11] Hwang, C., Leu, J.F., Tsay, S.Y., "A note on time-domain simulation of feedback fractional-order systems". *IEEE Trans Auto Contr* 2002;47:625–31.
- [12] Podlubny, I., Petras, I., Vinagre, B.M., O'Leary, P., Dorcak, L., "Analogue

- realizations of fractional-order controllers”. *Nonlinear Dyn* 2002;29:281–96.
- [13] Hartley, T.T., Lorenzo, C.F., Qammer, H.K., “Chaos in a fractional order Chua’s system”. *IEEE Trans CAS-I* 1995;42:485–90.
- [14] Arena, P., Caponetto, R., Fortuna, L., Porto, D., “Chaos in a fractional order Duffing system”. In: *Proc ECCTD, Budapest; 1997.p. 1259–62.*
- [15] Ahmad, W.M., Sprott, J.C. ,“Chaos in fractional-order autonomous nonlinear systems”. *Chaos, Solitons and Fractals* 2003;16:339–51.
- [16] Ahmad, W.M., Harb, W.M. ,“On nonlinear control design for autonomous chaotic systems of integer and fractional orders”. *Chaos, Solitons and Fractals* 2003;18:693–701.
- [17] Ahmad, W., El-Khazali, R., El-Wakil, A. ,“Fractional-order Wien-bridge oscillator”. *Electr Lett* 2001;37:1110–2.
- [18] Grigorenko, I., Grigorenko, E. ,“Chaotic dynamics of the fractional Lorenz system”. *Phys Rev Lett* 2003;91:034101.
- [19] Arena, P., Caponetto, R., Fortuna, L., Porto, D. ,“Bifurcation and chaos in noninteger order cellular neural networks”. *Int J Bifur Chaos* 1998;7:1527–39.
- [20] Arena, P., Fortuna, L., Porto, D. ,“Chaotic behavior in noninteger-order cellular neural networks”. *Phys Rev E* 2000;61:776–81.
- [21] Li, C.G., Chen, G. ,“Chaos and hyperchaos in fractional order *Rössler* equations”. *Phycica A* 2004;341:55–61.
- [22] Li, C.G., Chen, G., “Chaos in the fractional order Chen system and its control”. *Chaos, Solitons and Fractals* 2004;22:549–54.
- [23] Li, C.P., Peng, G.J., “Chaos in Chen’s system with a fractional order”. *Chaos, Solitons and Fractals* 2004;22:443–50.
- [24] Zaslavsky, G.M., “Chaos, fractional kinetics, and anomalous transport”. *Phys Rep* 2002;371:461–580.

- [25] Lu, J.G. ,“Chaotic dynamics and synchronization of fractional-order Arneodo’s systems”. Chaos, Solitons and Fractals 2005, in press.
- [26] Podlubny I. Fractional differential equations. New York: Academic Press; 1999.
- [27] Charef, A., Sun, H.H., Tsao, Y.Y., Onaral, B., “Fractal system as represented by singularity function”. IEEE Trans Auto Contr 1992;37:1465–70.
- [28] Pecora, L.M., Carroll, T.L., “Synchronization in chaotic systems”, Phys. Rev. Lett. 64:821–4;1990.
- [29] Carroll, T.L., Heagy, J.F., Pecora, L.M., “Transforming signals with chaotic synchronization”, Phys. Rev. E;54:4676–80;1996.
- [30] Kocarev, L., Parlitz, U., “Generalized synchronization, predictability, and equivalence of unidirectionally coupled dynamical systems”, Phys. Rev. Lett.;76:1816–9;1996.
- [31] Rosenblum, M.G., Pikovsky, A.S., Kurths J., “Phase synchronization of chaotic oscillators”, Phys. Rev. Lett.; 76:1804–7; 1996.
- [32] Yang, S.S., Duan, C.K., “Generalized Synchronization in Chaotic Systems”, Chaos, Solitons and Fractals; 9:1703–7; 1998.
- [33] Chen, G., Liu, S.T., “On generalized synchronization of spatial chaos”, Chaos, Solitons and Fractals; 15:311–8; 2003.
- [34] Kim, C.M., Rim, S., Kye, W.H., Ryu, J.W., Park, Y.J., “Anti-synchronization of chaotic oscillators”, Phys. Lett. A;320:39–46;2003.
- [35] Yang, S.P., Niu, H.Y., Tian, G., et al., “Synchronizing chaos by driving parameter”, Acta Phys. Sin.;50:619–23;2001.
- [36] Dai, D., Ma, X.K., “Chaos synchronization by using intermittent parametric adaptive control method”, Phys. Lett. A ;288:23–8; 2001.
- [37] Chen, H.K. “Synchronization of two different chaotic systems: a new system and each of the dynamical systems Lorenz, Chen and Lü ”, Chaos, Solitons and

Fractals Vol. 25; 1049-56, 2005.

- [38] Chen, H.K., Lin, T.N., “Synchronization of chaotic symmetric gyros by one-way coupling conditions”, *ImechE Part C: Journal of Mechanical Engineering Science* Vol. 217; 331-40, 2003.
- [39] Chen, H.K., “Chaos and chaos synchronization of a symmetric gyro with linear-plus-cubic damping”, *Journal of Sound & Vibration*, Vol. 255; 719-40, 2002.
- [40] Ge, Z.M., Yu, T.C., and Chen, Y.S., “Chaos synchronization of a horizontal platform system”, *Journal of Sound and Vibration* 731-49, 2003.
- [41] Ge, Z.M., Lin, T.N., “Chaos, chaos control and synchronization of electro-mechanical gyrostat system”, *Journal of Sound and Vibration* Vol. 259; No.3, 2003.
- [42] Ge, Z.M., Chen, Y.S., “Synchronization of unidirectional coupled chaotic systems via partial stability”, *Chaos, Solitons and Fractals* Vol. 21; 101-11, 2004.
- [43] Ge, Z.M., Chen, C.C., “Phase synchronization of coupled chaotic multiple time scales systems”, *Chaos, Solitons and Fractals* Vol. 20; 639-47, 2004.
- [44] Ge, Z.M., Lin, C.C. and Chen, Y.S., “Chaos, chaos control and synchronization of vibrometer system”, *Journal of Mechanical Engineering Science* Vol. 218; 1001-20, 2004.
- [45] Chen, H.K., Lin, T.N. and Chen, J.H., “The stability of chaos synchronization of the Japanese attractors and its application”, *Japanese Journal of Applied Physics* Vol. 42; No. 12, 7603-10, 2003.
- [46] Ge, Z.M. and Shiue, “Non-linear dynamics and control of chaos for Tachometer”, *Journal of Sound and Vibration* Vol. 253; No4, 2002.
- [47] Ge, Z.M. and Lee, C.I., “Non-linear dynamics and control of chaos for a rotational machine with a hexagonal centrifugal governor with a spring”, *Journal*

of Sound and Vibration Vol. 262; 845-64, 2003.

- [48] Ge, Z.M., Hsiao, C.M. and Chen, Y.S., “Non-linear dynamics and chaos control for a time delay Duffing system”, Int. J. of Nonlinear Sciences and Numerical Vol. 6; No. 2, 187-199, 2005.
- [49] Ge, Z.M., Tzen, P.C. and Lee, S.C., “Parametric analysis and fractal-like basins of attraction by modified interpolates cell mapping”, Journal of Sound and Vibration Vol. 253; No. 3, 2002.
- [50] Ge, Z.M. and Lee, S.C., “Parameter used and accuracies obtain in MICM global analyses”, Journal of Sound and Vibration Vol. 272; 1079-85, 2004.
- [51] Ge, Z.M. and Leu, W.Y., “Chaos synchronization and parameter identification for loudspeaker system” Chaos, Solitons and Fractals Vol. 21; 1231-47, 2004.
- [52] Ge, Z.M. and Chang, C.M., “Chaos synchronization and parameter identification for single time scale brushless DC motor”, Chaos, Solitons and Fractals Vol. 20; 889-903, 2004.
- [53] Ge, Z.M. and Lee, J.K., “Chaos synchronization and parameter identification for gyroscope system”, Applied Mathematics and Computation, Vol. 63; 667-82, 2004.
- [54] Ge, Z.M. and Cheng, J.W., “Chaos synchronization and parameter identification of three time scales brushless DC motor”, Chaos, Solitons and Fractals Vol. 24; 597-616, 2005.
- [55] Ge, Z.M. and Chen, Y.S., “Adaptive synchronization of unidirectional and mutual coupled chaotic systems”, Chaos, Solitons and Fractals Vol. 26; 881-88, 2005.
- [56] Chen, H.K., “Global chaos synchronization of new chaotic systems via nonlinear control”, Chaos, Solitons & Fractals 4; 1245-51, 2005.
- [57] Chen, H.K. and Lee, C.I., “Anti-control of chaos in rigid body motion”, Chaos,

- Solitons and Fractals Vol. 21; 957-965, 2004.
- [58] Ge, Z.M. and Wu, H.W., “Chaos synchronization and chaos anticontrol of a suspended track with moving loads”, Journal of Sound and Vibration Vol. 270; 685-712, 2004.
- [59] Ge, Z.M. and Yu, C.Y. and Chen, Y.S., “Chaos synchronization and chaos anticontrol of a rotational supported simple pendulum”, JSME International Journal, Series C, Vol. 47; No. 1, 233-41, 2004.
- [60] Ge, Z.M. and Leu, W.Y., “Anti-control of chaos of two-degree-of-freedom louder speaker system and chaos system of different order system”, Chaos, Solitons and Fractals Vol. 20; 503-21, 2004.
- [61] Ge, Z.M., Cheng, J.W. and Chen, Y.S., “Chaos anticontrol and synchronization of three time scales brushless DC motor system”, Chaos, Solitons and Fractals Vol. 22; 1165-82, 2004.
- [62] Ge, Z.M. and Lee, C.I., “Anticontrol and synchronization of chaos for an autonomous rotational machine system with a hexagonal centrifugal governor”, Chaos, Solitons and Fractals Vol. 282; 635-48, 2005.
- [63] Ge, Z.M. and Lee, C.I., “Control, anticontrol and synchronization of chaos for an autonomous rotational machine system with time-delay”, Chaos, Solitons and Fractals Vol. 23; 1855-64, 2005.
- [64] Morel, Cristina; Bourcier, Marc; Chapeau-Blondeau, François, “Generating independent chaotic attractors by chaos anticontrol in nonlinear circuits”, Chaos, Solitons and Fractals Vol. 26; 541-549, 2005.
- [65] Bondarenko, Vladimir E., “Control and `anticontrol' of chaos in an analog neural network with time delay”, Chaos, Solitons and Fractals Vol. 13; 139-154, 2002.
- [66] Codreanu, Steliana, “Desynchronization and chaotification of nonlinear dynamical systems”, Chaos, Solitons and Fractals Vol. 13; 839-843, 2002.

- [67] Yang, Ruoting; Hong, Yiguang; Qin, Huashu; Chen, Guanrong, “Anticontrol of chaos for dynamic systems in p -normal form: A homogeneity-based approach”, *Chaos, Solitons and Fractals* Vol. 25; 687-697 , 2005.
- [68] G. Chen and L. Yang, “Chaotifying a continuous-time system near a stable limit cycle”, *Chaos, Solitons and Fractals* Vol. 15, 245–253, 2003.
- [69] X. S. Yang and G. Chen, “Can state feedback stabilize a chaotic orbit uniformly and asymptotically in the sense of orbital stability?”, *Chaos, Solitons and Fractals* Vol.15, 297–301, 2003.
- [70] Li, Changpin; Chen, Guanrong, “On the Marotto–Li–Chen theorem and its application to chaotification of multi-dimensional discrete dynamical systems”, *Chaos, Solitons and Fractals* Vol. 18; 807-817, 2003.
- [71] Lu, Hongtao; Yu, Xinzhen, “Local bifurcations in delayed chaos anticontrol systems”, *Journal of Computational and Applied Mathematics* Vol. 181; 188-199, 2005.
- [72] Konishi, Keiji, “Generating chaotic behavior in an oscillator driven by periodic forces”, *Physics Letters A* Vol. 320; 200-206, 2003.
- [73] Andrew N. Cleland, “*Foundations of Nanomechanics.*” Springer, Germany, 2003.
- [74] Chen, G., “Control and anticontrol of chaos.” In: *Proceedings of the 1st International Conference on Control of Oscillations and Chaos*, p. 181–86, 1997.

Appendix

Table 1. FRACTIONAL OPERATORS WITH APPROXIMATELY
2 db ERROR FROM $\omega = 10^{-2}$ TO 10^2 rad/sec

$\frac{1}{s^{0.1}} \approx$	$\frac{220.4s^4 + 5004s^3 + 503s^2 + 234.5s + 0.484}{s^5 + 359.8s^4 + 5742s^3 + 4247s^2 + 147.7s + 0.2099}$
$\frac{1}{s^{0.2}} \approx$	$\frac{60.95s^4 + 816.9s^3 + 582.8s^2 + 23.24s + 0.04934}{s^5 + 134s^4 + 956.5s^3 + 383.5s^2 + 8.953s + 0.01821}$
$\frac{1}{s^{0.3}} \approx$	$\frac{23.76s^4 + 224.9s^3 + 129.1s^2 + 4.733s + 0.01052}{s^5 + 64.51s^4 + 252.2s^3 + 63.61s^2 + 1.104s + 0.002267}$
$\frac{1}{s^{0.4}} \approx$	$\frac{25s^4 + 558.5s^3 + 664.2s^2 + 44.15s + 0.1562}{s^5 + 125.6s^4 + 840.6s^3 + 317.2s^2 + 7.428s + 0.02343}$
$\frac{1}{s^{0.5}} \approx$	$\frac{15.97s^4 + 593.2s^3 + 1080s^2 + 135.4s + 1}{s^5 + 134.3s^4 + 1072s^3 + 543.4s^2 + 20.1s + 0.1259}$
$\frac{1}{s^{0.6}} \approx$	$\frac{8.579s^4 + 255.6s^3 + 405.3s^2 + 35.93s + 0.1696}{s^5 + 94.22s^4 + 472.9s^3 + 134.8s^2 + 2.639s + 0.009882}$
$\frac{1}{s^{0.7}} \approx$	$\frac{4.406s^4 + 177.6s^3 + 209.6s^2 + 9.179s + 0.0145}{s^5 + 88.12s^4 + 279.2s^3 + 33.3s^2 + 1.927s + 0.0002276}$
$\frac{1}{s^{0.8}} \approx$	$\frac{5.235s^3 + 1453s^2 + 5306s + 254.9}{s^4 + 658.1s^3 + 5700s^2 + 658.2s + 1}$
$\frac{1}{s^{0.9}} \approx$	$\frac{1.766s^2 + 38.27s + 4.914}{s^3 + 36.15s^2 + 7.789s + 0.01}$

Paper List

- [1] Zheng-Ming Ge and Chan-Yi Ou, “Chaos in a Fractional Order Modified Duffing System.”, *Chaos, Solitons and Fractals*, Nov. 2005, accepted and proofed.(SCI, Impact Factor:1.938)
- [2] Zheng-Ming Ge and Chan-Yi Ou, “Chaos Synchronization of Fractional Order Modified Duffing Systems with Parameters Excited by a Chaotic Signal.”, *Chaos, Solitons and Fractals*, May. 2006, accepted. (SCI, Impact Factor: 1.938)
- [3] Zheng-Ming Ge and Chan-Yi Ou, “Anti-control of Chaos of a Fractional Order Modified Duffing System.”, submitted to *Chaos, Solitons and Fractals*, 2006.
- [4] Zheng-Ming Ge and Chan-Yi Ou, “Anti-control of Chaos of a Fractional Order Modified Duffing System by Adding Noise.”, submitted to *Chaos, Solitons and Fractals*, 2006.

